HEINRICH HEINE
UNIVERSITÄT
DÜSSELDORF

Proteomic analysis of differentially expressed proteins in the heart following desflurane preconditioning

Inaugural-Dissertation

zur Erlangung des Doktorgrades
der Mathematisch-Naturwissenschaftlichen Fakultät
der Heinrich-Heine-Universität Düsseldorf

vorgelegt von

Nadine Dyballa
aus Würselen

Düsseldorf, Mai 2010

Aus
der Klinik für Anästhesiologie des Universitätsklinikum Düsseldorf
und
dem Biologisch-Medizinischen Forschungszentrum der Heinrich-Heine Universität Düsseldorf

Gedruckt mit der Genehmigung der
Mathematisch-Naturwissenschaftlichen Fakultät der
Heinrich-Heine-Universität Düsseldorf

Referent: Prof. Dr. William Martin
Koreferent: Prof. Dr. Wolfgang Schlack

Tag der mündlichen Prüfung: 14. Juli 2010

Die besondere Leistung einer Doktorarbeit ist es, sein Projekt über so viele Jahre pflichtbewusst und gewissenhaft zu erledigen –
Tag ein, Tag aus, und manches Mal auch des Nachts.

Die besondere Ehre die mir dabei zuteil wurde, ist die,
als Wissenschaftlerin Kompetenz bewiesen zu haben.

Danksagung

Mit großem Stolz habe ich die Verleihung meines Doktorgrades erlebt. Eine Vielzahl von Menschen hat mich auf diesem Weg dorthin begleitet. Diese Seite ist nur euch gewidmet.

Nicht zuletzt sondern zuallererst möchte ich mich bei meinen Eltern bedanken, die in jeglicher Hinsicht die Grundsteine für den Weg bis hierhin gelegt haben. Ohne ihre grenzenlose und uneingeschränkte Unterstützung könnte ich nicht in der Position sein, in der ich jetzt glücklicherweise bin. Sie waren immer für mich da und haben meine innere Ausgeglichenheit und Stärke aufgebaut.

In besonderem Maße danke ich meinem Freund und Verlobten Christian. Ich habe vieles unbewusst von ihm vorausgesetzt, was nicht immer selbstverständlich war. Vor allem in der Endphase hat er mir den Rücken freigehalten, meine schlechte Laune und meine Zeiten der überstrapazierten Nerven geduldet und immer ein offenes Ohr für mich gehabt.

Ein großer Dank geht an meinen Doktorvater Professor Wolfgang Schlack, bei dem ich stets Zuspruch für dieses Projekt erfahren habe. Von weiter Ferne hat er mich begleitet und mit hilfreichen Tipps und Anregungen unterstützt.

Bedanken möchte ich mich natürlich bei Professor William Martin, der trotz seines straffen Zeitplans bereit war, meine Doktorarbeit vor der Mathematisch-Naturwissenschaftlichen Fakultät zu vertreten.

Einen erheblichen Beitrag zum Gelingen meiner Doktorarbeit hat Nina Hauck-Weber geleistet, die mir in der Anfangsphase viele wertvolle Hinweise gegeben hat. Danke dafür, dass du dich fortwährend nach mir und meiner Arbeit erkundigt hast, und selbst am Ende der Doktorarbeit von Amsterdam aus stets als Ansprechpartnerin zur Verfügung standest.

Sabine Metzger, wie soll ich dir danken? Du hast nie ein Blatt vor dem Mund genommen, Kritik geübt und Verbesserungsvorschläge vorgebracht. Du standest mir moralisch immer zur Seite, hast mich in meiner Arbeit bestärkt wie kein anderer und mir dadurch ermöglicht, mich selbst zu verwirklichen. Du standest aber nicht nur mit deinem Fachwissen zur Seite, sondern bist mir nicht zuletzt auch durch private Gespräche zu einem wertvollen und freundschaftlichen Wegbegleiter geworden.

Zu meiner Doktorandenzeit gehörte aber auch das (Über)Leben im sozialen Laborgefüge – ich habe Viele kommen und gehen sehen:
die Hartgesottenen Lars A., Mark H. und Axel K., „meine“ Zöglinge Christian S., Hendrik V., Schirin K., Paul R. und auch Axel M., die Frischlinge Florian F. und Jana K., und natürlich die Chaoten Vicky G. und Werner B.! Danke euch allen für die unvergessene Zeit, ihr habt meinen Charakter sehr geformt.

Weiterhin danke ich meinen Freund(inn)en, dass sie für die erforderliche Abwechslung sorgten. Es war nicht selbstverständlich von euch, meine Zeit im Schneckenhaus zu tolerieren.

Mein Dank gilt der Jürgen Manchot Stiftung, die sie sich finanziell an meinem Projekt beteiligte; und Katrin Henze, die sich freundlicherweise bereit erklärt hatte meine Doktorarbeit gegenzulesen.

Ein besonderes Wort des Dankes richte ich an Angelika Simons, die bis zuletzt im Promotionsbüro alle Hebel für den erfolgreichen Abschluss dieser Arbeit bewegt hatte.

Abschließend bedanke ich mich bei Allen herzlich für die zahlreichen Glückwünsche und anerkennenden Worte, die ich am 14. Juli 2010 nach meiner Verteidigung entgegen nehmen durfte. Tut mir leid, dass ich nicht länger mit euch feiern konnte…

Eure Nadine

Table of content

I. List of figures

II. List of tables

III. Abbreviations

2-DE	two-dimensional gel electrophoresis
aa	amino acid
APC	anesthetic preconditioning
ATP	adenosine triphosphate
Ca^{2+}	calcium
CABG	coronary artery bypass graft
CHAPS	3-[(3-cholamidopropyl)dimethylammonio]-1-propanesulfonate
CPB	cardiopulmonary bypass
DES-PC	desflurane-induced preconditioning
dpi	dots per inch
DTT	dithiothreitol
ESI	electrospray-ionisation
g	gravity
H^+	proton
HED	hydroxyethyldisulfide
IEF	isoelectric focusing
IPC	ischemic preconditioning
IR	ischemia-reperfusion
ISO-PC	isoflurane-induced preconditioning
K^+	Kalium
kDa	kilodalton
MAC	minimum alveolar concentration

M+H	protonated molecular ion
M_r	relative molecular weight
MS	mass spectrometry
m/z	mass-to-charge ratio
Na^{2+}	natrium
NAD	nicotinamide adenine dinucleotide
NADH	reduced nicotinamide adenine dinucleotide
PC	preconditioning
RT	room temperature
SDS-PAGE	sodium dodecyl sulfate polyacrylamide gel electrophoresis
SEVO-PC	sevoflurane-induced preconditioning
OD	optical density
TCA	trichloroacetic acid
pI	isoelectric point
V	Volt
v/v	volume per volume
w/v	weight per volume
w/w	weight per weight

IV. Abstract

Zusammenfassung (German version)

In den letzten 20 Jahren konnte gezeigt werden, dass eine Vielzahl pharmakologischer Substanzen die Fähigkeit besitzt das Herz gegen die Folgen eines Ischämie-Reperfusionsschaden zu schützen. Interessanterweise können auch volatile Anästhetika, welche seit Jahrzehnten als Narkosemittel zum Einsatz kommen, eine solche pharmakologische Präkonditionierung hervorrufen. Während das Phänomen an sich gut beschrieben ist, sind die zugrunde liegenden Signalwege bislang noch nicht vollständig geklärt. Das Ziel der vorliegenden Arbeit war daher, die Kenntnisse auf proteinbiochemischer Ebene zu erweitern.

Mit Hilfe der zwei-dimensionalen Gelelektrophorese und Massenspektrometrie wurde das kardiale Proteom Desfluran-präkonditionierter und unbehandelter Ratten verglichen, wobei zunächst umfangreiche Optimierungsschritte zur Herstellung qualitativ hochwertige Trenngele durchgeführt wurden. Auf Grundlage dieser konnten letztlich 40 Proteinspots detektiert werden, welche im Verlauf der Desfluran-Präkonditionierung (DES-PC) auffällige Veränderungen aufwiesen (1.2-fache Expressionsänderung; $P<0.02$ *vs*. Kontrolle).

Insgesamt wurden 12 Proteine massenspektrometrisch identifiziert, von denen elf in metabolischen Prozessen involviert sind. Die Liste der durch DES-PC veränderten Proteine umfasst die Methylmalonat-Semialdehyd Dehydrogenase, Aspartat-Aminotransferase, die Ubiquinol-Cytochrome c Reduktase, NADH-Ubiquinon Oxidoreduktase und NADH Dehydrogenase Ubiquinon Flavoprotein, sowie die Carboanhydrase, Laktatdehydrogenase, Inorganische Pyrophosphatase und Aconitase. Das einzige nicht-metabolische Protein war Serumalbumin. Auffällig war hierbei, dass alle Proteine außer der Aspartat-Aminotransferase eine verringerte Expression aufwiesen. Dies lässt vermuten, dass DES-PC eine repressive Wirkung auf metabolische Prozesse ausübt. In diesem Zusammenhang könnte ein reduzierter Energieverbrauch einen Adaptionsmechanismus an zukünftige Ischämie-Reperfusionsschäden darstellen.

Während der vergleichenden Analyse fiel auf, dass post-translationale Modifikationen eine entscheidende Rolle zu spielen scheinen. Einige der angesprochenen Proteine wiesen multiple *pI* Varianten auf, jedoch zeigten nicht alle Varianten eine Veränderung im Verlauf der DES-PC. So scheint die Ubiquinol-Cytochrome c Reduktase selektiv durch Proteinphosphorylierung beeinflusst zu werden, die Aconitase vor oxidativer Modifikation geschützt zu werden und die Aminotransferase-2 verstärkt zu translozieren. Desweiteren wurden Albumin, NADH-Ubiquinon Oxidoreduktase und Aminotransferase-1 an veränderten Positionen im Gel nachgewiesen, möglicherweise aufgrund von Proteindegradation. Diese Hinweise deuten darauf hin dass DES-PC bedingte Änderungen in der Proteinexpression zum Großteil durch post-translationale Modifikationen vermittelt werden.

Summary (English version)

In the last 20 years it was shown that a group of structurally diverse pharmacological agents pre-condition the heart toward ischemia-reperfusion injury through a variety of biochemical mechanisms. Pharmacological preconditioning with volatile anesthetics emerged as effective cardioprotective intervention in a multitude of experimental settings, but the cellular and molecular mechanisms are still incompletely elucidated. The purpose of this study was to gain deeper insight into the underlying signaling pathways of anesthetic-preconditioning on the protein level.

Using a proteomic approach, the combination of two-dimensional gel electrophoresis (2-DE) and mass spectrometry was applied to investigate differentially expressed proteins in the myocardial proteome of *in vivo* desflurane-preconditioned rats. In an effort to overcome the limitations of 2-DE separation and to substantially increase the overall proteome coverage, initial experiments were performed to refine protein extraction, solubility and resolution. Based on the comparative analysis of high-resolution 2-DE gels, 40 protein spots were found to be differentially expressed during desflurane preconditioning (DES-PC) (1.2-fold; $P<0.02$ *vs*. control).

Among the identified proteins, 11 out of 12 were involved in various metabolic processes. These include methylmalonate-semialdehyde dehydrogenase and aspartate aminotransferase 1 and 2 (amino acid metabolism), NADH-ubiquinone oxido-reductase 75kDa subunit and ubiquinol-cytochrome c reductase core protein 1 (electron transport chain), and carbonic anhydrase 1 and 2 (one-carbon compound metabolism). Other metabolic proteins are associated with oxidative phosphorylation (NADH dehydrogenase ubiquinone flavoprotein 1), glycolysis (lactate-dehydrogenase B), polyphosphate catabolism (inorganic pyrophosphatase 2) and the Krebs cycle (aconitase-2). The only non-metabolic active protein takes part in transport (albumin). Except for the aspartate aminotransferases, all proteins were down-regulated indicating that the trigger phase of DES-PC seems to be partially associated with a decrease in metabolic active enzymes. This in turn might evoke an adaptive mechanism of the heart to reduce energy dissipation under a subsequent condition of hypoxia like during ischemia.

A finding of note was that proteins represented in a spot chain (aminotransferase-2 (AST-2), aconitase-2 (Aco-2) and ubiquinol-cytochrome c reductase core protein 1 (UQCRC1)) showed expression changes only for distinct *pI* variants, suggesting post-translational modifications. AST-2 seems to translocate during DES-PC, Aco-2 was demonstrated to circumvent oxidative modification, and UQCRC1 was found to be differentially phosphorylated. In addition, three proteins with altered molecular weight and *pI* significantly decreased in abundance (AST-1, albumin and NADH-ubiquinone oxido-reductase 75 kDa subunit), possibly indicating reduced protein degradation in response to DES-PC. These findings support the paradigm that protein modifications play a more important role in the triggering phase of preconditioning than cellular protein turnover.

V. Declaration of originality

Ich versichere an Eides statt, dass ich die hier vorgelegte Dissertation mit dem Titel

Proteomic analysis of differentially expressed proteins in the heart following desflurane preconditioning

eigenständig und ohne unerlaubte Hilfe angefertigt habe. Es wurden keine anderen als die angegebenen Hilfsmittel verwendet.

Die Dissertation wurde in vorgelegter oder in ähnlicher Form noch bei keiner anderen Institution eingereicht. Ich habe bisher keine erfolglosen Promotionsversuche unternommen.

Düsseldorf, Mai 2010

Nadine Dyballa

Proteomic analysis of differentially expressed proteins in the heart following desflurane preconditioning

1 Introduction

1.1 The phenomenon of anesthetic preconditioning

1.1.1 What does not kill you makes you stronger

The year 2009 was the bicentennial of Darwin's birthday, and the sesquicentennial of publication of his book 'The Origin of Species'. Darwin's work, along with those of many others both before and after him, laid the foundation for our increasingly detailed understanding of the history and diversity of life. Although much has changed in evolutionary biology over the past 150 years, Darwin's insights continue to play an important role. Survival of the fittest as a metaphor for "better adapted for immediate, local environment" is strongly reflected in the phenomenon of preconditioning. The term preconditioning describes the remarkable ability of tissue with high energy consumption to adapt to stress by changing its phenotype so that it becomes more resistant to a subsequent severe insult. This means that as long as the damaging stimulus remains sublethal, the tissue will emerge in a strengthened state to defend from further harm. According to Darwin this process might have developed evolutionary to increase cell survival within specialized tissues in response to temporal shortages of nutrient supply and repetitive noxious stimuli.

The phenomenon of preconditioning was first described in a pioneering paper by Murry and colleagues in 1986, discovering that brief episodes of coronary artery occlusion (inducing sublethal ischemia) interspersed with 5-minute periods of reperfusion (restoration of blood flow) paradoxically resulted in 75% infarct size reduction in dogs (101). The authors termed this myocardial adaptation ischemic preconditioning (IPC), due to the fact that it is induced by repetitive periods of subcritical ischemic events. Since then, IPC has been confirmed in almost all species, including mouse, rat and rabbit (55, 89, 150), as well as domestic animals like sheep and swine (14, 131), and indirectly in man (29, 33, 167). The preconditioning phenomenon or reducing ischemic injury is established for the heart as well as for a number of other organs including the brain, small intestine, lung, liver and kidney (90, 109, 102, 79, 61). Besides direct preconditioning where the target organ is exposed to brief ischemia prior to prolonged ischemia, remote (inter organ) ischemic preconditioning was also shown to confer protection on distant organs without direct stress to the organ (121).

During the last two decades, extensive research has been conducted towards the understanding of the mechanisms by which IPC possibly prevents myocardial infarction in the experimental setting. A fundamental finding was that preconditioning is associated with two forms of protection: a first window of protection occurring immediately after the preconditioning stimulus accompanied with a strong protection but just lasting approximately 2-3 hours (73, 74), followed 12-24 hours later by a second (delayed) window of protection that induces less protection but lasts approximately 3 days (8, 80). Moreover, numerous endogenous triggers, signaling pathways and mediators have been controversially discussed, such as activation of adenosine, α-adrenergic, opioid or bradykinin receptors, signal transduction via protein kinase C, tyrosine kinases or mitogen-activated protein kinases, and induction of cardioprotection through opening of ATP-dependent potassium (K_{ATP}) channels or release of reactive oxygen species (reviewed in (39)).

Besides gaining scientific knowledge, the ultimate goal of these investigations was to mimic the preconditioned state and its benefits. A multitude of alternative stressful stimuli, including oxidative (hypoxia), mechanical (stretch), electrical (rapid pacing), chemical (ionic) and thermal (hypothermia) stressors can induce the same early and late protective response in cardiac tissue (153, 139, 111, 95, 126). But the probably best way to elicit protection will be the use of pharmacological agents instead of stressors. Various therapeutic drugs have been identified to evoke cardiac preconditioning, encompassing functions as G protein-coupled receptor agonists, K_{ATP}- channel openers, activators of PKC, and sodium/hydrogen exchange inhibitors (reviewed in (31)). However, most of them are associated with side-effects such as occurrence of hypotension, arrhythmias or possible carcinogenic effects. Besides these pharmacological treatments, volatile anesthetics as another class of compounds have also been shown to reduce infarct size to an extent similar to that observed following IPC. Their clinical use in preconditioning therapies is particularly promising because of the long-term experience clinicians have in their administration as well as their favorable safety profile.

1.1.2 Cardioprotection using volatile anesthetics

1.1.2.1 Volatile anesthetics exhibit deeper properties

General anesthesia is administered each day to thousands of patients worldwide, exhibiting the characteristic to induce unconsciousness, to relax the musculature and to control pain. A large number of drugs are available to the modern anesthetist to produce general anesthesia, from intravenously administered hypnotics to halogenated vapors (volatile anesthetics) and gaseous agents such as xenon. But the effect of anesthetics is not limited to the desired short-term action in the operating room to allow surgery on patients. Especially volatile anesthetics have long been known to provide some protection against the effects of cardiac ischemia and reperfusion. Already in 1969, infarct-reducing properties were reported for the volatile anesthetic halothane during myocardial ischemia in the canine heart (142). Several other experimental studies further demonstrated that pretreatment with volatile anesthetics improved left ventricular systolic function (155), reduced dysrhythmias and improved contractile function (15), and decreased myocardial oxygen utilization (16).

The cardioprotective mechanisms reported in these studies might result from the cardiac depressant effect of volatile anesthetics which decreases myocardial oxygen demand and thus may indirectly improve myocardial oxygen balance during ischemia. But experimental research has clearly shown that volatile anesthetics also directly protect from ischemic myocardial damage. In 1997, three independent working groups provided first evidence that isoflurane directly preconditions myocardium against infarction, and that cardioprotection was conducted via activation of K_{ATP} channels (19, 71, 24). These findings suggest that volatile anesthetics mimic the cardioprotective effect of IPC, and in turn led to the adaption of the term anesthetic preconditioning (APC). Since then major interest arose to study the preconditioning effect of anesthetics.

A large amount of data using *in vitro* studies and *in vivo* animal experiments has been produced dealing with cardiac preconditioning by anesthetics. Today we know that nearly all halogenated volatile anesthetics (halo-, iso-, sevo-, des- and enflurane) protect the ischemic myocardium by preconditioning. Our working group actually could show that even the noble gas xenon induces cardioprotection in a preconditioning manner (158). Multiple different intracellular signaling

pathways have been investigated, encompassing triggers which initiate the cardioprotective signal, mediators that forward the signal during ischemia and end-effectors that finally render the myocardium resistant to cell death. But in contrast to the obvious cardioprotective effects reported from experimental studies, the benefits of APC in clinical situations are still a matter of debate.

1.1.2.2 Anesthetic preconditioning versus myocardial infarction in man

Myocardial infarction is the clinical term for a heart attack and is caused by occlusion of the coronary artery for example by a blood clot, resulting in the partial or total blockage of one of the coronary arteries (myocardial ischemia). When this occurs, the myocardium does not receive enough oxygen (ischemia-injury). A mild ischemia leads to first cellular dysfunction, but the heart muscle may recover its original state. However, severe ischemia results in necrosis and finally causes permanent damage as the heart muscle dies. When ischemia is stopped by the restoration of blood flow, a second series of harmful events produce additional reperfusion-injury. Factors like older age, tobacco smoking, diabetes, high blood pressure, obesity, chronic kidney disease, heart failure, excessive alcohol consumption, the abuse of drugs, and chronic high stress levels additionally enhance the risk for myocardial infarction (114). Ischemia-reperfusion injuries are thus a common complication in medicine even in non-cardiac surgeries. It is interesting to note that during non-cardiac surgeries of patients with high risk of myocardial infarction, the recent American College of Cardiology/American Heart Association Guidelines recommend the use of volatile anesthetics for maintenance of general anesthesia (44).

The most commonly used inhalational anesthetics are desflurane and sevoflurane, which gradually replace isoflurane as the leading volatile for human use. Their cardioprotective properties during coronary surgery were already revealed several years ago (30). Recent data from a meta-analysis of randomized clinical trials indicated that the choice of the anesthetic regimen based on administration of volatile anesthetics is associated with a better outcome after cardiac surgery (82). But whereas the volatile anesthetics regimen continuously gains clinical evidence, the phenomenon of APC remains controversial in cardiac surgery. Despite the fact that the concept of APC offers the opportunity to improve the tolerance of the myocardium to ischemia-reperfusion events, like they are predictable in cardiac

and vascular surgery, neurosurgery, and transplant surgery, its application remains controversial.

The first study designed to assess the clinical relevance of APC investigated isoflurane-induced preconditioning in patients undergoing elective coronary artery bypass graft (CABG) surgery. It was shown that administration of isoflurane (after the onset of cardiopulmonary bypass (CPB) via a 5-minute exposure to 2.5 MAC isoflurane followed by a 10-minute washout) before aortic cross-clamping resulted in less postoperative release of creatine kinase MB and troponin, both biomarkers for acute myocardial infarction (11). So far, five clinical studies were designed to verify the preconditioning properties of the new volatile anesthetics sevoflurane and desflurane. In all cases, the cardioprotective effect was assessed by biochemical markers in patients undergoing CABG. The first study demonstrated a preconditioning effect for sevoflurane using 2 MAC administration during the first 10 minutes of CPB (63). Four years later, cardioprotective effects following sevoflurane-preconditioning were negated, using 1 MAC sevoflurane applied for 15 minutes followed by a 15 minutes washout before CPB (118). Sevoflurane-preconditioning in an interrupted manner (2x 1 MAC sevoflurane prebypass interrupted by a 10-minute washout phase) was then shown to be preferable toward continuous administration (1 MAC sevoflurane until initiation of CPB) (10). Recently, our working group underscores the important role of the cycles of the preconditioning stimulus for the protective effect. Whereas a single sevoflurane administration (5-minute exposure of 1 MAC sevoflurane followed by 10 minutes of washout) had no cardioprotective effect, two periods of sevoflurane significantly reduced cellular damage (46). Concerning desflurane, only one study exists that demonstrated evidence for preconditioning-induced cardioprotection in man (5 minute exposure of 2.5 MAC desflurane followed by 10 minute washout during established CPB) (94).

The current results of clinical APC studies in cardiac surgery show highly variable outcomes and fail to demonstrate a definite beneficial effect on post-ischemic myocardial performance (reviewed in (31)). This is mainly due to the fact that there is still no consensus on the method of administration of volatile anesthetics for myocardial preconditioning, including the time to begin administration, its duration, the dosage, and selection of volatile anesthetics. This clearly

demonstrates that much more (molecular) information is necessary to understand the intracellular events responsible for APC.

1.1.3 Desflurane-induced cardiac preconditioning

In the mid 90s the volatile anesthetics desflurane and sevoflurane were launched onto the German market, featuring low blood-gas partition coefficients which allow a more rapid emergence from anesthesia than isoflurane does. Isoflurane is still frequently used for veterinary anesthesia and is the best investigated anesthetic in APC, accounting for nearly 50% of the articles published between 1997 and 2009. While sevoflurane-induced preconditioning currently gains popularity, less is known about cardiac protection by desflurane preconditioning.

Infarct-limiting properties of desflurane were first described in 2000 (151). The experimental design was rather a treatment study than a preconditioning study as no memory phase before the index ischemia was embedded. Desflurane reduced myocardial infarct size in dogs *in vivo*, and the results further suggested that both sarcolemmal and mitochondrial KATP channels could be involved. This hypothesis was confirmed to some extend *in vitro* (56). They further provided evidence that stimulation of adenosine A1 receptor, α- and β-adrenoreceptors are involved in desflurane mediated cardioprotection. But again, myocardial tissue was only exposed to desflurane and not in a classical preconditioning manner with memory phase. The first desflurane-preconditioning (DES-PC) experiment was conducted in 2002, when comparing the potency of desflurane, sevoflurane, isoflurane and halothane to induce preconditioning in the rabbit myocardium (117). In this study (inhalation of the halogenated anesthetic for 30 minutes followed by a 15-minute washout phase), desflurane was the most effective agent at preconditioning the myocardium against ischemia.

In the last six years, molecular pathways of DES-PC were investigated by deducing targets from already known signaling in IPC. In this context, our working group showed in rodents that DES-PC does not depend on tyrosine kinase activation (38), but is mediated by protein kinase C (PKC) and extracellular-regulated kinases (ERK) through phosphorylation of PKC-ε and ERK-1/2 (152). Further *in vivo* studies revealed that DES-PC is mediated by nitric oxide and in parts by activation of mitochondrial large-conductance calcium-activated K^+-channels via protein kinase A (125, 141). Recently, DES-PC induced cardioprotection was shown to be

abolished by the specific β2-adrenoreceptor blocker ICI 118,551 (84). *In vitro* experiments provide evidence that DES-PC protects isolated rat cardiomyocytes from oxidative stress-induced cell death via stimulation of reactive oxygen species production (135). In summary, only fragments are known regarding the overall alterations responsible for the progression of the preconditioning signal.

1.2 Cardiovascular proteomics

The social, economic and human costs of cardiovascular diseases continue to escalate. Predicting cardiovascular risk on the one hand and designing new prophylactic-cardioprotective strategies on the other hand are therefore the main challenges of modern cardiovascular medicine. Gene therapy has been appreciated as the future of medicine but becomes subordinate as the *Human Genome Project* has reinforced the importance of the study of proteins. Classical approaches target candidate proteins as being potentially involved in the pathology of cardiovascular disease and aim to test hypothesis-based on previously reported data. The application of proteomics to cardiovascular diseases like ischemia-reperfusion injury creates a renaissance that allows understanding complex systems and pathologies at a global level.

1.2.1 Brief history of proteomics

Proteins are the final products manufactured in living cells according to the blueprint contained in the genome, but were for a long time ignored to play a major role in life due to the boom in genome research. However, soon after the conclusion of the genome project most efforts in biochemical research were focused on the study of “the protein complement of the genome”. But it was not until 1994 that the former PhD student Marc Wilkins was looking for an alternative to this phrase, and introduced the term proteomics at the first Siena 2-D Electrophoresis meeting.

In the beginning, proteomics implied the integrated study of the entire sum of all proteins produced by an organism or cell or tissue, constricted to a defined time point, particular condition and selected circumstance in order to set up a map of the proteome. This concept of a global protein analysis to set up an inventory of

proteins was already proposed 40 years ago (70). But progression in biochemical technologies has created a renaissance toward understanding complex proteomes at a global level, thus allowing an expanded experimental view. Most notably were following three developments:

1. Improvements in protein separation techniques, especially regarding two-dimensional gel electrophoresis and high-resolution liquid chromatography.
2. Refinements in mass spectrometry, in particular the implementation of the soft ionization methods electrospray ionization and matrix-assisted laser desorption/ionization, which markedly enhanced the ability to analyze biomolecules.
3. Development of bioinformatics tools such as databases that catalogue sequences from large-scale genome research, or search engines that query these databases via the Internet.

Today the scope of proteomics encompasses the identification and quantification of proteins, characterization of post-translational modifications and protein-protein interaction, but is most commonly applied to comparative approaches.

1.2.2 Methodological aspects of comparative proteomics

In comparative proteomic approaches, the investigator does not preselect the proteins to be examined, but makes use of high sensitive protein separation technologies to search for changes in any proteins that occur in control-case studies. Two-dimensional gel electrophoresis (2-DE), mass spectrometry (MS) and bioinformatics tools are still the key elements of comparative proteomics.

In the early 1970s, the pioneers of 2-DE immediately recognized the potential use of combining isoelectric focusing (IEF) with sodium dodecyl sulfate polyacrylamide gel electrophoresis (SDS-PAGE) to study multiple proteins at the same time (70). Shortly after, O'Farrell and Klose independently adopted the 2-DE technique for the simultaneous analysis of cellular proteins (75, 106), and made the use of 2-DE gels an attractive method of protein separation. As the name implies, the system separates proteins according to two distinct physicochemical properties, resulting in high resolution power for sample separations.

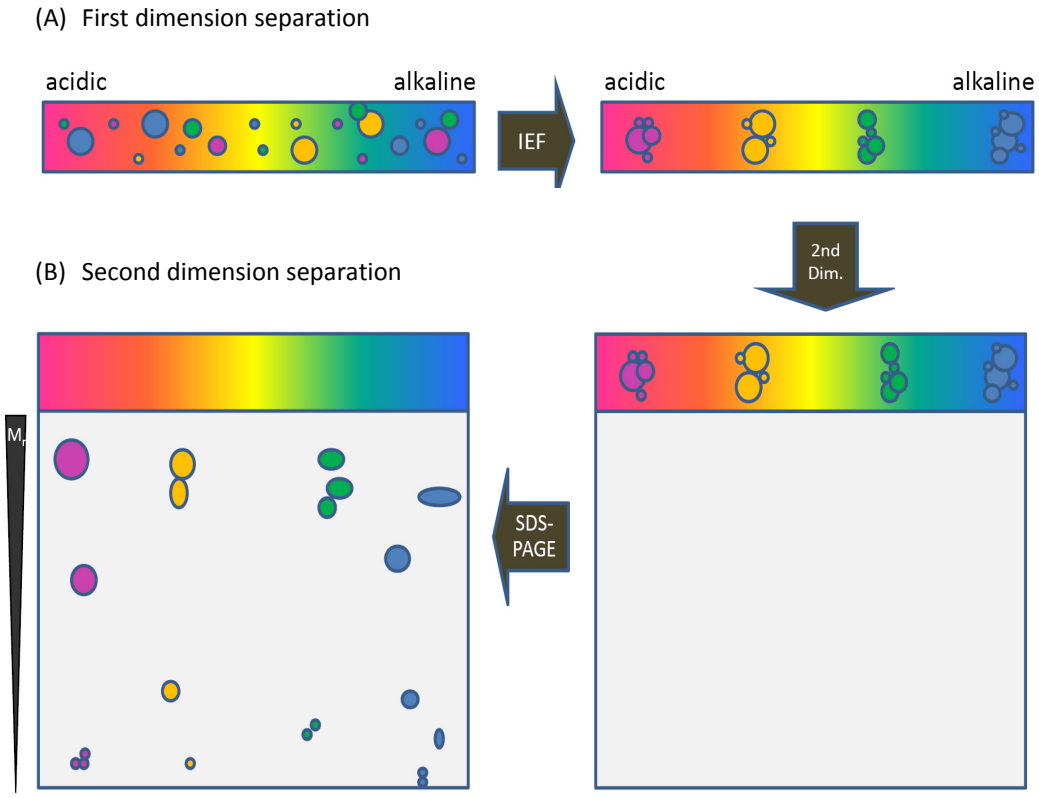

Figure 1.1: Schematic illustration of IEF and SDS-PAGE as part of 2-DE. In a pH gradient and under the influence of an electric field, a protein will move to the position in the gradient where its net charge is zero. This is the focusing effect. (B) After IEF, SDS-PAGE is used to separate the protein sample according to the molecular weight in the second dimension.

During the first dimension, IEF, proteins are separated on the basis of their ionic character via an ampholyte pH gradient and are allowed to migrate to their respective isoelectric points (*pI*) in the gel (Figure 1.1A). The *pI* is the specific pH at which the net charge of the protein is zero. In the second dimension, the IEF gel is subjected to a SDS-PAGE gel, and proteins are separated on the basis of their molecular weight (Figure 1.1B). This orthogonal separation results in a 2-DE pattern typically in form of protein spots where each spot potentially corresponds to a single protein species in the sample. In the last 30 years, numerous improvements finally led to its ability to display thousands of proteins simultaneously and differentially, including refinements of ampholytic technology, the introduction of a variety of staining methods, and the establishment of image capture devices and image analysis software to finally represent the pattern of 2-DE gels. Besides being currently the most powerful protein separation technique, a comparative 2-DE approach is only meaningful when the resolution and reproducibility of the gels are high-quality.

1.2.2.1 The problem of proteomic coverage

The human catalog of protein-coding genes was actually scaled down to only 20.500 rather than the 100.000–150.000 proteins we were once told to expect (3). But the respective proteome is most complex due to alternative splicing and post-translational modifications. Subcellular localization and interaction partners additionally influence protein abundances in the proteome so that the number of proteins expressed at a given time under defined biological conditions is likely to be in the range of 10^6 orders of magnitude for cells and tissues, ranging from several million copies for high-abundant proteins to a few copies for low-abundant proteins (27). Thus the principal goal for a global proteomic analysis of a complex system like the heart is mandatory to elicit the maximum amount of information on the investigated proteins.

In general, 10.000 proteins can be resolved on a large-format (46 x 30 cm) 2-DE gel (76), but difficulties in handling such large gels plus the high consumption of protein sample preclude their routine use for comparative analyses. In practice, only a subset of the expressed proteins can be displayed by 2-DE using standard wide-range gels (18 cm IPG strips pH 3-10/ 20 x 20 cm SDS–PAGE gels). It is therefore preferable to carry out pre-fractionation steps to reduce sample complexity to access all expressed proteins at once to the greatest possible extent. In most instances it is even crucial to enrich and visualize low-copy number proteins. Depending on the chosen fractionation technique, utilizing properties of protein classifications like subcellular localization, *pI* and/or M_r, solubility and specific functional characteristics, additional information about the topology of the proteins can be obtained.

A survey of the literature reveals that proteomic analyses are mostly performed using pH 3-10 and 4-7 IPG gels for first dimension separation. On the contrary, alkaline proteins (*pI* > 8) are infrequently analyzed even if they represent almost 50% of the total predicted proteome in organisms (Figure 1.2). This is due to the fact that IEF of alkaline proteins still seems to be a challenging job because of horizontal and vertical streaks, detergent smear and poor protein transfer from the first to second dimension.

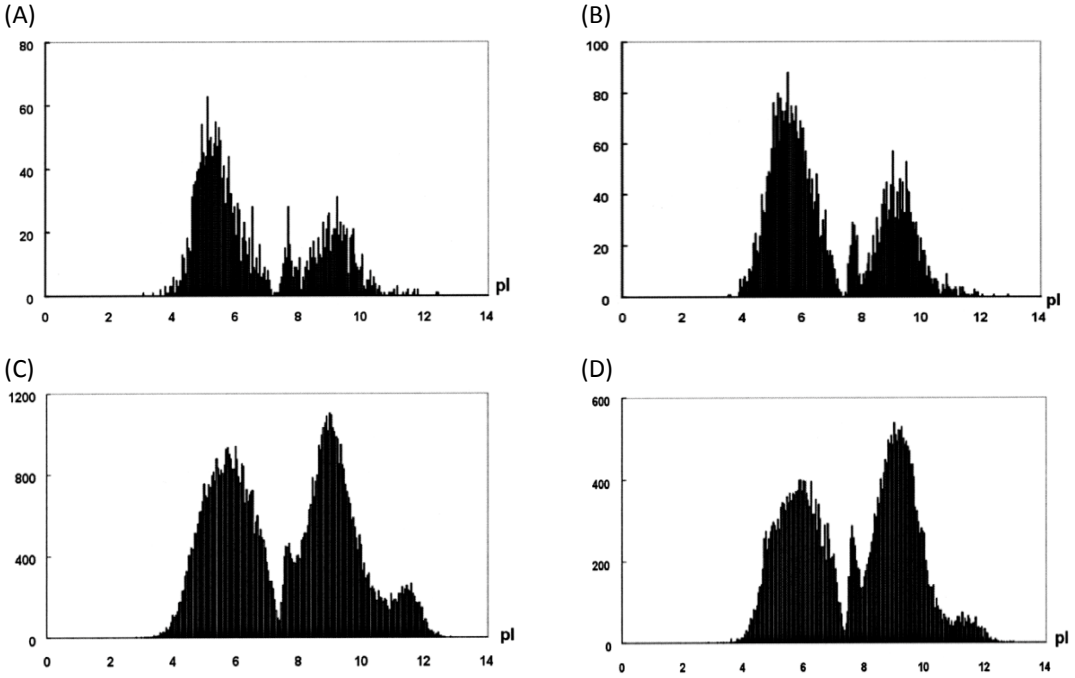

Figure 1.2: Histograms of *pI* distributions for predicted proteomes. (A) *Archaeoglobus fulgidus* (Achaea, 2420 proteins); (B) *Escherichia coli* (bacteria, 4279 proteins); (C) *Homo sapiens* (animal, 27 941 proteins); (D) *Oryza sativa* (plant, 83 159 proteins). The multi-modality character is demonstrated by *pI* values ranging from 3 to 13 with two main accumulations in the range from *pI* 4 to 7.8 and 7.9 to 10.5, and a third small peak around *pI* 11. [Figure modified from Wu *et al*., 2006 (164)].

The analysis of alkaline proteins is not a weakness of 2-DE but rather implies a "streak business" that can be overcome for the most part by different optimization steps (49, 108, 50, 48, 59, 66). Strategies include:

- use of zoom-range pH gradients
- anodic cup-loading sample application
- shortening IEF duration
- addition of a DTT wick to replenish reducing agent at the cathode
- use of an alternative reducing agent such as organic disulfides.

All these improvements were mainly applied for setting up reference maps of diverse organisms, carried out for *S. melliferum* (26), *H. influenza* (45), *B. subtilis* (107), HeLa cells (54), human placental mitochondria (85), adipose tissue (28) and colon crypt (87) as well as barley (5) and wheat seeds (21). The only comparative proteome analyses that especially addressed basic proteins were conducted for *E.coli* (154) and *T.cruzi* life forms of epimastigote and trypomastigote stages (92). Reports on comparative 2-DE analysis of cardiac proteomes have not focused on basic proteins so far.

1.2.2.2 Comparative quantification of protein species from gels

To analyze spot pattern the gels must be digitized, converting the raw pixel values into optical density (OD). The algorithms of 2-DE analysis software measure the amount of protein present in each spot using the relative volume [%Vol.]. Measuring the protein quantification values this way has the advantage of being more robust and reproducible when calculating protein expression variations. Statistical analyses of the spot volumes between populations of gels allow analyzing variations in protein expression among treatment groups. However, when comparing five commercially available programs using 18 replicate gels of a rat brain protein extract, the results demonstrated that an accurate, unbiased, and rapid gel analysis is still a major bottleneck (22). For this reason, a careful investigation of data reproducibility should be carried out to avoid misinterpretation of protein expression changes.

1.2.2.3 Mass spectrometric protein identification

Although the technology to separate proteins by 2-DE has existed since the 1970s, the only methods available to identify the separated proteins at the time was N-terminal sequencing by Edman degradation or immunoblotting. Because the Edman degradation proceeds from the N-terminus of the protein it fails if the N-terminal amino acid has been modified due to post-translational modifications. Western blotting on the other hand is presumptive and requires the availability of a suitable antibody, and the confidence of the identification can be limited by problems with the specificity of the antibody. These limitations were overcome by technical developments in mass spectrometry (MS) instrumentation in the 1990s. With the introduction of ionization techniques suitable for biomolecules, the group around Fenn (electrospray ionization, 1985), Tanaka and co-workers (liquid matrix method of laser desorption ionization, 1988) and Karas & Hillenkamp (crystalline matrix-assisted laser desorption/ionization, 1988) opened a new era in protein analysis (68, 162, 147). In nowadays proteomics, the soft ionization techniques electrospray ionization (ESI) and matrix-assisted laser desorption/ionization (MALDI) are the ionization techniques used for protein and peptide identification.

1.2.3 The heart proteome

In the mid 90s, extensive research was conducted to generate 2-DE databases for heart proteins, with the aim to offer descriptive information accessible via the World Wide Web. The databases “HP-2DPAGE” (64), “HEART-2DPAGE" (119) and “HSC-2DPAGE” (40) were established on the basis of human, rat, dog and mouse ventricle proteins. New proteomics data have continuously been added to the databases. At present, the proteome map of the human heart represents 2683 spots with about 400 identifications from 110 unique proteins (160). The identified proteins were found to be associated with numerous types of processes, functions and components. Interestingly, the vast majority of the proteins identified (from the human heart left ventricle) are mitochondria-associated and, surprisingly, relatively few are associated with what would perhaps be expected for proteins from the heart (such as muscle contraction, heart regulation, *etc.*). Figure 1.3 illustrates the “top ten” associations for the mentioned categories in the human heart.

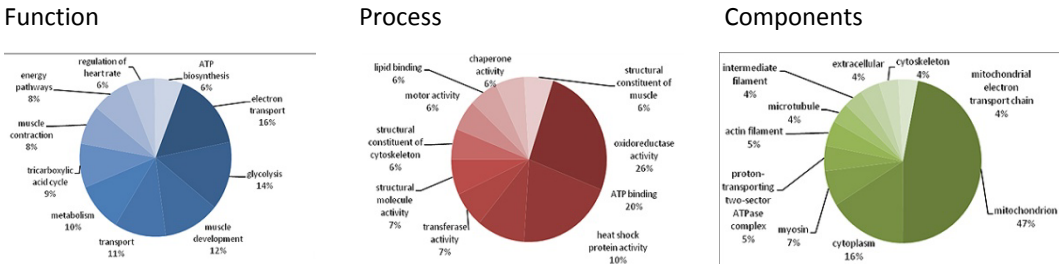

Figure 1.3: Functions, processes and components in the human heart proteome. 110 left ventricle proteins were categorized into 97 types of process, 144 types of function and 54 types of component using Gene Ontologies (GO). Charts adapted from Westbrook *et al.* (2006).

The rodent 2-DE proteome map currently consists of 1163 protein spots. Depending on their intracellular localization these proteins were assigned to seven different compartments: mitochondria, cytosol, nucleus, sacromere and cytoskeleton, extracellular, multiple subcellular localizations, and other (including Golgi, membrane, peroxisomal and endocytic vesicle). The majority of the identified proteins was mitochondrial (34%), and predominantly identified as metabolic enzymes. They represent multiple pathways with >90% coverage for enzymes involved in glycolysis and the Krebs cycle, oxidative phosphorylation and fatty acid metabolism (124).

1.2.4 Cardiac preconditioning enters proteomics

Several years ago, proteomic studies started focusing on ischemia-reperfusion (134, 129, 130, 161, 166, 43). These approaches provided an overall assessment of the cellular response to ischemia-reperfusion (IR) injury and identified a pronounced subset of enzymes and protein complex subunits. The majority of changes were observed to proteins from four functional groups: (i) the sarcomere and cytoskeleton; (ii) redox regulation; (iii) energy metabolism and (iv) stress response. Recently, cardiac preconditioning entered the era of cardiovascular proteomics. Ten studies were conducted to clarify the underlying mechanisms of ischemic tolerance in the heart so far (Table 1.1) but concerning anesthetic-induced preconditioning, published data is still limited to one proteomic study (41).

Table 1.1: Proteomic studies investigating cardiac preconditioning.

Species	Experimental approach	Major experimental findings	Reference
rat	Mito-Phosphoproteome analysis of ISO-PC; Langendorff model	45 differentially phosphorylated proteins. Categorization: Oxidative Phosphorylation, Krebs cycle, fatty acid metabolism, transport and chaperones	(41)
	PC with ethanol, PKC-epsilon activator and inhibitor	ALDH-2 activation correlates with reduced ischemic heart damage	(20)
	IPC and PC with diazoxide and insulin; Langendorff model	No IPC-mediated changes, but IPC inhibits MPTP opening in mitochondria	(23)
	PC with PKC-epsilon activating peptide in adult and aged hearts; Langendorff model	10 differentially expressed spots in aged but not adult hearts; 1 protein identification: F1-ATPase β-subunit	(78)
	Pharmacological PC with resveratrol; Langendorff model	Identification of several PC-associated proteins in context to IR	(12)
	Biomarker discovery in blood samples; IPC and RIPC *in vivo*	2 differentially regulated proteins: albumin and LRRG03	(83)
Mouse	Phosphoproteome analysis; IPC and PC with GSK-3 inhibitor; Langendorff model	Identification of 4 common protein levels/posttranslational modifications: increased cytochrome c oxidase subunits Va and VIb, ATP synthase-coupling factor 6, and cytochrome b-c1 complex subunit 6; decreased cytochrome c	(163)

Table 1.1 continued: Proteomic studies investigating cardiac preconditioning.

Species	Experimental approach	Major experimental findings	Reference
rabbit	Mitochondrial proteomics of IR and IPC hearts; Langendorff model	25 proteins differentially expressed in IR compared with control and IPC. Categorization: Krebs cycle; α-keto acid dehydrogenase; respiratory chain; mitochondria membrane channels, β-oxidation; proliferation and cytoskeleton	(72)
cell culture	Phosphoproteomic analysis of diazoxide-induced PC; adult rat ventricular myocytes	Identification of 6 proteins with different abundance	(86)
	PC with diazoxide and adenosine; isolated ventricular myocytes	19 protein identifications. Characterization: mitochondrial energetic including subunits of Krebs cycle enzymes and complexes of Oxidative Phosphorylation	(4)

1.3 Aim of the study

The cardioprotective benefits of anesthetic-preconditioning are well described but the phenomenon is still largely unexplained on the molecular level. Current research on the molecular mechanisms of DES-PC has been limited to the examination of factors or pathways already believed to contribute to cardioprotection. A proteomics approach would allow the evaluation of global changes in protein expression by focusing on several biological parameters and molecules at a time.

The classical combination of 2-DE and MS was chosen to study the impact of desflurane-induced preconditioning on the heart proteome in a time-course analysis. The specific aims of the study were as follows:

- Establishing protein extraction protocols and 2-DE the separation for the comparative analysis of proteins from rat heart tissue samples.
- Optimizing 2-DE analysis of alkaline proteins.
- Determining protein expression changes during the exposure to and recovery from desflurane-preconditioning *in vivo*.
- Mass spectrometric identification of protein spots with altered expression.

2 Material and Methods

2.1 Animals

The animal experiments were performed in accordance with the regulations of the German Animal Protection Law (Tierschutzgesetz, Germany) and were approved by the Bioethics Committee of the District of Duesseldorf, North Rhine-Westphalia, Germany. Male Wistar rats were obtained from the Animal Facility (Tierversuchsanlage) of the University Hospital in Duesseldorf. They received standard feed *ad libitum*, free access to water and human care. Animals had a 12:12 hour light-dark cycle and were kept under temperature controlled environmental conditions and constant humidity before entering the study.

2.1.1 Surgical preparation

Surgical preparation was performed like described in Toma *et al.* (152). Anesthesia of male Wistar rats weighting 250-300 g was induced by an intraperitoneal injection of S (+) -ketamine (150 mg/kg) (Pfizer Pharma, Berlin, Germany). After tracheal intubation, the lungs were ventilated with oxygen-enriched air and a positive end-expiratory pressure of 2–3 cm H_2O. Respiratory rate was adjusted to maintain partial pressure of carbon dioxide within physiologic limits. Body temperature was maintained at 38°C by the use of a heating pad. The right jugular vein was cannulated for infusion, and the left carotid artery was cannulated for measurement of aortic pressure. Anesthesia was maintained by a continuous infusion of a saline solution containing α–chloralose (Sigma-Aldrich, Taufkirchen, Germany). A lateral left sided thoracotomy followed by pericardiotomy was performed and a ligature using 5–0 prolene (Ethicon, Norderstedt, Germany) was passed below the main branch of the left coronary artery. The ends of the suture were threaded through a propylene tube to form a snare. After surgical preparation rats were left untreated for 30 minutes to allow for recovery before starting the preconditioning protocol.

2.1.2 Preconditioning protocol

The study protocol of desflurane-induced preconditioning is shown in Figure 2.1. Desflurane was purchased from Baxter Deutschland GmbH (Unterschleissheim, Germany). 22 rats were randomly assigned to one of the six groups and either

received 1 MAC (minimum alveolar concentration) desflurane (DES-PC groups) or did not undergo any further treatment (control groups). To investigate time-dependent protein changes, the hearts were excised at four different time points during DES-PC and at two different time points in baseline (Figure 2.1). A number of 3-5 animals per treatment is usually chosen for proteomic analyses due to animal experiments constraints.

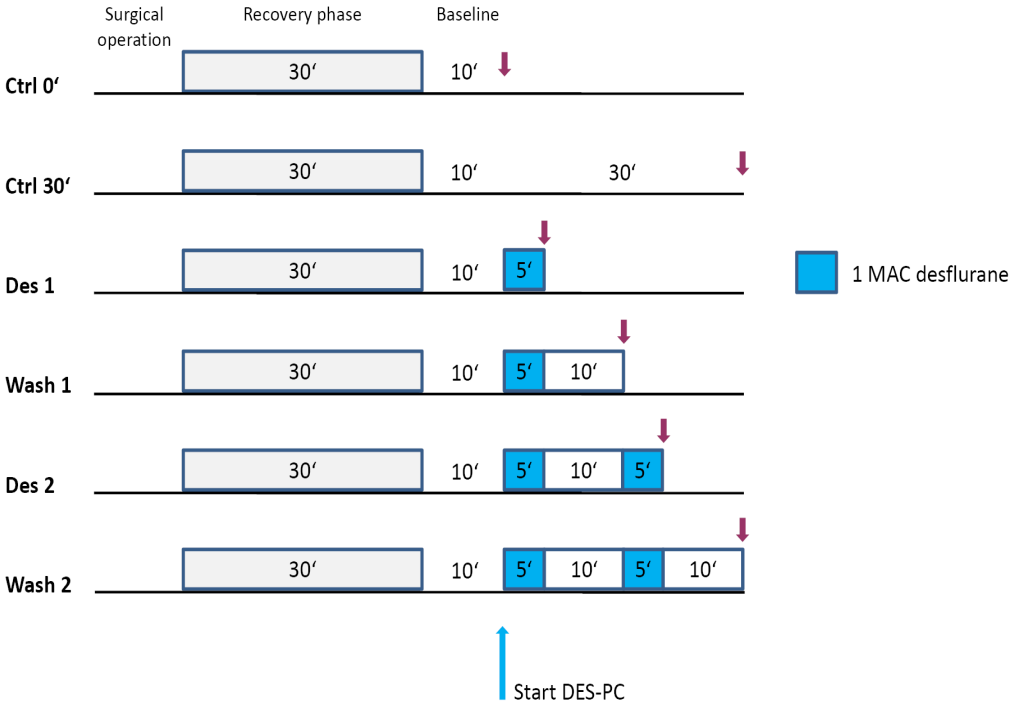

Figure 2.1: Experimental protocol of DES-PC. After surgical preparation and recovery time, animals were aligned at baseline levels. Myocardial tissue samples were extracted at indicated points (↓) during DES-PC. Control samples were taken at the beginning and the end of the scheduled DES-PC protocol, respectively.

Ctrl 0' group (n = 3): hearts were excised at the starting point (t = 0 min [0']) of the preconditioning protocol.

Ctrl 30' group (n = 4): hearts were excised 30 min after the scheduled starting point of DES-PC (t = 30 min [30']), corresponding to the end of the preconditioning protocol.

Des 1 group (n = 4): rats received 1 MAC desflurane for one 5-minute period before excision of the hearts (total treatment phase: 1x5 minutes PC = 5 minutes).

Wash 1 group (n = 4): rats received 1 MAC desflurane for one 5-minute period with one 10-minute washout phase before excision of the hearts (total treatment phase: 1x5 minutes PC + 10 minutes washout = 15 minutes).

Des 2 group (n = 4): rats received 1 MAC desflurane for two 5-minute periods interspersed with one 10-minute washout phase before excision of the hearts (total treatment phase: 2x5 minutes PC + 1x10 minutes washout = 20 minutes).

Wash 2 group (n = 4): rats received 1 MAC desflurane for two 5-minute periods, interspersed with one 10-minute washout phase and one final 10-minute washout phase before excision of the hearts (total treatment phase: 2x5 minutes PC + 2x10 minutes washout = 30 min).

After heart excision, the tissue was shock-frozen in liquid nitrogen and stored at -78°C.

2.2 Chemicals and equipment

For the preparation of buffers and solutions, chemicals with high quality such as analytical grade (*p.a.*) and water of high purity from a Millipore system (Milli-Q) was used. Chemicals were purchased from Sigma-Aldrich (Taufkirchen, Germany), Carl Roth (Karlsruhe, Germany) or Merck (Darmstadt, Germany) if not otherwise stated.

The equipment and consumables for isoelectric focusing (*IPGphor 3*, *Manifold*, *Multiphor*, *EPS 3501 XL power supply*, *Immobiline DryStrip Kit*, *Reswelling tray*, *Immobiline DryStrips and IPG buffers*) and quantitative gel analysis (*ImageScanner*, *LabScan* and *ImageMaster 2D Platinum*) were purchased from GE Healthcare (Freiburg, Germany).

2.3 Tissue homogenization and protein extraction

For tissue disruption, the method of mechanical homogenization was chosen as it is well-established in the laboratory of the Department of Anesthesiology. Briefly, shock-frozen tissue was pulverized between two nitrogen-cooled metal blocks (Dick, Deizisau, Germany), suspended in the respective lysis buffer and homogenized using a motorized blender with different shear force adaptors (IKA,

Staufen, Germany). In general, sample preparation should be kept as simple as possible to avoid protein loss, but additional steps may improve the quality of the final 2-DE results. For this reason, different protocols from a literature search were investigated to work out a suitable lysis buffer for proper protein extraction prior to IEF. Ideally, the procedure will result in complete protein solubilization and disaggregation. Subsequent protein determination was conducted either according to Lowry or Bradford (chapter 2.4), depending on the compatibility of buffer components used for solubilization. In the end, samples were either directly used for first dimension gel electrophoresis separation or stored at -78°C.

2.3.1 One-step protein extraction in IEF-buffer

The tissue powder was directly dissolved in denaturing isoelectric focusing (IEF) buffer [8 M urea; 4% CHAPS; 40 mM DTT]. Mechanical homogenization was conducted at room temperature to avoid urea crystallization. The homogenate was incubated for 1h at room temperature with occasional vortexes. After centrifugation at 1000 *g* and 20°C for ten minutes the supernatant was twice centrifuged at 16000 *g*, 20°C for 20 minutes. Protein determination of the supernatant was performed by the Bradford method.

2.3.2 Two-step protein extraction in TCA/acetone

This procedure allows a selective separation of proteins from contaminating species such as salts, detergents, nucleic acids or lipids. The crushed heart tissue was suspended in TCA-buffer [10% (w/v) TCA with 0.3% (w/v) DTT in ice-cold acetone], homogenized keeping the sample on ice and further incubated at -20°C for two hours. After centrifugation at 16000 *g* at 4°C for 20 minutes the resulting pellet was washed twice with ice-cold acetone (80%) and finally dried at room temperature. At last proteins were resolved in IEF-buffer and remained at room temperature for at least one hour while shaking for full denaturation and solubilization. Protein quantification was determined using the Bradford protein assay.

2.3.3 Physiological protein extraction followed by TCA/acetone precipitation

Soluble proteins were extracted using a Tris-based homogenization buffer with increasing solubilization power, and subsequently precipitated with the aid of TCA and acetone. Shock-frozen tissue powder was dissolved in Tris-lysis buffer containing phosphatase and protease inhibitors [5 mM Tris base; 2 mM EGTA; 2 mM Na_3VO_4; 50 mM NaF; 0.2 µM okadaic acid; aprotinin, pepstatin A and leupeptin each 0.01% (w/v) in 500 mM Tris-HCl (pH 7.4)]. Sample homogenization was performed on ice to reduce protein degradation. After adding 1% (v/v) Triton X-100 to the sample, the extract was kept on ice for one hour with occasional vortexes and finally centrifuged at 16000 *g*, 4°C for 20 minutes. The resulting supernatant contained all soluble proteins. Protein concentration analysis was performed by the Lowry method. The subsequent precipitation step was also employed to prepare protein samples of defined concentration. Samples were incubated with 10% (w/v) TCA in 8 volumes (of sample volume) acetone (80%) for a minimum of two hours at –20°C. The precipitate was collected by centrifugation at 16000 *g* and 4°C for 45 minutes. The pellet was finally washed twice with ice-cold acetone (80%) and then air-dried to remove residual acetone.

2.3.4 Prefractionation of proteins with subsequent TCA/acetone precipitation

Prefractionation of cardiac proteins was conducted similar to the physiological extraction procedure (chapter 2.3.3), but in this case protein fractions of different solubilization degrees were kept separately. Briefly, tissue was resolved in Tris-lysis buffer as mentioned above and homogenate was centrifuged at 1000 *g* at 4°C for ten minutes. The supernatant containing the crude water-soluble fraction was centrifuged again at 16000 *g* 4°C for 15 minutes to clean up cytosolic proteins. The remaining pellet of the first centrifugation step was solubilized in Tris-lysis buffer that additionally contained 1% (v/v) Triton X-100. The sample was incubated for one hour on ice and afterwards centrifuged at 16000 *g* at 4°C for 15 minutes. The resulting supernatant contained the detergent-soluble fraction including membrane-associated proteins. The pellet was re-suspended in Tris/Triton X-100 lysis buffer to recover the particulate fraction. Protein concentrations were

determined by the Lowry protein assay and TCA/acetone precipitation was performed like described before.

2.4 Protein quantification

Protein quantification prior to 2-DE is crucial for ensuring that equivalent amounts of protein were compared between samples. Knowing the precise concentration of the protein extract is important as small changes in the amount of protein loaded onto the 2-DE gels will influence the protein pattern between matched groups. Thus, protein concentration in the extracts must be determined in a reliable manner. Due to several buffer components in the sample solutions, not every common protein assay could be applied. Therefore, protein samples resolved in Tris-lysis buffer were analyzed by the Lowry assay (91) whereas determination of proteins solubilized in IEF-buffer was performed by the Bradford method (13). In both cases, diluted samples were calculated against a BSA standard curve of known concentrations.

2.5 Two-dimensional gel electrophoresis

Animal samples were randomized for 2-DE to avoid systematic artifacts. To verify the data with a small number of replicate experiments (n=3/4) we factor experimental variations with a stringent threshold. Each organ was run in triplicate but not in batch to factor differences due to technical variations (i.e. 2-DE processing). In general, isoelectric focusing was performed in parallel for six samples, and two IPG Strips were run simultaneously during second dimension SDS-PAGE.

2.5.1 Protein solubilization prior to IEF

Besides proper protein extraction, optimal sample solubilization is absolutely essential to achieve a well-resolved 2-DE separation. The key feature of this preparation step is not only to solubilize proteins but also to keep them soluble during all steps of 2-DE. For this reason, several IEF-buffer compositions with different denaturants, detergents, reductants and solvents were tested.

Urea is used as denaturant and unfolds most proteins to their fully random conformation, with all ionizable groups exposed to solution. The use of thiorurea in addition to urea has been found to further improve solubilization, particularly for hydrophobic proteins (123, 97, 122). A nonionic or zwitterionic detergent is always included in the sample solution to ensure complete sample solubilization and to prevent aggregation through hydrophobic interactions. CHAPS is the most commonly used detergent but in the last years new zwitterionic detergents like ASB-14, ASB-16 and SB 3-10 have been developed, providing an alternative reagent for protein stability. DTT is frequently used to break disulfide bonds and to maintain the proteins in their fully reduced state during IEF. For the reduction of basic proteins, the use of hydroxyethyldisulfide (HED) is recommended (51). Furthermore, the use of isopropanol and glycerol in the IEF buffer was reported to improve resolution in the neutral and alkaline region of zoom-gels (59).

Stock solutions (Table 2.1) were prepared with traces of bromphenol blue and stored at -20°C. For isoelectric focusing, an appropriate volume of IEF-buffer (125 µl for 7 cm and 250 µl for 13 cm IPG strips) was applied to the sample. IPG Buffer and DTT or HED were freshly added to the solution, and where indicated supplementary isopropanol / glycerol. The protein sample was kept on a vortex (Scientific Industries, New York, USA) for at least 1 hour to ensure complete denaturation and solubilization before 2-DE separation.

Table 2.1: IEF buffer compositions.

Stock solution		
U	**TU**	**TUA**
8 M **U**rea	2 M **T**hiourea / 7M **U**rea	2 M **T**hiourea / 7 M **U**rea
4% CHAPS	4% CHAPS	2% CHAPS / 2% **A**SB-14
Add-ons		
0.5% (v/v) IPG Buffer pH 3-10, 4-7	40 mM DTT	10 % isopropanol /
or	or	5% glycerol
2% (v/v) IPG-Buffer pH 6-11	50 mM HED	

2.5.2 First dimension separation

Isoelectric focusing (IEF) is an electrophoretic method that separates proteins according to their isoelectric points (*pI*). IEF is performed with Immobiline DryStrip gels using a flatbed electrophoresis system.

2.5.2.1 Sample application, IPG strip rehydration, and IEF

Two different sample application methods are commonly used for IEF: in-gel rehydration and sample cup-loading. In-gel rehydration loading offers advantages like loading and separation of larger sample volumes as well as larger sample amounts and is therefore the most commonly used application method in 2-DE. Cup loading is generally recommended for analytical loadings (up to 100 µg protein) on alkaline or very acidic IPG strips. Furthermore, it is preferable for high molecular mass as well as hydrophobic proteins.

In-gel rehydration was chosen for isoelectric focusing of neutral-acidic proteins in pH range 4-7 gels. The solubilized protein sample was directly pipetted into the slots of the Reswelling tray. The IPG strips were inserted with gel side down into the grooves without trapping air bubbles, and covered with mineral oil to minimize evaporation and prevent urea crystallization. During overnight rehydration, proteins enter the IPG strip by absorption and are distributed over the entire length of the strip (passive rehydration). Prior to IEF, strips were briefly drained of excess mineral oil and transferred with gel side facing upwards into the Manifold tray (IPGphor) which was previously placed on the cooling unit of the electrophoresis system. Electrode wicks were soaked with 500 µl distilled water and blotted onto Whatman paper to ensure that they were damp but not excessively wet. The damp wicks were placed on each end of the strip, and the electrodes were fixed onto the paper wicks. IEF was started using the respective running conditions listed in Table 2.2.

IEF of proteins in basic IPG strips (pH 6-11) was performed using the cup-loading procedure which allows active sample application during IEF. The IPG strips were rehydrated in pure IEF buffer overnight using the Reswelling tray. The rehydrated strips were drained of excess mineral oil and transferred with gel side facing upwards into the DryStrip Kit placed on the cooling unit of the Mulitphor. Damp paper wicks and electrodes were adjusted before the sample cup bar was placed at the desired point of application (either near to the anode or the cathode). The

sample previously solubilized in 100 µl IEF buffer (maximum volume of cup) was applied into the positioned sample cups being properly covered with mineral oil. IEF runs were performed following the focusing conditions listed in Table 2.2.

Table 2.2: Focusing conditions for running IPG strips.

Strip length	pH interval	Voltage mode	Voltage [V]	Time [h]	IEF system
13 cm	**3-10 / 4-7**	Step and Hold	500	1:00	IPGphor
		Gradient	1000	1:00	
		Gradient	8000	2:30	
		Step and Hold	8000	3:00	
13 cm	**6-11**	Step	350	0:01	Multiphor
		Gradient	3500	1:30	
		Step and Hold	3500	4:00	
7 cm	**3-10 / 4-7**	Step	200	0:01	Multiphor
		Gradient	3500	1:30	
		Step and Hold	3500	4:00	
7 cm	**4-7$^{\$}$**	Step and Hold	300	1:00	IPGphor
		Gradient	1000	0:30	
		Gradient	2400	1:30	
		Step and Hold	2400	1:00	
7 cm	**6-11§**	Step	500	0:01	Multiphor
		Step and Hold	500	2:00	
		Gradient	3500	1:30	
		Step and Hold	3500	1:00	

IEF was performed at constant 20°C. The focusing conditions correspond to the guidelines of the manufacturer's protocol, except for IEF of cytosolic proteins in 7cm IPG strips pH 4-7$^{\$}$ and 6-11§. After termination of IEF, the IPG strips were either stored at -78°C or directly equilibrated for second dimension separation.

2.5.3 Second dimension separation

The second-dimension step, sodium-dodecyl sulfate polyacrylamide gel electrophoresis (SDS-PAGE), separates proteins according to their molecular weights (M_r).

2.5.3.1 Equilibration

Prior to second dimension separation, the IPG strips were blotted onto filter paper to remove excess oil. Equilibration to the SDS buffer system was performed in two steps, reduction and alkylation, each for 15 minutes with gentle shaking. Each IPG strip was incubated in 2.5 ml of an equilibration stock solution containing 50 mM Tris-HCl (pH 8.8), 6 M urea, 30% (v/v) glycerol, 2% (w/v) SDS and a trace of bromphenol blue, whereas 1% (w/v) DTT was added to the first, and 2.5% (w/v) iodoacetamide to the second equilibration step. The equilibrated IPG strips were rinsed with Milli-Q water, again blotted onto filter paper and finally dipped in electrophoresis buffer [25 mM Tris base; 192 mM glycine; 0.1% (w/v) SDS in Milli-Q water].

2.5.3.2 SDS-PAGE

Second dimension separation was performed by SDS-PAGE in vertical electrophoresis units (Bio-Rad Laboratories, Munich, Germany; or PEQLAB Biotechnologie, Erlangen, Germany) with a total acrylamide concentration of 10-12%, depending on the protein fraction investigated. The equilibrated IPG strips were placed upright on the top of the acrylamide gel surface and covered with heated (75°C) agarose-sealing solution [0.5% (w/v) agarose, traces of bromphenol blue in electrophoresis buffer], avoiding introduction of air bubbles. Prestained protein molecular weight marker (*Dual Color*, Bio-Rad Laboratories) dropped on a piece of filter paper was placed onto the separating gel next to the end of the IPG strip. The gel system was filled with electrophoresis buffer and proteins were separated for 2.5 hours, starting at 80 V for 15 minutes followed by 120 V until the dye front reached the bottom of the gel.

2.6 Protein staining

The final step in a gel electrophoresis experiment is the visualization of the proteins to evaluate the results of their separation. There exists a great variety of methods, each featuring pros and cons regarding their toxicity, sensitivity, linear range for quantitation and compatibility with mass spectrometry. Because the relative amount of a protein determined based on the intensity of the staining is used to analyze differential protein expression, the choice of the staining method has a great impact on the outcome of a differential analysis by 2-DE.

2.6.1 Silver staining

Silver staining is extremely sensitive with a detection limit as low as 0.1ng of protein per spot, and is widely used in 2-DE (36). However, due to its limited dynamic range (10- to 40-fold range), less repeatable procedure (subjective end-point of staining), and its partial compatibility with subsequent MS identification (despite any improvements avoiding cross-linkage), silver staining is rather unfavorable for the quantitative analysis of protein expression changes on 2-DE gels.

Silver staining was performed on the basis of Shevchencko's protocol published in 1996 (138). This protocol claims full compatibility with subsequent mass spectrometric analysis by omitting glutardialdehyde from the sensitizer and formaldehyde from the silver nitrate solution. All steps took place on a rocking platform shaker (*Duomax 1030*, Heidolph, Schwabach, Germany). First, the gels were fixed in 50% (v/v) methanol, 5% (v/v) acetic acid in Milli-Q water for 20 minutes, followed by two fixation steps each in 50% (v/v) methanol for ten minutes. After a washing step with Milli-Q water for ten minutes, the gel was sensitized by one-minute incubation in 0.02% (w/v) sodium thiosulfate and rapidly washed with three fast changes of Milli-Q water for 20 seconds. The gel was then submerged in 0.2% (w/v) silver nitrate solution and incubated for 20 minutes. The silver nitrate solution was discarded and the gel was rinsed three times with Milli-Q water for 20 seconds. Development was started with a staining solution containing 0.5% (w/v) sodium thiosulfate, 3% (w/v) sodium carbonate and 0.05% formalin. After the desired intensity of staining was achieved, developing was stopped by fast washing steps (3x20 seconds) with Milli-Q water and terminated with 5% (v/v) acetic acid. The gels were finally kept overnight in 1% (v/v) acetic acid.

2.6.2 Colloidal Coomassie staining

Coomassie Brilliant Blue (CBB) is a dye commonly used for the visualization of proteins in gels but is said to be 50-100-fold less sensitive than silver or fluorescent staining and therefore rarely used for the detection of proteins in analytical gel-based proteomic approaches (113). Several improvements of the well-known Coomassie protocol by Neuhoff and collegues (104) have been made to increase

the sensitivity of the CBB stain. In comparison to the others, the aluminum-based formula shows superior sensitivity that detects as low as 1 ng protein/band (37, 67).

Coomassie G-250 staining was performed on a rocking platform shaker. After second dimension separation, the gels were carefully washed three times with Milli-Q water each for ten minutes and afterwards incubated with Coomassie G-250 solution [0.02% (w/v) CBB G-250, 5% (w/v) aluminium sulfate-18-hydrate, 10% (v/v) ethanol, 2% (v/v) orthophosphoric acid] overnight. When staining procedure was completed, Coomassie G-250 solution was removed and the gels were briefly washed with Milli-Q water twice. Proteins were destained with destaining solution [10% (v/v) ethanol, 2% (v/v) orthophosphoric acid] for 60 minutes and finally rinsed with Milli-Q water to improve the color to background ratio.

2.6.3 Pro Q Diamond Phosphoprotein stain

The fluorescent stain ProQ was used to detect phosphorylated proteins at tyrosine, serine or threonine residues. The staining was performed according to the manufacturer's standard protocol (Molecular Probes, Eugene, USA). The gel was immersed in fixing solution [50% methanol, 10% acetic acid] and incubated with gentle agitation for 30 minutes. The fixation step was repeated overnight to ensure washout of residual SDS. Following three washing steps a 10 minutes, gels were stained with ProQ for 1.5 hours in the dark and destained by 3x30-minute washes using a solution containing 20% acetonitrile, 50 mM sodium acetate (pH 4.0). ProQ gels were scanned on a Typhoon 9400 variable mode imager (GE Healthcare, Freiburg, Germany) at 480V / 200 microns (excitation source 532 nm laser; emission filter 560 nm longpass).

2.7 Comparative 2-DE image analysis

For comparative proteome analyses, the Coomassie stained gels were digitalized using the flatbed ImageScanner and LabScan software (GE Healthcare, Freiburg, Germany). Converting gray density values into OD values was performed using the Kodak step tablet. Gels were scanned with blank filter type in transparent mode and a scanning resolution of 300 dpi. Spot identification, normalization and

matching were performed with ImageMaster (IM) 2D Platinum (GE Healthcare). Variations in protein expression among the treatment groups were calculated using descriptive statistics by means of overlapping measures as obtained by the software's integrated data analysis tools.

2.7.1 Gel image analysis

Spot registration was started with automatic detection, but manual intervention was conducted in cases where residual artifacts had to be deleted and wrongly registered spots to be edited. Normalization of the image was performed including background subtraction and noise filtering. Spot quantification was determined on the basis of the relative volume [%Vol.], representing the spot volume (integrated intensity above 75% of the spot height) divided by the total volume of all spots in the gel.

Matching was performed using 3-5 landmarks to achieve proper spot sets between gels. For the analysis of pH 4-7 gels, IM software version 6 was used to create a composite gel image that contains only representative spots of a population. The composite gel is a statistically derived, synthetic gel of a batch of matched gels and comprises only spots that appeared on at least two out of the three technical replicate gels per organ. Final matching of all composite images against a unique arbitrary reference image was carried out to link biological groups. Matching of pH 6-11 gels was performed with IM software version 7 that provides an improved matching algorithm. It combines the parameter-free matching algorithm with hierarchical population matching and allows more efficient comparisons without the use of composite gels.

For comparisons of protein expression between treatment groups, spot sets were analyzed using a special release of IM 2D Platinum 7.0 that allows the analysis of synthetic gels. Changes in spot volume were determined using the statistical descriptors *central tendency* and *dispersion*, which define the %Vol. interval for each spot set. In order to avoid type I errors (false positives), spot sets with overlapping differences between the treatment groups were ignored.

2.7.2 Evaluation of variability in dynamic protein expression

Technical variability can generally be minimized by the setup of standardized protocols but should, nevertheless, be taken into consideration in the interpretation of the results. Within a given group of homogenous animals using age, sex and genetic background matched rats, the major source of biological variation is the variation resulting from different genotypes and environmental factors. Determining the degree of both, technical and biological variability, allows setting a threshold for the reproducibility of the present 2-DE protocol. Differences in protein expression above this threshold can then be considered as real preconditioning-induced changes.

Protein samples were separated by 2-DE in triplicate and protein spots were detected and quantified using the ImageMaster algorithm. Variation analyses were performed with samples from the control 0' group (n=3). Thus, a total of nine 2-DE gels were obtained for each investigated subproteome [water-soluble/neutral-acidic (ws_4-7), water-soluble/alkaline (ws_6-11) and detergent-soluble/neutral-acidic (ds_4-7)].

2.7.2.1 Technical variability

The technical error inherent to the 2-DE procedure was investigated from pair-wise comparisons of one biological sample (organ #1n) using normalized volumes [%Vol.] of matched spots (intra-experiment analysis). The scatter plot function of the ImageMaster software allows assessing the relationship (correlation) between the spot values. On the basis of the best-fit line through the data points and the goodness-of-fit for this approximation gel similarities or experimental variations can be analyzed. Representative digital gel images and scatter plots are shown in Figure 2.2: **Evaluation of technical variability of 2-DE by regression analysis.** Representative 2-DE gels and scatter plots of the subproteome ws_6-11. (Left) Digital images of replicate gels from organ #1n of the control 0' group. The spot outline corresponds to the area from which the relative volume [%Vol] was quantified. (Right) Scatter graphs on logarithmic scale for the specified replicate gel (x-axis) and the reference gel (y-axis). Technical variations were compared between matched normalized spot volumes. Regression analysis yielded the best fit line, the correlation coefficient Corr and the number of matches (count). The pair-wise comparisons yield the following output values: (i) the number of matched spots corresponding

in the two gels (counts), (ii) the correlation coefficient *Corr* among the matching spot intensities and (iii) the regression equation of the best fit line. If matched spots have the exact same quantity, the spots will be plotted on a line with slope 1.0. Further, matched spots whose quantities differ between a pair of gel will result in correlation coefficients less than 1.0.

Digital 2-DE image Scatter plot

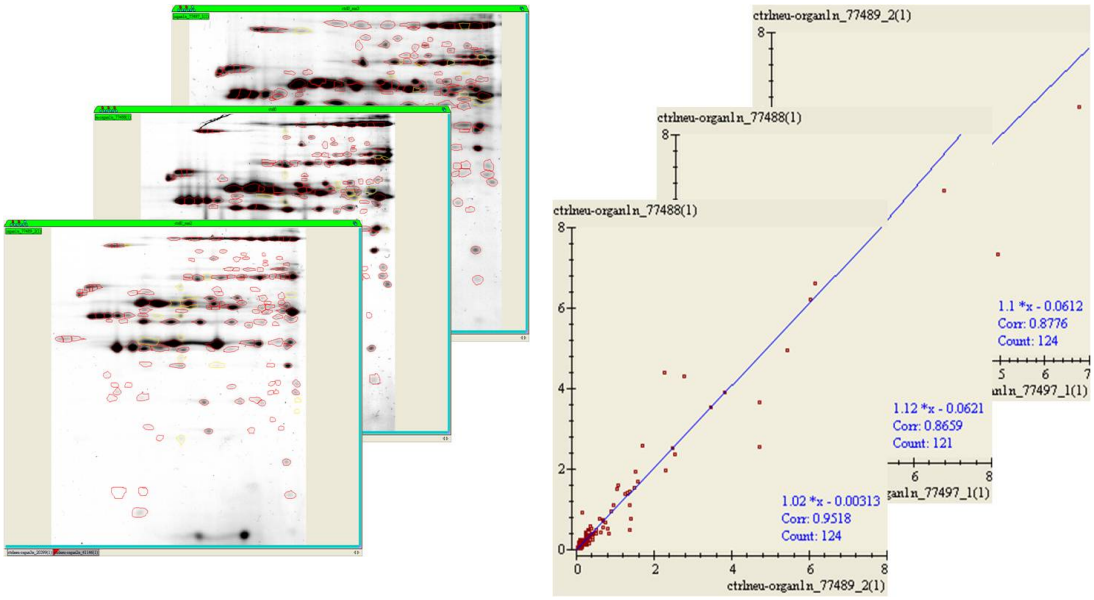

Figure 2.2: Evaluation of technical variability of 2-DE by regression analysis. Representative 2-DE gels and scatter plots of the subproteome ws_6-11. (Left) Digital images of replicate gels from organ #1n of the control 0' group. The spot outline corresponds to the area from which the relative volume [%Vol] was quantified. (Right) Scatter graphs on logarithmic scale for the specified replicate gel (x-axis) and the reference gel (y-axis). Technical variations were compared between matched normalized spot volumes. Regression analysis yielded the best fit line, the correlation coefficient Corr and the number of matches (count).

2.7.2.2 Biological variability

To evaluate the extent of variation between individual animals of the control group (inter-experiment), composite (average) gels for each organ (#1n, #2n, #3n) were created from representative spots of technical replicate gels. However, every technical replicate gel contained several spots which were seen only on a few other gels. These spots were mainly low abundant and close to the detection limit, or appeared at the edge of the pH range and showed irregular shapes. Thus, only spots that were on at least two out of three technical replicate gels were included in the composite image.

In analogy to the intra-experiment comparisons, scatter plot analysis was conducted for inter-experiment gels to evaluate sample-to-sample variations resulting from disparities in protein extraction / sample fractionation. The CV was then determined for all spot volumes on the composite gels. Match sets that only consist of one organ were not included in the present analysis.

2.7.3 Determining differential protein expression

Protein expression changes were calculated for each subproteome separately using overlapping measures statistics. The overlapping measures quantify the overlap between the intervals (defined by the ranges 'mean - dispersion, mean + dispersion`) of the comparing groups (ctrl 0' *vs*. DES-PC groups). To get meaningful data, the maximum difference (gap) between the range of the control group and the range of one of the treatment groups was set to gap > 0, indicating non-overlapping ranges. Protein spots were further processed by determining the fold-rage between the treatment groups compared to the control group. As the ratio is calculated between the extremes of the dispersion an absolute value higher than 1 represents an over- or under-expression of the spot matches. In this study, the threshold was set to ratio > 1.2. Because this is just a marginal threshold, one-way ANOVA values were used as qualitative indicators. Protein spots with $P<0.05$ were considered as substantially regulated. The spot list was finally verified by comparing the values of the control groups 0' and 30' against each other to exclude alterations that are caused by the resting time.

2.8 Electrospray mass spectrometry

Mass spectrometric identification of differentially expressed proteins was performed on an electrospray hybrid mass spectrometer (ESI Qq-TOF) equipped with a *Nanospray* source (*Q-STAR XL,* Applied Biosystems, Darmstadt, Germany).

2.8.1 Fundamentals in instrumentation

Mass spectrometers consist of three major components: the ion source, the mass analyzer and the detector. The ion source of a mass spectrometer converts the analyte molecules into ions that can be transported to and analyzed by the mass

analyzer. For electrospray (ESI)-MS, the peptide mixture is transferred into a small-diameter capillary tube. A high electric field is applied between this capillary and an electrode and induces a charge accumulation in the liquid at the end of the capillary, whereby multiply charged droplets are formed and sprayed out from the end of the capillary. These droplets are forced by the electric field to enter a region of decreasing pressure, where evaporation of the solvent will cause explosion of the droplets and produce singly or multiply charged ions (Charged Residue Model).

The mass analyzer/filter then separates the ions according to their mass-to-charge ratio (m/z) – with the mass of the ion expressed in units and the charge expressed as the number of charges that the ion possesses. Important parameters of mass analyzers are resolution, sensitivity and mass accuracy. Nowadays, four types of mass analyzers are used in protein analysis: time-of-flight (TOF), quadrupole (Q), ion trap (IT) and Fourier transform ion cyclotron resonance (FT-ICR). These analyzers are sometimes combined in a single instrument, e.g. quadrupole ion trap (QIT). In the present study protein identification was performed on a Q-TOF instrument.

The operating principles of the TOF mass spectrometer involve measuring the time required for an ion to travel from an ion source to a detector usually located 1 or 2 meters from the source. Ions obtain their kinetic energy by acceleration in an electric field. The ion velocities depend on m/z values and correspondingly ions of different m/z will reach the detector at different times. The quadrupole analyzer consists of four parallel rods where a superimposed radio- frequency potential is applied. The field on the quadrupole then determines which ions are allowed to reach the detector. As an electric field is imposed, ions moving into this field region will oscillate depending on their m/z ratio and chosen radio frequency. Only ions of a particular m/z are allowed to pass through.

For detection of the ions which are emerging from the mass analyzer, and measurement of their m/z and abundances all mass spectrometers are supplied with multi-channel-plates. These detectors most often used in modern mass spectrometers involve secondary emission of electrons. Positive or negative ions cause the emission of one or several secondary particles (usually electrons) while colliding with the detector. These secondary particles pass into an electron multiplier causing the emission of more and more electrons as they travel toward the ground potential. Thus a cascade of electrons is created that finally results in a

measurable current at the end of the electron multiplier. The detector signals are transferred to a computer for recording of the signal, and the sum of all detected signals represents the characteristic mass spectrum for the investigated peptide ions.

2.8.2 Proteolytic digestion

The 2-DE gels were placed on a clean glass plate positioned on a light table and protein spots of interest were excised from gels using a disposable scalpel. The gel slices were cut into 1 mm^3 plugs and transferred into a *Protein LoBind* tube (Eppendorf, Hamburg, Germany). The following washing steps were carried out each for 10 minutes at RT on a continuously shaking vortex instrument unless otherwise indicated. The solutions were removed after any incubation step using *GELoader* tips (Eppendorf, Hamburg, Germany). At first residual Coomassie stain was rinsed out by repetitive washing with 10% (v/v) ethanol / 2% (v/v) phosphoric acid. The destained gel plugs were then washed twice with 50 mM NH_4HCO_3/50% (v/v) acetonitrile, and once with 100% (v/v) acetonitrile. The gel plugs were finally evaporated in a vacuum *Concentrator* (Eppendorf, Hamburg, Germany). *Proteomics grade trypsin* (Sigma, Taufkirchen, Germany) resolved in digestion buffer [25 mM NH_4HCO_3, pH 8.0] was added to the dried gel pieces until swelling. Rehydration was allowed to proceed for 30 minutes whereby samples were kept on ice to prevent auto-digestion of trypsin. The chosen trypsin concentration depended on the protein amount in the spot and varied between 0.1 – 0.01 µg/µl. Following rehydration, excessive trypsin solution was discarded and samples were amply covered with digestion buffer. Protein digestion was carried out for at least 12 hours at 37°C.

After digestion, sample was centrifuged at 8000 *g* for 60 seconds and peptide-containing supernatant was collected into a fresh LoBind tube. To gain peptides from the gel plug, two volumes of Milli-Q water were added to the sample and gel plugs were shaken on a vortex and sonicated in a sonication bath (*Sonorex*, Bandelin, Berlin, Germany) for 5 minutes. The washing out was transferred to the peptide fraction, and extraction of peptides from the gel plugs was further proceeded by adding two volumes of elution buffer [50% (v/v) acetonitrile / 5% (v/v) formic acid]. The sample was placed on a vortex for 30 minutes, and after centrifugation the elution fractions were also added to the peptide fraction. This

extraction procedure was repeated three times. A final elution step with 100% ACETONITRILE was performed to squeeze out last digestion products. United peptide extracts were lyophilized in the vacuum concentrator and stored at -20°C for future MS analysis.

2.8.3 Sample desalting

Protein digests were desalted by solid-phase extraction to remove components of the sample that might otherwise interfere with the direct analysis by electrospray ionization mass spectrometry. At first, 7 µl of washing solution [4% (v/v) methanol/1% (v/v) formic acid] was added to the dried peptides allowing to resuspend for at least 5 minutes. In the meantime the small reversed-phase column, *PerfectPure C-18 Tip* (Eppendorf, Hamburg, Germany) was prepared by aspirating 7 µl of elution solution [60% (v/v) methanol / 1% (v/v) formic acid] into the tip and expelling the solution into the waste. This process was repeated twice. Afterwards, the C-18 Tip was equilibrated using 7 µl of washing solution, once again aspirating and expelling the solution. The equilibration step was repeated another two times. The resolved peptides were then bound to the C-18 Tip by repeatedly aspirating the digested sample into the tip and expelling it back into the microfuge tube, a total of ten cycles. The C-18 Tip was washed three times using wash solution, keeping all wash fractions in a separate microfuge tube for any contingency. The peptides were subsequently eluted from the C-18 Tip using 7 µl of elution solution, aspirating and expelling the peptide-containing solution into a clean LoBind tube. Desalted protein samples were finally pipetted into *NanoES Capillaries* (Proxeon Biosystems, Odense, Denmark) and transferred into the electrospray source.

2.8.4 Determining protein identity by ESI mass spectrometry

Protein identification using mass spectrometry is based on the information in mass spectra acquired from peptides of digested proteins. A measurement of the masses of the peptides yields a peptide mass fingerprint (PMF) of the digested protein. For PMF-based protein identification, a sequence collection containing all possible peptide sequences that can be present in an organism is needed. A computer performs a virtual digestion of entire proteins in a sequence collection in the same way as in a real experiment and creates a theoretical mass list of

peptides. Mass values obtained from the acquired mass spectrum (the PMF) are then compared to the theoretical masses from the mass list in order to find matches.

A more specific method for identifying proteins and peptides is provided by tandem mass spectrometry. The term “tandem mass spectrometry” reflects the fact that two stages of mass analysis (MS/MS) are used in a single experiment. This technique employs isolation of a product ion which then undergoes fragmentation. A number of different fragmentation techniques are available that lead to the detection of different types of fragment ions. The ESI Qq-TOF used for this study operates with collision-induced dissociation: the ion of interest is fragmented as a result of collision with inert molecules of nitrogen. The resulting set of proteolytic peptide fragment mass values provide sequence information that can be utilized for identifying the peptide that was fragmented (Figure 2.3). MS/MS- based identification has several advantages since it provides detailed information about a peptide sequence and its modifications. It allows working with complex peptide mixtures and does not require all the peptides of a given protein to be confirmed to achieve confident identification of a protein.

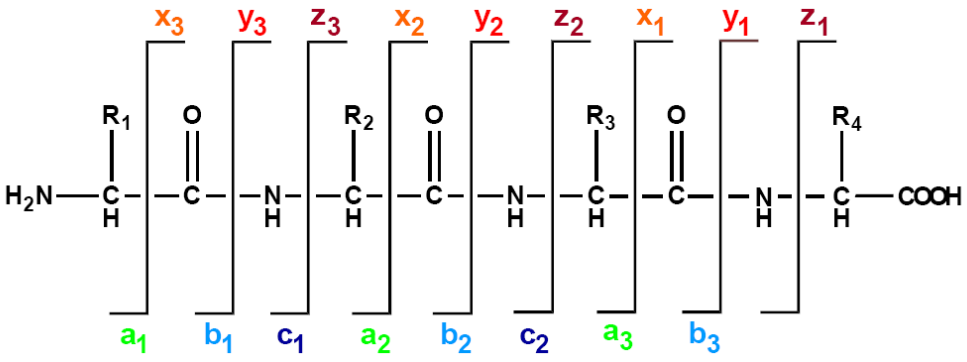

Figure 2.3: Nomenclature of peptide fragmentation according to Roepstorff and Fohlmann. Fragmentation following collision-induced dissociation leads to peptide backbone cleavage resulting in fragments that either retain the positive charge on the C-terminus component (represented by symbols x, y, z) or on the N-terminus of the original peptide (indicated with the lettering a, b, c) (128).

The most frequently used computer-based identification is library searching, where peptides are identified by comparing the experimental MS/MS spectrum with previously acquired spectra of identified peptides stored in a library. This

approach can be very sensitive, since the comparison involves real already existing spectra, but of course is useless for analysis of peptides not already detected. If a peptide of interest features exceptional amino acid modifications or is not present in any sequence collection, peptide identification has to be performed by *de novo* sequencing using the MS/MS-data. *De novo* sequencing means that the peptide sequence tag is manually derived directly from the mass spectrum by systematical identification of b- and y-ion series.

2.8.5 MS data acquisition

One mass spectrum (scan type *TOF-MS*) and up to five tandem mass spectra (scan type *Product Ion*) were recorded for each sample spot. Mass spectra and collision MS/MS data were analyzed with the *Analyst QS* software (Applied Biosystems). For protein identification, tryptic monoisotopic peptide masses of collision-induced ion fragments were searched against the equivalent theoretical masses derived from the *NCBInr* protein database. Using *Mascot* (http://www.matrixscience.com), following search parameters were employed: taxonomy unspecified, one missed cleavage site, peptide tolerance 1.2 Da and MS/MS tolerance ± 0.6 Da. Partial chemical modification such as oxidation of methionine and carbamidomethylation of cysteine were considered for the queries. In general, Mascot searches are scored using the MOWSE algorithm. Here, the given probability value was used as indicator for a proposed protein, but manual *de novo* sequencing was applied to confirm the amino acid sequence suggested by Mascot. Peptide mapping was considered positive when theoretical and experimental M_r and *pI* were expected to be similar. The criteria used to accept protein identification included the extent of sequence coverage (> 10%), the number of peptides matched (minimum of three) and the mass accuracy.

3 Results

3.1 Strategies for improving 2-DE separation of cardiac tissue proteins

The prerequisite for gel-based proteomics analysis of differential protein expression is establishing optimal protocols for protein extraction and subsequent 2-DE. To fully represent the proteome of interest, as many proteins as possible have to be released and extracted from the respective tissue. The main elements accounting for a satisfactory sample preparation are protein extraction, pre-fractionation and protein solubility. For optimal 2-DE separations, different established protocols were examined and optimized for the application in heart tissue analyses.

3.1.1 Impact of protein extraction protocol on 2-DE pattern

Three methods of protein extraction for 2-DE were evaluated (chapter 2.3), all generally recommended for gentle and/or more vigorous lysis of crude tissue samples (52). In all cases, the frozen heart tissue was disrupted by mechanical devices and further homogenized in different lysis buffers. Protein samples were either (a) directly solubilized in IEF-buffer containing urea and CHAPS (one-step extraction); (b) dissolved in TCA-buffer and subsequently solubilized in IEF-buffer (two-step extraction); or (c) homogenized in physiological Tris-buffer containing detergents followed by a subsequent precipitation step with TCA/acetone and a final solubilization in IEF buffer (multi-step extraction).

Following 2-DE separation, the urea-CHAPS homogenized tissue was found to be successful for a handful of highly abundant proteins, but less effective for the majority of proteins (Figure 3.1 left). The TCA-acetone extraction method was even worse to subject any cardiac proteins properly to 2-DE (Figure 3.1 middle). However, the physiological protein extraction strategy offered a well suited protocol for soluble proteins from myocardial tissue. Figure 3.1 illustrates the superiority of the multi-step extraction protocol in terms of quantity and quality of protein spots resolved on the 2-DE gel.

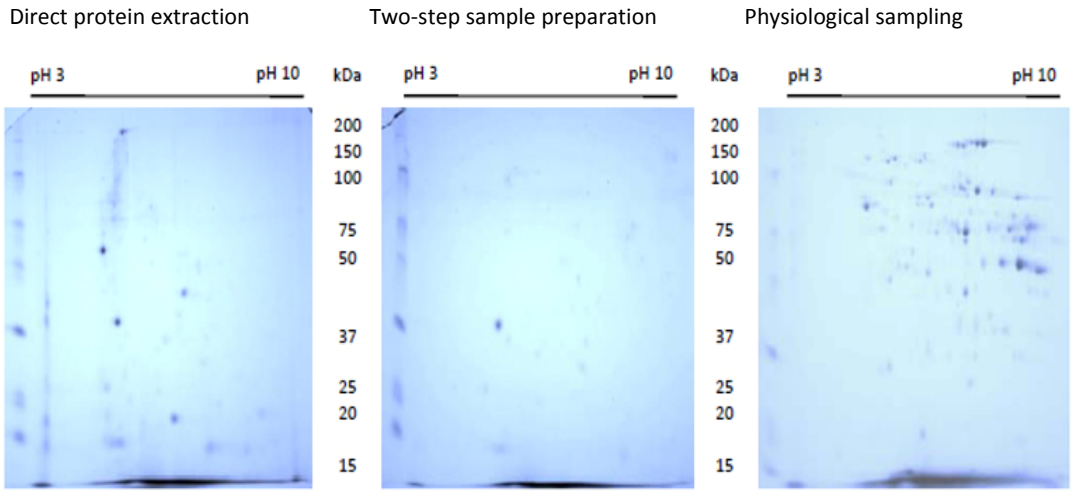

Figure 3.1: Efficiency of different protein extraction methods. 200 µg protein extracts were separated in 13 cm IPG strips pH 3-10 and transferred to 12% SDS-PAGE gels. (Left) Direct protein extraction in urea-CHAPS containing sample buffer; (middle) Two-step sample preparation by homogenization in TCA/acetone; (right) Physiological Tris-based sampling followed by TCA/acetone precipitation.

To exclude the possibility that the Coomassie staining protocol is not sensitive enough to visualize the bulk of proteins, silver and fluorescent staining as high sensitivity detection methods were used for comparison. Preliminary experiments with fluorescent Cy dyes were performed during a *Difference Gel Electrophoresis* (DIGE) workshop by GE Healthcare. DIGE is very sensitive staining method with a detection limit of around 500 pg of a single protein, but fails to uniformly stain gels in cases of varying protein abundances (Figure 3.2). Proteins of low abundance were shown to fall below the detection range and conversely, proteins of extremely high abundance exceed the tolerance of the system, causing poor resolution (trains, doubling of spots).

Compared to silver staining, Coomassie was able to visualize equal numbers of protein spots, similar protein patterns and reached nearly the same detection limit (Figure 3.2). Coomassie even performed better in staining high molecular weight proteins, but silver showed superior detection of low molecular weight proteins.

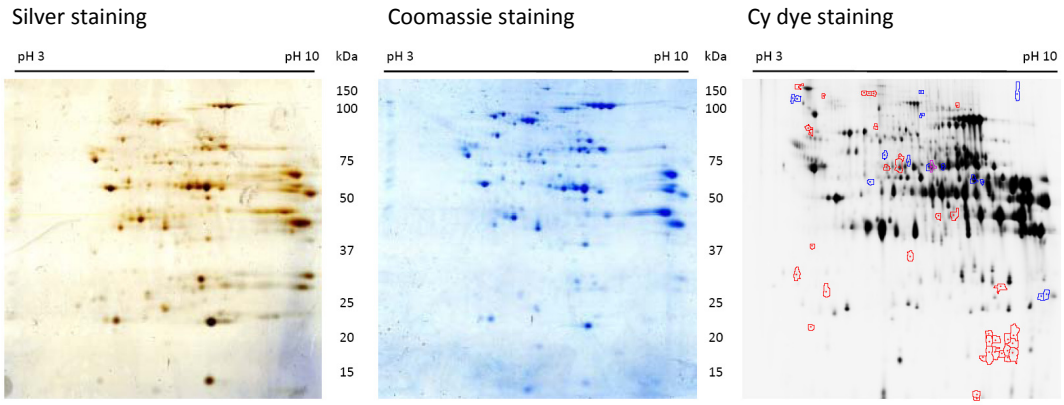

Figure 3.2: Comparison of protein spot resolution between different staining methods. Coomassie performed as strongly as silver staining, but did not reach detection limits of the fluorescent Cy dye staining. In return, the phenomenon of spot masking is quite prominent in the fluorescent staining but not apparent for Coomassie or silver staining.

3.1.2 Protein pre-fractionation enhances proteome coverage

In order to display as many proteins as possible on the one hand and to overcome the complexity of the sample on the other hand, a prefractionation strategy was applied. In general, diversity in tissue organization and protein content affect protein solubility, thus a sequential extraction procedure with increasing solubilization power was tested. Proteins were first extracted with an aqueous buffer, followed by a solubilization step using a detergent-based extraction solution by means of differential centrifugation. The resulting fractions were thus enriched in water-soluble (cytosolic), detergent-soluble (mitochondria-enriched) and particulate (nuclear) proteins.

All three protein fractions were separated by 2-DE without great restrictions (Figure 3.3). Moreover, the prefractionation strategy allowed displaying sample-specific spot patterns in the respective protein fraction (proteins encircled in red). Inspection of the particulate protein fraction versus the water-soluble and detergent-solubilized proteins suggests that there is more protein resolved from the cytosolic and membrane-associated fraction. As a result of restricted tissue quantities, a sufficient number of replicate gels cannot be run to finally reach statistic significance. For this reason, further 2-DE analyses were conducted without the particulate fraction.

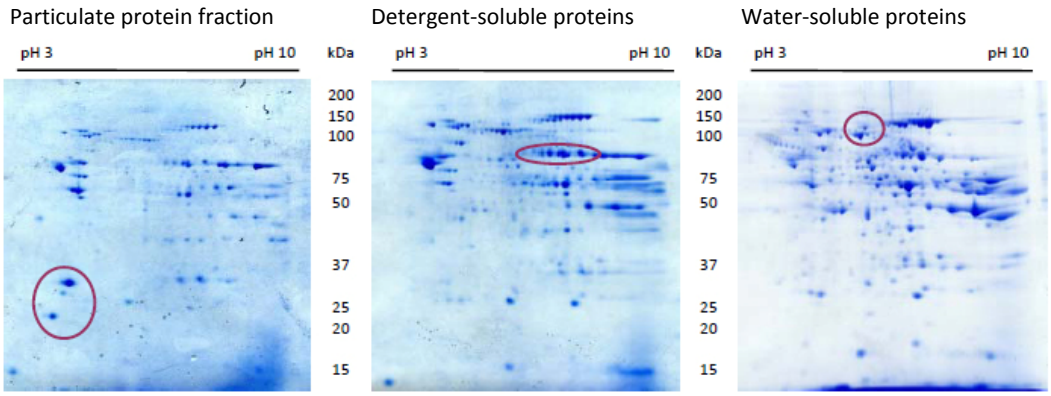

Figure 3.3: Improving resolution in 2-DE separation by the use of a pre-fractionation protocol. Protein samples (400 µg) extracted using differential centrifugation and increasing buffer solubilization power were separated in 13 cm IPG strips pH 3-10 and 12% SDS-PAGE. Protein pattern which are predominantly visible in the respective protein fraction were encircled.

A wide-range linear IPG 3-10 pH gradient is often useful for the initial analysis of a new type of sample. For ongoing analysis this can result in loss of resolution due to compressed areas where high-abundant proteins mask sparse protein spots. To increase protein resolution without restricting the protein amount to be loaded on a single 2-DE gel, the use of partially overlapping pH gradients for first dimension separation provides better proteome coverage.

In silico analyses of eukaryotic proteomes (Figure 1.2) showed a *pI* dependant bimodal distributions of proteins with two main accumulations between pI 4-7 and 9-11 (164). For this reason, the application of partially overlapping IPG strips is much more appropriate to enhance the resolution over shorter pH ranges. In this study, IPG 4-7 and 6-11 strips were used to particularly improve 2-DE pattern in neutral-acidic proteins and basic proteins.

To obtain maximum information from this subproteomic approach, optimization of IEF in the investigated pH intervals is absolutely necessary. Whereas 2-DE analysis of acidic and neutral proteins is generally quite simple to carry out, isoelectric focusing of basic proteins with pH's > 8 prevalently results in severe horizontal streaking (52). The *streak-business* of basic proteins will be detailed in chapter 3.1.4.

3.1.3 Optimal IEF depends on protein solubility

In order to improve the recovery of proteins prior to IEF (after the TCA/acetone precipitation step), protein solubility was optimized using different IEF-buffer compositions. Several combinations of chaotropes, detergents, reductants and solvents were tested for each protein fraction (Table A.1). Solubilization power of the respective buffer was determined by two distinct parameters: the number of visible protein isoforms, and the sharp of the protein stripes in the gel matrix.

The highest efficiency of protein solubilization in IPG 4-7 strips was demonstrated for the thiourea containing stock solution as it showed quantitatively and qualitatively the best focusing results for both solubility fractions (Figure A.1). No buffer including HED as reducing agent was short-listed. The use of ASB-14 as zwitterionic detergent was appropriate only in few cases. And the mixture of isopropanol and glycerol just improved marginally protein sharpness.

Subsequently, 2-DE separations were performed with the three most successful IEF conditions to figure out which buffer composition was the most suitable. Evaluation was based on the number of protein spots that were detectable on the 2-DE gel as well as on spot resolution within the protein pattern. In both cases, the TU-CHAPS-DTT buffer gave the most satisfying results. Figure 3.4 shows the representative 2-DE gels of water- and detergent-soluble proteins ran under optimized IEF (pH 4-7) and SDS-PAGE conditions. The 2-DE gels finally reveal highly resolved protein spots across the entire pH range and therefore provide good initial conditions for analyses of differential protein expression.

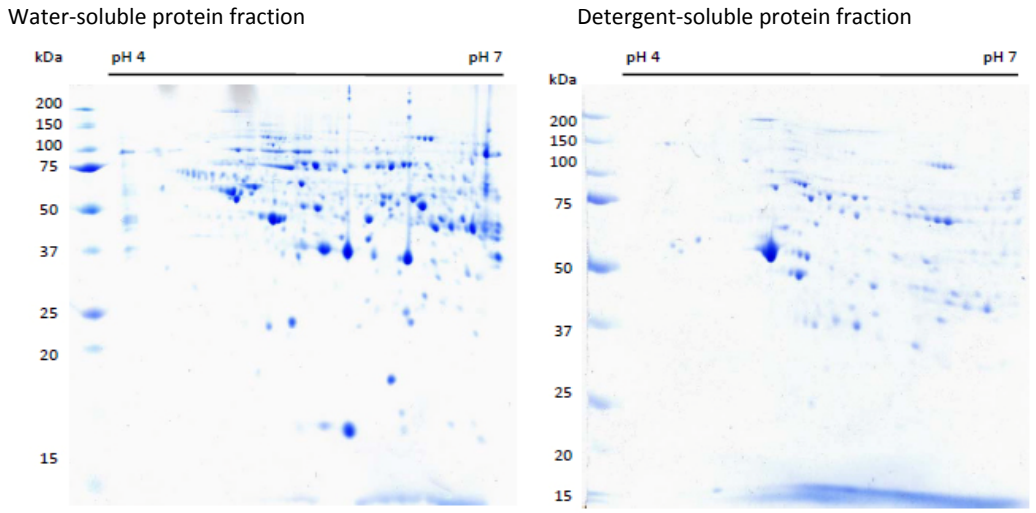

Figure 3.4: Optimized 2-DE gels of pre-fractionated cardiac tissue samples in pH 4-7 strips. Representative protein pattern of water- (left) and detergent-soluble protein fractions (right) separated in minigel (7cm) SDS-PAGE format. IEF was optimized for proteins within *pI* 4-7 showing clear and well resolved spots uniformly distributed in each 2-DE gel.

Concerning alkaline proteins, the best solubilization power was shown for the TUA-containing buffer (Figure 3.5). The detergent mixture of CHAPS and ASB-14 in combination with the chaotropes urea and thiourea profoundly enhanced intensity as well as sharpness of the protein spots. However, sample preparation alone did not address all resolution problems since protein streaking was consistently observed towards the cathode.

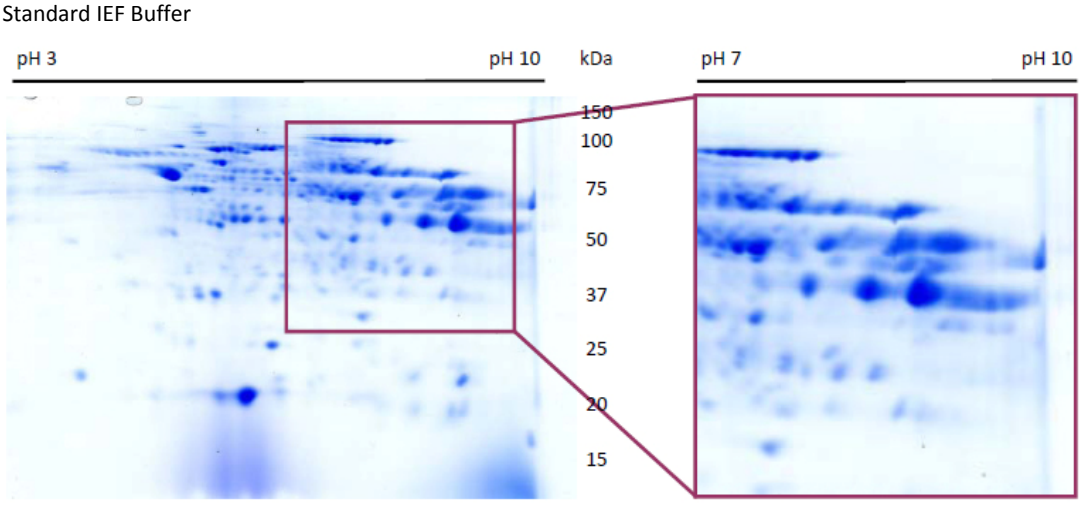

Figure 3.5a: Bad solubilization of alkaline proteins using the standard IEF buffer.

Thiourea-ASB-14 Buffer

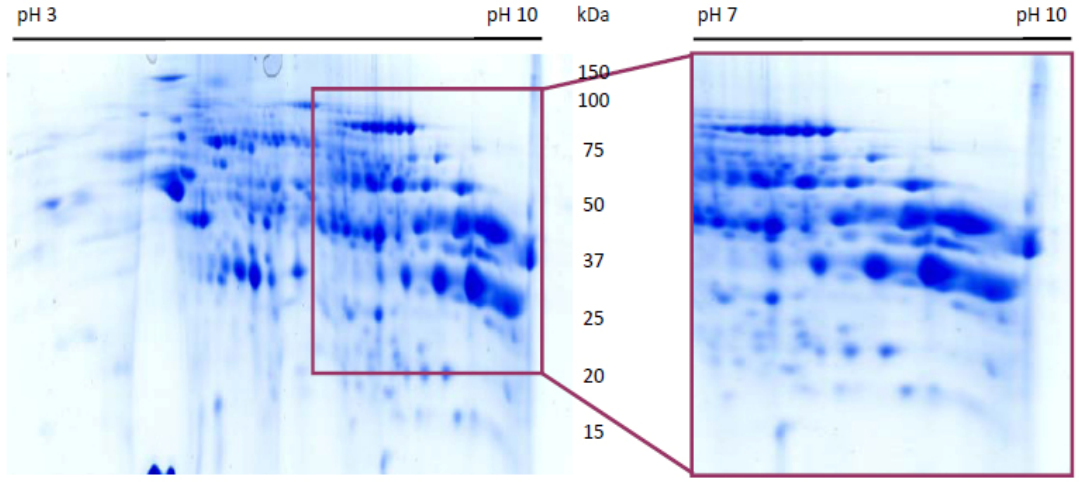

Figure 3.5b: Improved solubilization of alkaline proteins by the additon of thiourea and ASB-14. Enlarged areas of the basic regions in IPG pH 3-10 demonstrate the superiority of the TUA-buffer (lower panel) over the standard buffer (upper panel) to solubilize alkaline proteins.

3.1.4 De-streaking the alkaline proteome

The use of IPGs covering the alkaline pH range 6-11 did not facilitate IEF of alkaline proteins to any considerable degree, as they still have a tendency to form pronounced streaks rather than discrete spots in 2-DE gels (Figure 3.6). When using these basic pH gradients it is recommended to apply the sample by anodic cup-loading (51). Cup loading is generally used for analytical loadings as the maximal sample load is limited to 100 µg in 100 µl. Sample application takes place following overnight IPG strip rehydration, immediately prior to IEF. Thus depletion of reducing agent in the sample is avoided and therefore should support “de-streaking”. Cup-loading additionally facilitates the uptake of proteins that tend to stick at the barrier of the IPG strip matrix, like high molecular mass or hydrophobic proteins.

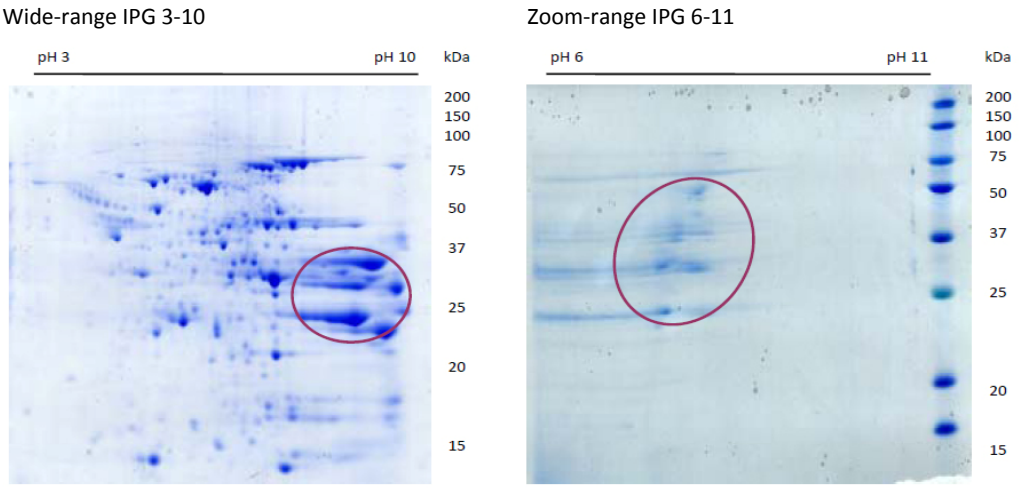

Figure 3.6: Poor resolution of basic proteins (*pI*>8) in 2-DE gels. Proteins of the soluble extraction fraction were applied by in-gel rehydration and separated in 13 cm wide-range pH 3-10 IPG strips (left) and zoom IPG strips pH 6-11 (right). Both 2-DE gels showed horizontal streaking along with numerous spot trains (encircled) at the cathodic end of the gels.

The optimal point of sample application needs to be determined empirically as it may vary with the nature of the protein sample. Sample application near the cathode is recommended for proteins with acidic *pI*'s or when SDS has been used in sample preparation. But for the most IPG strip gradients anodic sample application is suitable (51). Here both application points were tested for cup-loading, using the recommended sample load 100 µg/100 µl.

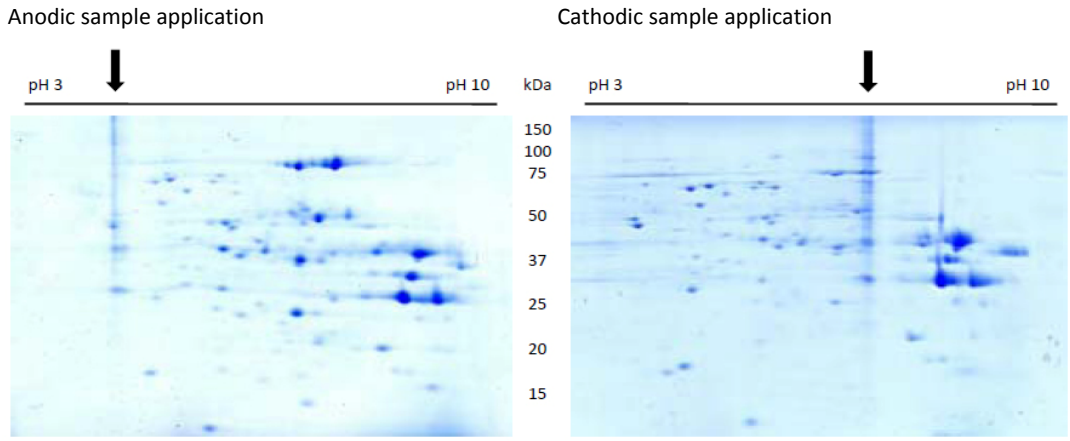

Figure 3.7: Effect of application point during cup-loading on proteome representation. Proteins (100 µg / 100 µl) were applied via cup-loading either at the anodic (left) or the cathodic edge (right) of the IPG strip pH 3-10 / 7cm. The application point is indicated by an arrow and easy to identify by the precipitation stripe.

Regarding proteins in the acidic-neutral pH range, similar 2-DE results were obtained with both application methods (Figure 3.7). The protein patterns displayed within pH 3-7.5 were similar and spot boundaries were well-defined in both cases. Concerning proteins in pH 7-9, sample application near the anodic end was superior to cathodic loading. The superiority is characterized by improved protein coverage and enhanced spot intensity. Furthermore, the precipitate at the cathodic sample application point masked a couple of spots in the area of interest whereas in anodic cup-loading the precipitate was beyond the alkaline region. Unfortunately, protein precipitation as a collapsed line of unresolved spots implies that less protein was separated than originally loaded.

To remedy protein aggregation and to overcome limited loading capacities, application of diluted samples in repetitive fillings was tested. The cup was refilled with diluted sample when the rest has almost completely entered the IPG strip. For the analysis of basic proteins, preparative loadings of 150-250 µg sample are recommended (51). "Refilling" was investigated for the double amount of protein normally applied using sample cups (100 µg → 200 µg). One has to bear in mind that insufficient focusing time during the refilling process will result in incomplete protein migration and consequently poor IEF separation. To ensure constant sample entry and proper focusing, the IEF protocol was therefore prolonged by a low-voltage step at 500 V for 2 hours whereby the final high-voltage step was reduced by the same Vhours.

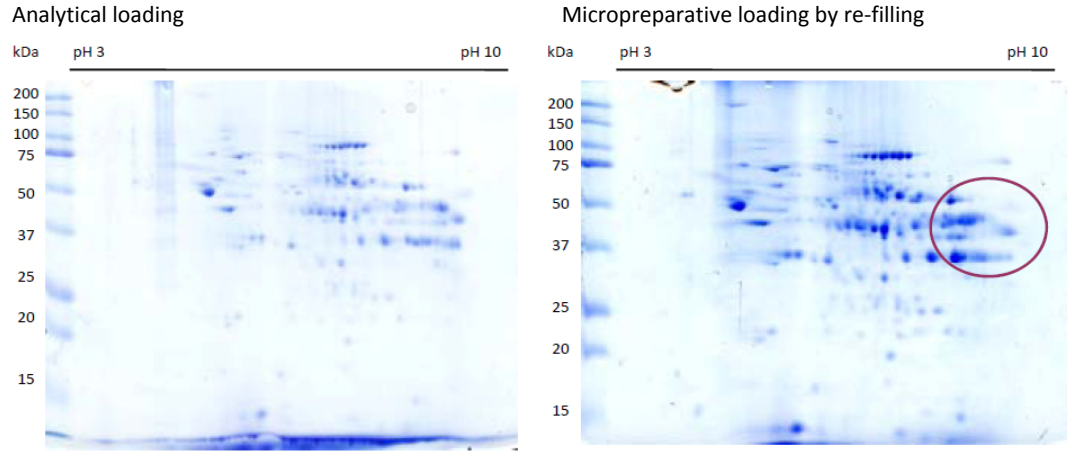

Figure 3.8: Overcoming restricted sample cup loading capacities by repetitive refilling. Sample application was performed by anodic cup-loading, whereby the recommended maximum protein load of 100 µg protein per cup (left) was risen above by re-filling of the sample cup during a low-voltage step at 500 V (right). In both cases, protein concentration was kept at 100 µg/ 100 µl.

Almost all protein abundances were effectively enhanced using the refilling approach (Figure 3.8). When IEF was performed in IPG 6-11 strips using the sample cup-loading method, profound streaking above pH 7 is still a problem of spot resolution (Figure 3.9). The most basic protein spot that was properly resolved in the basic pH strip had an approximate *pI* of 8.5.

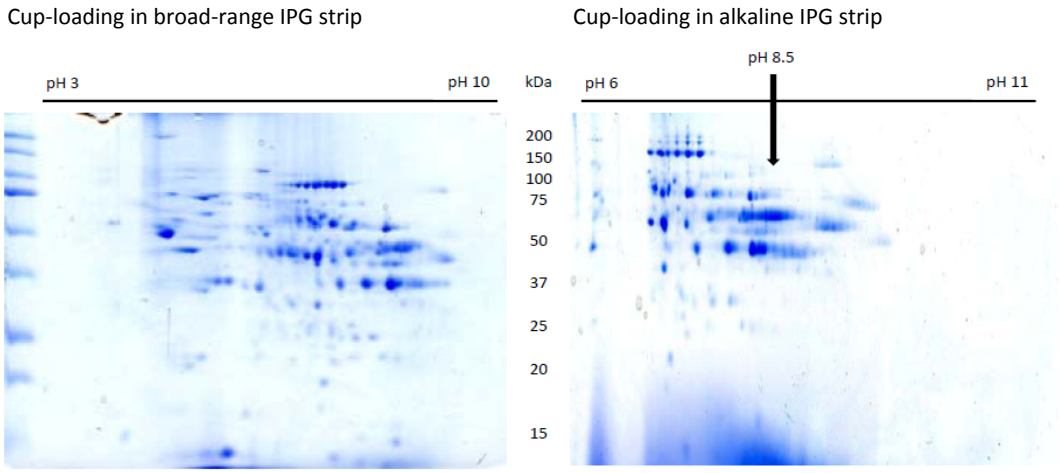

Figure 3.9: Comparison of cup-loading experiments in IPG 3-10 and 6-11 strips. 200 µg protein was applied by anodic cup-loading and either separated on wide-range IPG strips pH 3-10 (left) or on zoom IPG strips covering pH 6-11 (right). No de-streaking effect was observed in the basic pH range above *pI* 9 when using IPG strips which are designed for the analysis of alkaline proteins.

Furthermore, the basic zone near the cathode was evidently devoid of protein. This is mainly caused by active water transport toward the anode during IEF, the so called endosmotic flow (EOF) (49). To counteract EOF, water-moistened electrode pads were placed between the IPG strip and the electrodes every 2 hours. Besides maintaining the water content, the electrode pad was also used as salt trap.

Another problem in the basic pH range is cysteinyl related streaking that follows from disappearance of DTT in the basic part of the IPG strip (50). The formation of extra spots in elongated trains (Figure 3.9 right) can usually be eliminated when alternative reducing agents are utilized for IEF. For the present analysis of rat heart proteins, the use of HED seems to be proficient as it was found to work well with thiourea containing IEF solutions and did also show well resolved spots of mouse liver proteins (108). For de-streaking experiments of cardiac tissue proteins, IEF was performed with 50 mM HED instead of 40 mM DTT. Indeed, horizontal streaking along with numerous spot trains disappeared when replacing the

reducing agent (Figure 3.10). The greatest improvement was seen in the region above pH 8 where intra- and inter-disulfide exchange was expected to be most prevalent. At the same time, an enhanced protein distribution over the given pH range was achieved. The observed *pI* shifts towards the cathode are consistent with the hypothesis that HED converts negatively charged thiol groups of proteins into uncharged, mixed disulfides (108).

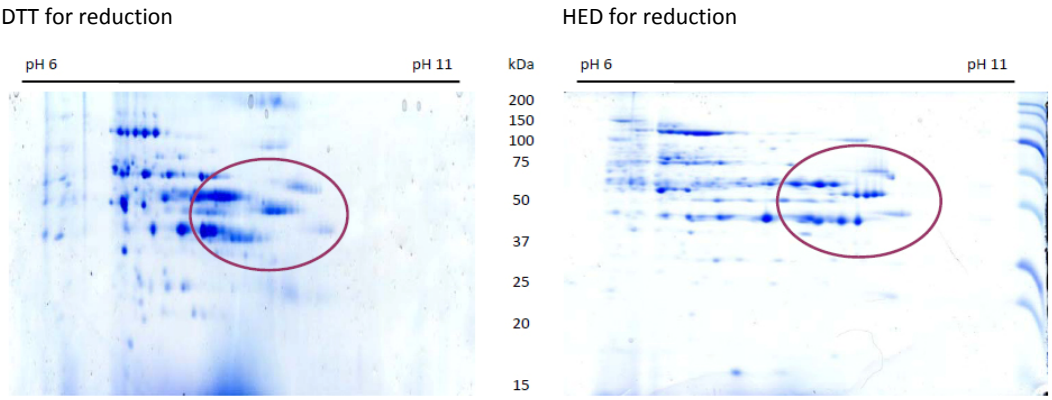

Figure 3.10: Spot de-streaking by the use of HED. Replacing the reducing agent DTT (left) by HED (right) positively affects spot resolution in IPG 6-11 gels. Protein pattern in the encircled areas show reduced artificial streaks.

Protein spots were well resolved in IPG 6-11 strips although vertical trains persist at the position of abundantly expressed proteins. In some cases, horizontal streaks are still prominent when proteins are expressed in multiple isoforms. The most basic protein spot present in the cardiac proteome of cytosolic proteins was identified as succinyl-CoA ligase, α unit with a theoretical *pI* ~ 9.9 and M_r ~ 37 kDa (Figure 3.11; Table A.3). The remaining gap lacking protein spots around pH 10-11 is probably caused by the hydrolysis of the amide groups present in the polyacrylamide strip matrix. This problem generally occurs when using basic IPG strips and becomes more serious with focusing time (personal communication with R. Westermeier/ GE Healthcare).

In summary, the proposed protocol combining enhanced protein solubility, micropreparative cup-loading sample application by repetitive filling and de-streaking by the use of HED as reducing agent was found to efficiently resolve alkaline proteins from myocardial tissue (Figure 3.15). The high-quality spot

pattern even reveals the occurrence of low-abundant proteins (indicated by arrows) which were previously masked by severe streaks.

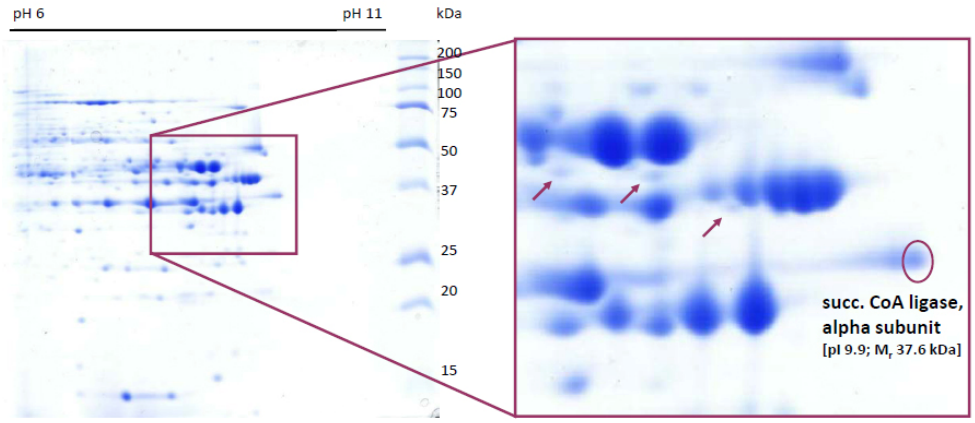

Figure 3.11: Optimized 2-DE separation of basic proteins. Optimization of sample preparation and focusing permits supreme proteome coverage in IPG 6-11 strips. 200 µg protein of the water-soluble fraction was solubilized in TUA buffer containing HED as reducing agent, and was applied via anodic cup-loading in micropreparative sample loads by repetitive filling. (Right) Focus on gel region exceeding pH 9. Arrows indicate low-abundant protein spots. The most basic spot was identified as succinyl CoA ligase, α subunit (*pI* 9.9).

3.1.5 Summary

The improvements provided in this chapter allow a higher coverage of the myocardial proteome that consequently enhances the potential success rate in the identification of novel targets for further differential analyses. Depending on the subproteome of investigation, different protein extraction protocols, solubilization procedures and isoelectric focusing conditions were necessary. In the current study, protein extraction from myocardial tissue samples was only feasible using a physiological Tris-based buffer and subsequent TCA/acetone-based protein precipitation. For the visualization of proteins, the improved Coomassie protocol according to Kang *et al.* (2002) was shown to provide detection limits similar to silver staining (1-10 ng) (67, 37). Pre-fractionation in water- and detergent-soluble proteins considerably enhanced proteome coverage of myocardial tissue proteins. 2-DE was performed in overlapping pH ranges for the analysis of neutral-acidic (IPGs 4-7) and alkaline proteins (IPGs 6-11). Mix and matching different IEF buffer compositions further provided optimal protein solubilization of neutral-acidic (Urea-Thioruea-CHAPS buffer) and basic proteins (Urea-Thiourea-ASB-CHAPS buffer). For de-streaking alkaline proteins in gel regions above pH 8, sample

application by repetitive anodic cup-loading and the use of HED instead of DTT as reducing agent were shown to considerably improve 2-DE pattern.

3.2 Proteomic profiles of DES-PC treated rat hearts

The *in vivo* preconditioning of small animals is a well-established model in the working group of Prof. Wolfgang Schlack (Academic Medical Research Center, Amsterdam, The Netherlands) and is used to study the cardioprotective effect of different pharmacological agents. For desflurane preconditioning in male Wistar rats it was shown that the administration of 2x5 minutes desflurane (1 MAC) interspersed by ten minutes wash-out phases significantly reduces experimental infarct size from 57.2±4.7% in controls to 35.2±16.7% (measured as % of area at risk) (152). The application of 1 MAC in rats corresponds to 5.7% of the inspired gas. The use of this concentration is a common dose for clinical anesthesia.

To study the impact of desflurane preconditioning on the rat heart proteome, a broad-based proteomics approach in the classical combination of 2-DE and MS was chosen. For better proteome coverage, complementary subproteomes were analyzed [water-soluble/neutral-acidic proteins (ws_4-7), water-soluble/alkaline proteins (ws_6-11) and detergent-soluble/neutral-acidic proteins (ds_4-7)]. When performing comparative proteomics it is important to determine the contribution of inherent variability in measuring relative differences between data sets. Table 3.1 shows the raw data of the 2-DE gels, encompassing the number of spots, number of matches (corresponding spots between replicate gels) and the match efficiency. The average number of protein spots detected in the gels of the different subproteomes ranged from 135 for ds_4-7, 289 spots for ws_4-7 to 172 for ws_6-11. Of these, 114, 265 and 163 spot sets were found to be in common between all replicate gels of the respective subproteome, resulting in a match efficiency of 90% on average. In summary, the comparability of spot pattern within the subproteome was quite high for all protein populations, providing a good basis for comparative analyses.

Table 3.1: Characteristics of spot sets calculated from replicate gels of control animals. For each subproteome, the number of spots and matches (spot sets between comparing groups) were calculated and averaged [mean+SD] from the nine replicate gels. The match efficiency indicates the percentage of spots that were consistent within the control group of each subproteome.

Subproteome	Number of spots	Number of matches	Match efficiency
Detergent-soluble/ pH 4-7	135 (± 16)	114 (± 13)	85 %
Water-soluble/ pH 4-7	289 (± 24)	265 (± 18)	92 %
Water-soluble/ pH 6-11	172 (± 14)	163 (± 10)	93 %

As can be seen from the gel-to-gel analyses (Table 3.2), *Corr* values were in the range of 0.866 - 0.996, and average coefficients were calculated to be 0.995 (±0.1%), 0.961 (±2.4%) and 0.898 (±4.7%) for samples from ds_4-7, ws_4-7 and ws_6-11, respectively. The data from the subproteomes in pH range 4-7 (ds_4-7 and ws_4-7) were highly correlated (*Corr* close to 1), indicating good reproducibility between replicate gels. This demonstrates less disparity in sample loading, and high similarity among the sample preparation. On the other hand, the alkaline subproteome (ws_6-11) slightly differed from goodness-of-fit, but the values of the subproteome ws_6-11 were not systematically biased by the cup-loading sample application method. The linear dependences between the data points of scatter plots from ws_4-7 and ds_4-7 were also not far away from identity (1.0 * x + 0). Altogether, matching performance, regression line and correlation coefficient give confidence to the consistency of the 2-DE procedure.

Additionally, the average technical coefficient of variation (CV) was determined for protein expression levels from the three replicate 2-DE gels (Table 3.2, intra-experiment analyses). On average, samples applied by in-gel rehydration showed equal CVs (26.2% and 26.6% for the detergent- and water- soluble subproteomes in pH range 4-7, respectively). However, the cup-loading strategy for alkaline proteins introduces technical variances to a greater extent (CV of 39.6%).

Table 3.2: Gel-to-gel and sample-to-sample variations in 2-DE gels. Intra-experiment compares repeat 2-DE gels from an identical sample (organ #1n); inter-experiment compares gels from different organ preparations (#1n, #2n, #3n).

Subproteome	Type of comparison	Evaluation values	Data set 1 vs. 2	Data set 1 vs. 3	Data set 2 vs. 3	Average	CV[e] (%)	SD[f] (%)
Water-soluble/ pH 4-7[a]	Intra-experiment	*Corr*	0.947	0.948	0.989	0.961	26.5	7.3
		Spot match	271	274	261	269		
	Inter-experiment[c]	*Corr*	0.924	0.831	0.846	0.867	45.3	9.3
		Spot match	271	296	260	276		
Detergent-soluble/ pH 4-7[a]	Intra-experiment	*Corr*	0.995	0.996	0.994	0.995	26.2	14.7
		Spot match	106	109	109	108		
	Inter-experiment[c]	*Corr*	0.994	0.994	0.993	0.994	31.1	15.6
		Spot match	110	101	100	104		
Water-soluble/ pH 6-11[b]	Intra-experiment	*Corr*	0.952	0.866	0.878	0.898	39.6	13.7
		Spot match	124	121	124	123		
	Inter-experiment[d]	*Corr*	0.822	0.916	0.841	0.860	54.0	20.2
		Spot match	135	148	132	138		

[a] Sample was applied by in-gel rehydration.
[b] Sample application via cup-loading.
[c] Values were calculated from synthetic (composite) gels.
[d] Mean values determined from three experimental 2-DE runs of the same dataset.
[e] Standard deviation divided by Mean for matched spots in an experimental series was averaged.
[f] Average SD of CVs for all matched spots in an experimental series.

To evaluate the impact of biological variation, *Corr* and CV values were analyzed by inter-experiment comparisons. The *Corr* and match values of each subproteome were quite similar between intra- and inter-experiments (Table 3.2), indicating the sample preparation procedure to be highly standardized. CV values for each subproteome were distributed over a broad range, whereby the median CV was 0.22, 0.37 and 0.50 for ds_4-7, ws_4-7 and ws_6-11 (Figure 3.12). Eight alkaline and 15 acidic spots of the water-soluble fractions even had a CV value above 1. Inspection of spot sets exhibiting high CVs revealed that these were mainly those ones that are part of crowded areas and partly masked by neighboring spots, or represented spot sets containing obvious outliers. However, in both subproteomes nearly three-quarters of the spots had a CV value below 0.70. Thus one has to keep in mind that there are notable differences in the CVs from one match set to the next within the same experimental group. In contrast, the detergent-soluble subproteome seems to be consistent, due to the fact that 75% of the spots sets

had a CV value below 0.35. The average CV and SD for each subproteome were high (31.1±15.6%, 45.3±9.3% and 54.0±20.2%, respectively; Table 3.2) meaning that variation on the scale of 46-74% (sum of the average CV plus the average SD) needs to be factored into the threshold for determining differential protein expression later on.

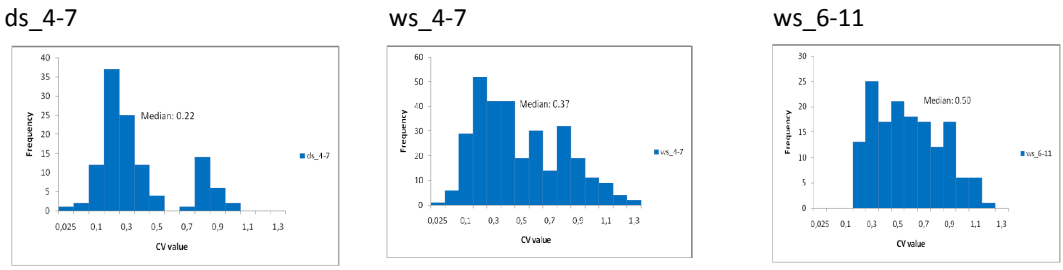

Figure 3.12: Frequency distribution of coefficient of variation in 2-DE experiments. Experimental frequency was determined by summing the number of occurrences corresponding for each nominal CV integer value.

3.2.1 Differential protein expression in the time course of DES-PC

Using the optimized 2-DE conditions described in chapter 3.1.5, differential protein expression was investigated for the different protein fractions of the myocardial tissue (water- and detergent- soluble proteins separated in pH 4-7 and 6-11 IPG strips). To gain a comprehensive view of proteomic alterations effected by desflurane preconditioning, proteins were considered as differentially regulated between control and DES-PC treated samples if they were up- or down-regulated by at least 1.2 fold and a *P*-value < 0.05 (ANOVA for comparison of multiple gel populations). Protein spots that are in accordance with these criteria are indicated in Figure 3.13.

Interestingly, in contrast to the hemodynamic data which demonstrated little difference in heart rate and aortic pressure between the experimental groups (152), DES-PC induces changes in the abundance of a number of proteins. In total, 70 protein spots were found to be affected in the water- and detergent-soluble protein fraction. The most spot alterations were detected in the detergent-soluble protein fraction pH 4-7 (35 spots; Figure 3.13 left), followed by the water-soluble fraction with 22 and 12 spot alterations for pH 4-7 and 6-11 separations (Figures

3.13 middle and right), respectively. At this point, no concrete information is given about the time course of expression change. The idea was to quickly find matches that distinguish the preconditioning groups from the control group to get an impression of the cellular response. Strikingly, the multiplicity of differentially expressed spots is represented in protein chains. Especially in the subproteome ds_4-7 nearly all influenced protein spots seem to belong to multiple protein spots. This is not unexpectedly as mitochondrial proteins will be accumulated in the detergent extraction fraction, and components of the mitochondrial proteome like the respiratory chain are highly expressed in multiple isoforms (subunits).

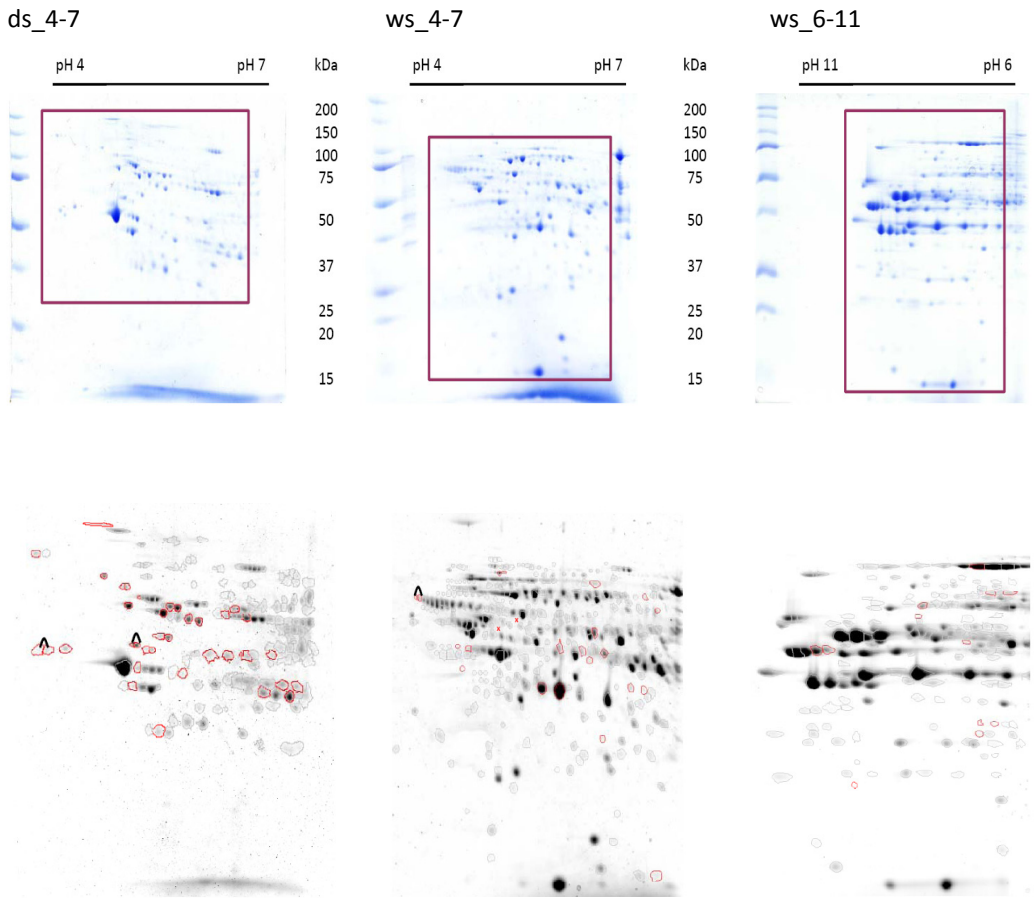

Figure 3.13: Proteomic alterations in the rat heart evoked by DES-PC *in vivo*. Representative 2-DE gels of the control group from subproteomes ds_4-7, ws_4-7 and ws_6-11. The boxes determine the area used for the software-based image analysis. The digital images in the lower panel show the respective area of investigation. Protein spots that are affected during DES-PC are outlined. Missing spots that are not present in the control group are indicated by x. Joined spots represent a merged spot set.

Although this set of spots might represent interesting proteins it was decided to narrow the hit list with respect to the varying CVs of the respective subproteomes. Individual thresholds for meaningful and representative statistic analyses regarding spot variation were set to *P*< 0.02, 0.01 and 0.005 for ds_4-7, ws_4-7 and ws_6-11, respectively. To further avoid errors due to a lower technical reproducibility close to the limit of detection, a minimal spot value [%Vol.] of 0.015 was imposed for further data analysis. In the end, 40 protein spots met the criteria whereby each subproteomes contributes relative equally (17, 14 and 9 spots for ds_4-7, ws_4-7 and ws_6-11). 2-DE gel images from the control group of each subproteome and the representative proteins which had a significant altered abundance between control and preconditioned animals are shown in Figures 3.14 and 3.15.

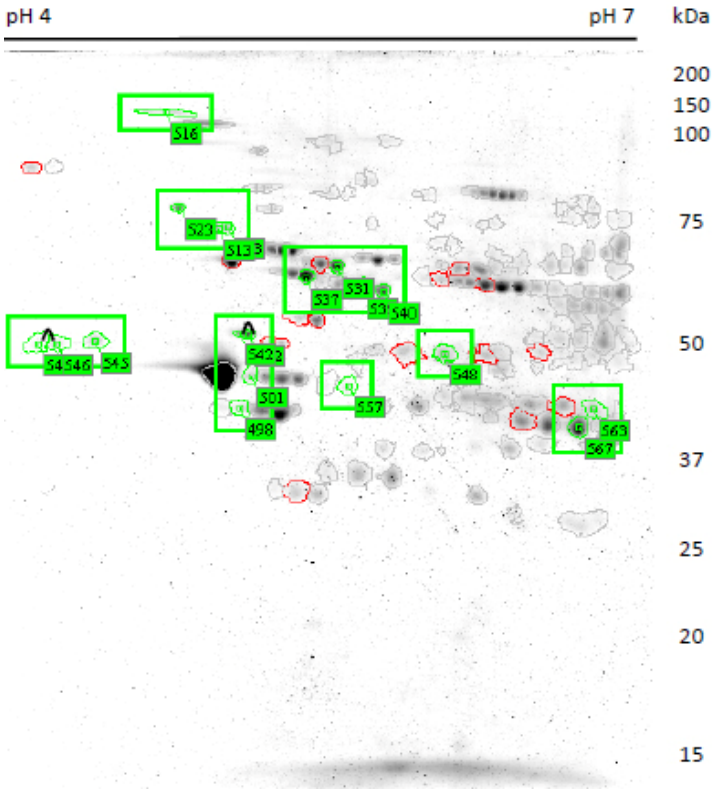

Figure 3.14: Differentially expressed proteins in the detergent-soluble fraction. Control gels of protein fraction ds_4-7. Protein spots that undergo significant expression alterations of > 1.2-fold and *P* < 0.02 are shown in green boxes and indicated by their match ID. Missing spots that are not present in the control group are indicated by x.

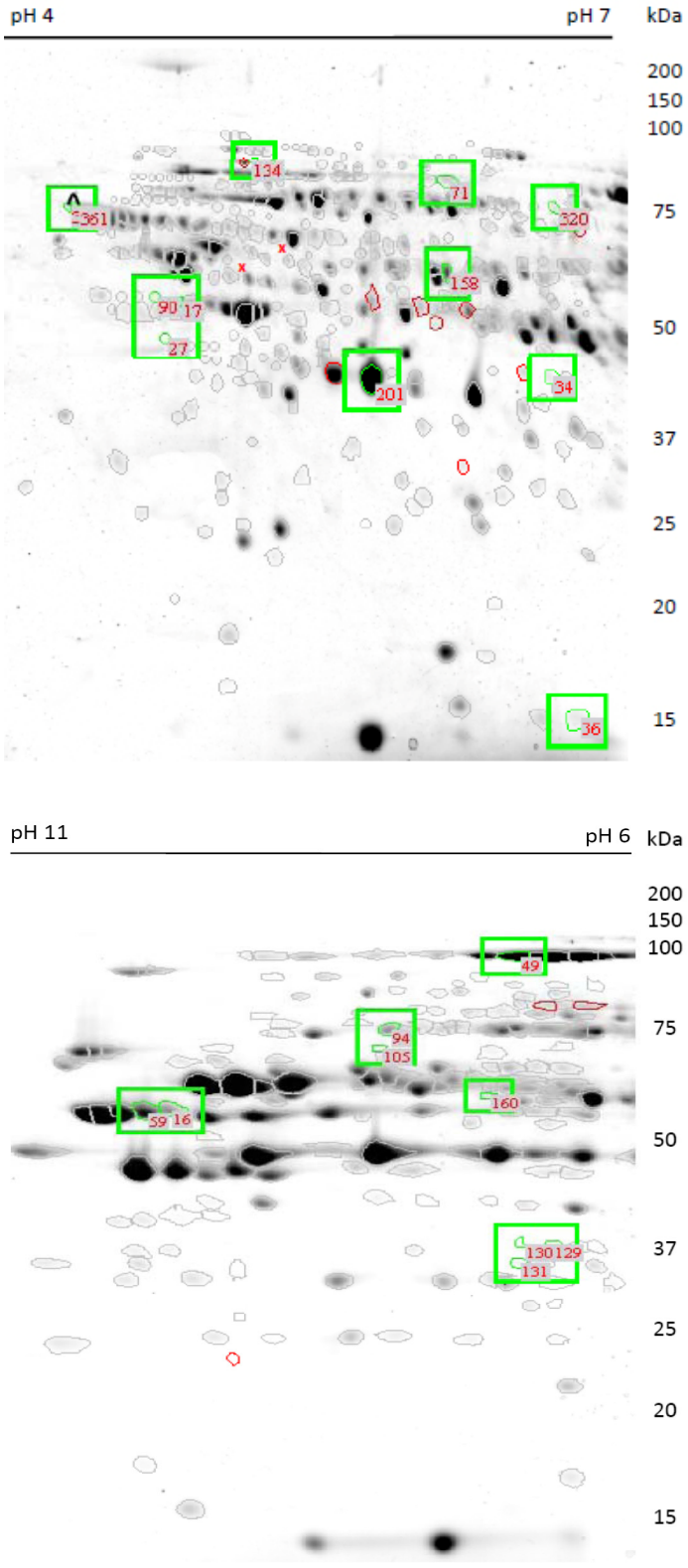

Figure 3.15: Differentially expressed proteins in the water-soluble fraction. Control gels of the protein fractions ws_4-7 (upper panel) and ws_6-11 (lower panel). Protein spots that undergo significant expression alterations of > 1.2-fold and $P < 0.01$ (ws_4-7) and $P < 0.005$ (ws_6-11) are shown in green boxes and indicated by their match ID.

In general, the majority of spots (32/40) showed a decreased abundance in the heart of preconditioned rats compared to the control (Table 3.3) indicated by green). Only eight protein spots were increased in response to DES-PC (indicated by red). Regarding protein changes in the time-course of DES-PC, most proteins seem to respond in particular to Des 2. The expression factors in all experimental groups were moderate, ranging from 4.90-fold down-regulation to 1.46-fold up-regulation.

Table 3.3: Significant protein expression changes in the heart induced by DES-PC. Changes were highlighted if they were significantly decreased (green) or increased (red) (Anova *P* values are shown). 1,0E-06 characterizes the case where the software cannot compute ranges because of missing values.

Match ID[§]	Average normalized intensity[b)]					Relative change in spot intensity[c)]			
	Control	DES-PC				Des 1 vs. Ctrl 0'	Wash 1 vs. Ctrl 0'	Des 2 vs. Ctrl 0'	Wash 2 vs. Ctrl 0'
	Ctrl 0' (n= 3)	Des 1 (n= 4)	Wash 1 (n= 4)	Des 2 (n= 4)	Wash 2 (n= 3)				
Subproteome ds_4-7 (threshold *P*<0.02)									
498	0,346	0,179	0,029	0,069	0,086	-1,024 *(P=0,109)*	-3,847 *(P=0,001)*	-1,933 *(P=0,008)*	-1,486 *(P=0,044)*
501	0,260	0,130		0,050		-0,842 *(P=0,208)*	1,0E-06 *(P=1,86E-04)*	-1,846 *(P=0,010)*	1,0E-06 *(P=0,001)*
503	0,388	0,229	0,890	0,066	0,490	-0,710 *(P=0,293)*	1,373 *(P=0,027)*	-2,069 *(P=0,009)*	0,606 *(P=0,547)*
513	0,228	0,134	0,495	0,038	0,129	-1,052 *(P=0,141)*	1,610 *(P=0,023)*	-2,594 *(P=0,002)*	-1,013 *(P=0,202)*
516	1,233		0,880			1,0E-06 *(P=0,004)*	-0,554 *(P=0,494)*	1,0E-06 *(P=0,004)*	1,0E-06 *(P=0,013)*
523	0,569	0,269	0,813	0,081	0,412	-0,976 *(P=0,096)*	0,733 *(P=0,318)*	-2,712 *(P=0,003)*	-1,003 *(P=0,164)*
531	1,407	1,158	2,104	0,403	1,139	-0,701 *(P=0,636)*	1,217 *(P=0,017)*	-1,595 *(P=0,019)*	-0,815 *(P=0,478)*
537	2,203	1,341	2,919	0,455	1,706	-0,883 *(P=0,217)*	1,059 *(P=0,042)*	-2,118 *(P=0,004)*	-0,864 *(P=0,310)*
539	0,853	0,452	0,821	0,180	0,281	-1,092 *(P=0,085)*	-0,795 *(P=0,805)*	-2,033 *(P=0,006)*	-1,763 *(P=0,010)*
540	1,135	0,868	1,558	0,308	0,762	-0,666 *(P=0,517)*	1,003 *(P=0,077)*	-1,444 *(P=0,024)*	-0,812 *(P=0,293)*
542	0,867	0,741	1,488	0,293	0,868	-0,621 *(P=0,698)*	1,093 *(P=0,075)*	-1,195 (P=0,025)	0,520 *(P=0,995)*
545	0,594	0,328	0,937	0,101	0,587	-0,901 *(P=0,142)*	0,773 *(P=0,264)*	-2,281 *(P=0,005)*	-0,586 *(P=0,970)*
546	1,016	0,375	0,967	0,138	0,327	-1,368 *(P=0,022)*	-0,651 *(P=0,853)*	-3,006 *(P=0,002)*	-1,536 *(P=0,026)*
548	0,587	0,434	0,754	0,153	0,299	-0,756 *(P=0,431)*	1,033 *(P=0,055)*	-1,557 *(P=0,021)*	-1,123 *(P=0,084)*
557	0,260	0,109	0,159	0,041		-1,051 *(P=0,067)*	-0,724 *(P=0,280)*	-2,189 *(P=0,008)*	1,0E-06 *(P=0,005)*
563	0,740	0,067	0,422	0,050	0,202	-2,744 *(P=0,008)*	-0,753 *(P=0,207)*	-5,253 *(P=0,005)*	-1,037 *(P=0,108)*
567	2,162	1,622	3,228	0,567	1,799	-0,666 *(P=0,473)*	0,980 *(P=0,099)*	-1,504 *(P=0,020)*	-0,598 *(P=0,677)*

Match ID[a]	Average normalized intensity[b]					Relative change in spot intensity[c]			
	Control	DES-PC				Des 1 vs. Ctrl 0'	Wash 1 vs. Ctrl 0'	Des 2 vs. Ctrl 0'	Wash 2 vs. Ctrl 0'
	Ctrl 0' (n= 3)	Des 1 (n= 4)	Wash 1 (n= 4)	Des 2 (n= 4)	Wash 2 (n= 3)				
Subproteome ws_4-7 (threshold *P*<0.01)									
17	0,108	0,010	0,024		0,033	-3,261 *(P=0,032)*	-1,393 *(P=0,057)*	1,0E-06 *(P=0,004)*	-0,960 *(P=0,149)*
27	0,014					1,0E-06 *(P=2,94E-04)*	1,0E-06 *(P=2,94E-04)*	1,0E-06 *(P=2,94E-04)*	1,0E-06 *(P=0,002)*
34	0,054	0,004		0,026		-4,899 *(P=2,03E-04)*	1,0E-06 *(P=8,17E-06)*	-1,481 *(P=0,004)*	1,0E-06 *(P=9,86E-05)*
36	0,245	0,028		0,004		-1,909 *(P=0,042)*	1,0E-06 *(P=0,015)*	-9,642 *(P=0,026)*	1,0E-06 *(P=0,056)*
71	0,104	0,024	0,065	0,027	0,032	-1,395 *(P=0,030)*	-0,919 *(P=0,121)*	-2,358 *(P=0,009)*	-1,255 *(P=0,066)*
77		0,091	0,083	0,082	0,097	1,0E+06 *(P=9,94E-05)*	1,0E+06 *(P=0,013)*	1,0E+06 *(P=0,004)*	1,0E+06 *(P=0,029)*
90	0,039	0,009	0,002		0,012	-2,271 *(P=0,002)*	-5,523 *(P=3,06E-04)*	1,0E-06 *(P=6,74E-05)*	-2,057 *(P=0,006)*
100		0,009	0,045		0,037	1,0E+06 *(P=0,437)*	1,0E+06 *(P=0,001)*		1,0E+06 *(P=0,118)*
128		0,066		0,036	0,157	1,0E+06 *(P=0,072)*		1,0E+06 *(P=0,064)*	1,0E+06 *(P=0,022)*
134	0,008	0,025	0,042	0,031	0,295	1,0E+06 *(P=0,490)*	0,569 *(P=0,187)*	1,347 *(P=0,028)*	9,061 *(P=0,014)*
158	0,497	0,122	0,429	0,568	0,328	-2,828 *(P=0,001)*	-0,764 *(P=0,493)*	0,871 *(P=0,325)*	-0,877 *(P=0,226)*
201	8,378	7,075	8,944	8,506	4,744	-0,937 *(P=0,239)*	0,975 *(P=0,171)*	0,821 *(P=0,892)*	-1,490 *(P=0,002)*
319	0,077	0,021		0,036	0,036	-2,299 *(P=0,001)*	1,0E-06 *(P=5,09E-05)*	-1,360 *(P=0,013)*	-1,211 *(P=0,056)*
349	0,119	0,027		0,051	0,054	-1,534 *(P=0,023)*	1,0E-06 *(P=0,003)*	-1,010 *(P=0,073)*	-0,997 *(P=0,119)*
Subproteome ws_6-11 (threshold *P*<0.005)									
16	0,485	0,718	0,983	1,165	0,582	0,447 *(P=0,154)*	0,684 *(P=0,018)*	1,449 *(P=2,91E-07)*	0,396 *(P=0,463)*
49	3,311	2,544	2,060	1,236	2,638	-0,623 *(P=0,198)*	-0,758 *(P=0,022)*	-1,509 *(P=6,86E-07)*	-0,659 *(P=0,199)*
59	1,159	1,722	1,984	2,506	1,503	0,638 *(P=0,064)*	0,597 *(P=0,050)*	1,231 *(P=3,61E-05)*	0,582 *(P=0,192)*
94	0,434	0,273	0,263	0,162	0,351	-0,681 *(P=0,034)*	-0,665 *(P=0,036)*	-1,451 *(P=7,23E-06)*	-0,534 *(P=0,353)*
105	0,049	0,009	0,009		0,009	-1,534 *(P=1,53E-05)*	-1,238 *(P=6,75E-05)*	1,0E-06 *(P=1,21E-07)*	-1,052 *(P=0,001)*
129	0,028	0,017	0,003		0,003	-0,139 *(P=0,266)*	-0,500 *(P=0,003)*	1,0E-06 *(P=0,001)*	-0,500 *(P=0,009)*
130	0,018	0,007			0,001	-0,130 *(P=0,087)*	1,0E-06 *(P=0,001)*	1,0E-06 *(P=0,001)*	-0,457 *(P=0,010)*
131	0,029	0,014	0,006	0,007	0,002	-0,355 *(P=0,055)*	-0,578 *(P=0,004)*	-0,489 *(P=0,007)*	-1,449 *(P=0,002)*
160	0,081	0,116	0,130	0,211	0,123	0,452 *(P=0,185)*	0,410 *(P=0,139)*	1,465 *(P=3,01E-05)*	0,333 *(P=0,213)*

a) Match IDs refer to numbers in Figure 3.14 and 3.15.

b) Average intensities were determined based on spot volumes [%Vol.]; cells are blank when the protein spot is completely absent from the group.

3.2.2 Mass spectrometry identification of altered proteins during DES-PC

Among the altered protein spots, 14 out of 40 could be identified by mass spectrometry (Table 3.4). These proteins were sequenced by excising the respective spot from the 2-DE gel, digestion with trypsin and ESI-MS/MS analysis. The respective protein sequences are listed in the appendix (Table A.2).

Table 3.4: Identification of protein spots with abundance differences during DES-PC. Acc. No.: NCBI accession numbers; M_r: relative molecular mass; pI: protein isoelectric point; Calc: calculated values from GPMAW; Obs: observed value by manual inspection.

Spot ID[a)]	Sub-proteome	Acc. No.	Protein Name (short name)	No. of peptides[b)]	Sequence coverage	M_r [kDa]		*pI*	
						Calc	Obs	Calc	Obs
16	ws_6-11	NP_037309	Aspartate aminotransferase 2, mitochondrial precursor (AST-2)	9	24,9%	47	45	9,3	9,4
17	ws_4-7	NP_001005550	NADH-ubiquinone oxido-reductase 75 kDa subunit, mitochondrial precursor (NDUFS1)	1	3,9%	79	45	5,6	4,6
34	ws_4-7	NP_001129343	pyrophosphatase (inorganic) 2 (PPA2)	2 / 4	25,5%	38	37	6,7	6,5
49	ws_6-11	NP_077374	Aconitase 2, mitochondrial precursor (Aco-2)	4 / 9	18,6%	85	83	7,6	7,8
59	ws_6-11	NP_037309	Aspartate aminotransferase 2, mitochondrial precursor (AST-2)	2 / 7	24,4%	47	45	9,3	9,5
71	ws_4-7	NP_599153	Albumin precursor (ALB)	3	9,9%	69	75	6,0	6,4
94	ws_6-11	NP_112319	Methylmalonate-semialdehyde dehydrogenase, mitochondrial precursor (MMSDH)	11	24,7%	57	56	8,2	8,0
105	ws_6-11	NP_001006973	NADH dehydrogenase ubiquinone flavoprotein 1 precursor (NDUFV1)	6	12,9%	50	47	7,9	8,0
129	ws_6-11	NP_062164	Carbonic anhydrase II (CAII)	2	18,1%	29	28	7,1	6,6

Spot ID[a)]	Sub-proteome [c)]	Acc. No.	Protein Name (short name)	No. of peptides [b)]	Sequence coverage	M_r [kDa]		*pI*	
						Calc	Obs	Calc	Obs
130	ws_6-11	NP_062164	Carbonic anhydrase II (CAII)	3	16,2%	29	28	7,1	6,8
131	ws_6-11	NP_001101130	Carbonic anhydrase I (CAI)	4	17,6%	28	27	7,0	6,8
160	ws_6-11	NP_036703	Aspartate aminotransferase 1 (AST-1)	8	22,5%	46	39	6,8	7,4
201	ws_4-7	NP_036727	L-lactate dehydrogenase B (LDH-B)	6	24%	37	40	5,7	5,7
501	ds_4-7	NP_001004250	Ubiquinol-cytochrome c reductase core protein 1 precursor (UQCRC1)	4	15,4%	53	55	5,2	5,5

[a)] Match ID refers to numbers in Figure 3.14 and 3.15.
[b)] Number of sequenced peptides by ESI MS/MS, where necessary number of peptides used for PMF.
[c)] The protein spots of the neutral-acidic subproteomes (ds_4-7 and ws_4-7) were analyzed by Ch. Schuh and H. Vogt.

In general, the success rate of protein identifications by mass spectrometry was considerably higher for spots with alkaline *pIs* although their protein content was even smaller in certain cases. This might be due to the fact that the basic amino acids lysine and arginine are more frequently distributed in alkaline proteins and therefore (a) more peptides can be achieved following trypsin digestion and (b) these peptides are easier to protonate and therefore simplify MS-based identification. Spot #17 revealed only one peptide for identification, but due to the fact fact that the sequenced peptide was quite long (aa 646-673) and no further peptides were identified from the tryptic digest, protein identification was accepted.

The estimated molecular weights (M_r) and *pIs* of the spot positions in the 2-DE gels were generally in agreement with the theoretical values calculated by GPMAW (Table 3.4). Only spot #17, 71 and 160 showed divergent values for both, M_r and *pI*. The possible reason for this divergent manner might be protein degradation. Especially the reduced molecular weight supports this hypothesis. In the end, 12 non-redundant proteins were identified. Of these, six can be allocated to the mitochondrial compartment (spot #16/59, 17, 49, 94, 105 and 501). Interestingly, the most putative mitochondrial proteins were found in the water-soluble fraction, however, these spots do actually represent precursor proteins. Nearly the same set of protein spots was also collocated in spot chains (spot #16/59, 49, 94, 501).

3.2.3 Time-course of differentially expressed proteins during DES-PC

Various expression patterns were observed for the 14 identified protein spots during the course of desflurane preconditioning (Figure 3.16). Proteins which had a decreased abundance in the DES-PC group relative to the control group were: L-lactate dehydrogenase B (LDH-B), NADH-ubiquinone oxidoreductase 75 kDa subunit and NADH dehydrogenase ubiquinone flavoprotein 1, 51 kDa subunit (NDUFS1 and NDUFV1), inorganic pyrophosphatase (PPA2), albumin (ALB), ubiquinol-cytochrome c reductase core protein 1 (UQCRC1), mitochondrial aconitase (Aco-2), methylmalonate-semialdehyde dehydrogenase (MMSDH), and carbonic anhydrase I and II (CAI and CAII). Conversely, proteins which showed increased abundance during DES-PC compared to controls were the cytosolic and mitochondrial aspartate aminotransferases (AST-1 and AST-2, respectively).

Spot ID	Time course during DES-PC	DES-PC regimen				
		Ctrl 0'	Des 1	Wash 1	Des 2	Wash 2
# 17 NDUFS1	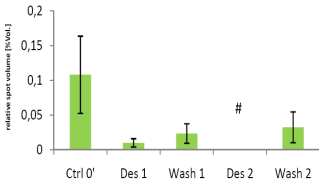	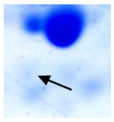	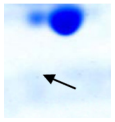	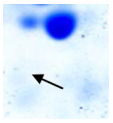	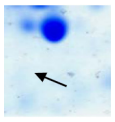	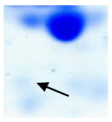
# 34 PPA2	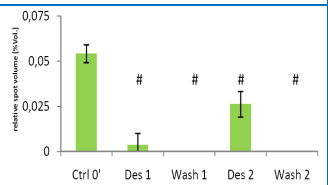	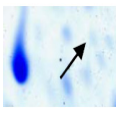	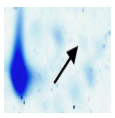	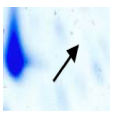	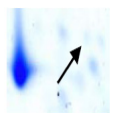	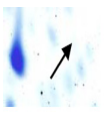
# 49 Aco-2	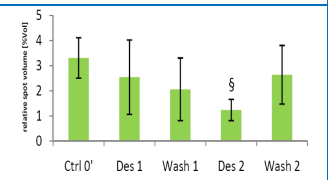	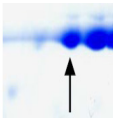	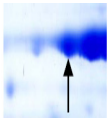	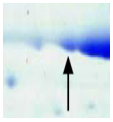	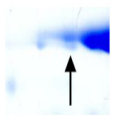	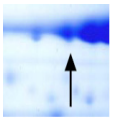
# 71 ALB	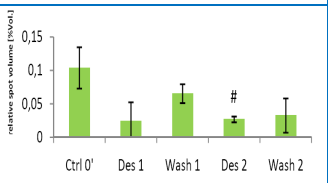	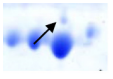	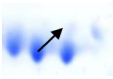	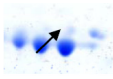	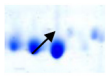	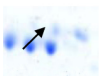

Spot ID	Time course during DES-PC	DES-PC regimen				
		Ctrl 0''	Des 1	Wash 1	Des 2	Wash 2
#94 MMSDH	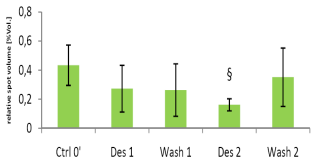	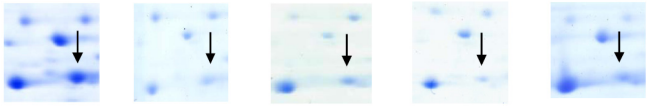				
# 105 NDUFV1		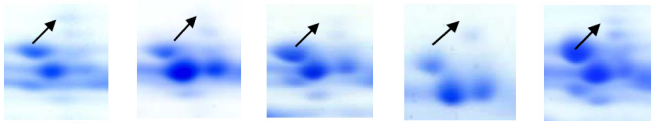				
# 129 CAII	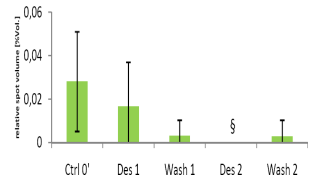					
# 130 CAII	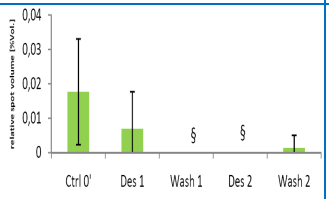	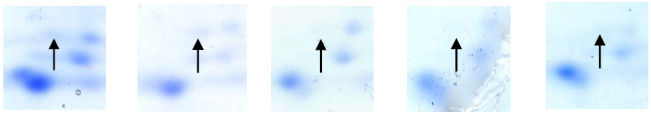				
# 131 CAI	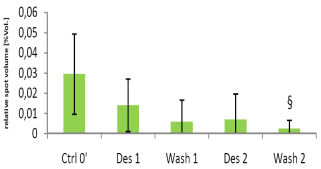	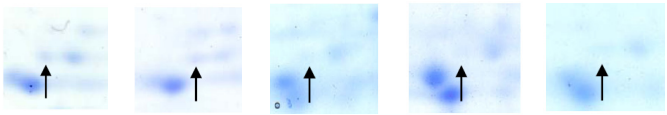				
# 201 LDH-B	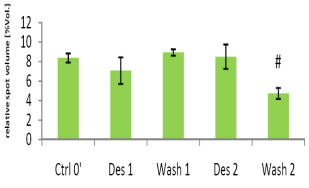	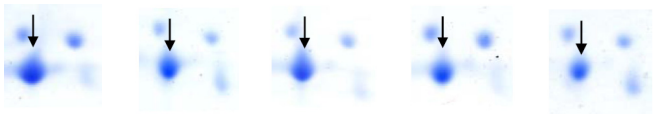				
# 501 UQCRC1	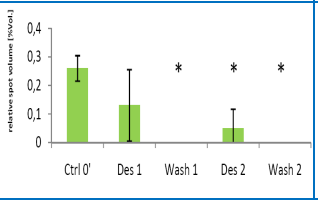	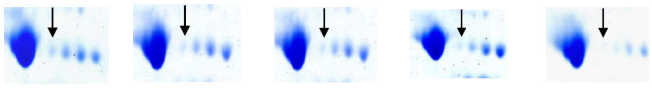				

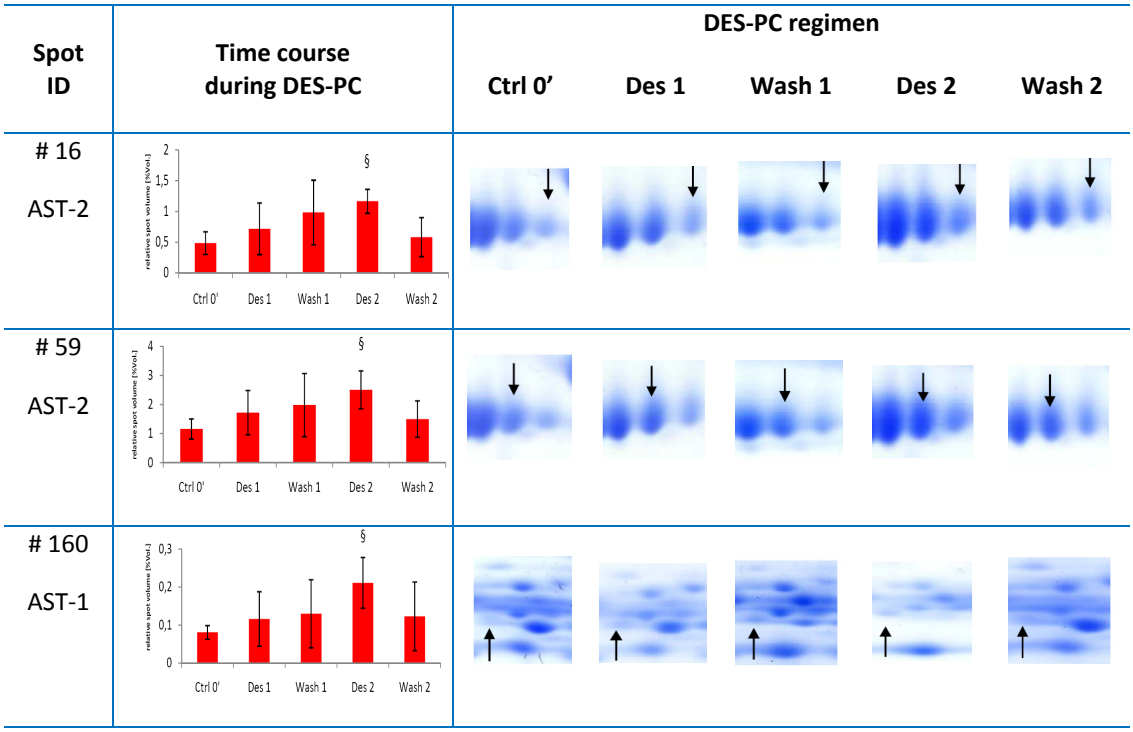

Figure 3.16: Protein expression changes in the course of DES-PC. Quantification of proteins was performed from DES-PC groups relative to the control 0' group. Data are presented as Mean (100%) and M.S.D. Statistically significant changes are indicated for the respective treatment group (**P*<0.02, #*P*<0.01, and §*P*<0.005 for ds_4-7, ws_4-7 and ws_6-11, respectively). In the enlarged regions of 2-DE gels from control and preconditioned rats, those proteins which had abundance difference between groups were indicated with an arrow.

Most protein spots were altered just at one treatment condition during DES-PC, in 7 of 9 cases after the second desflurane administration (Aco-2, albumin, MMSDH, AST-1, two protein spots of AST-2 and one protein spot of CAII). The other two spots, representing CAI and LDH-B, showed decreased abundance exclusively at the end of the preconditioning protocol (Wash 2). Four proteins (NDUFS1, NDUFV1, UQCRC1 and one protein spot of CAII) were significantly affected at several conditions during DES-PC, but all including treatment Des 2. Only one protein spot was found to be differentially expressed consistently in all experimental groups (PPA2).

Protein spots #16/59, 49 and 501 corresponding to AST-2, Aco-2 and UQCRC1 are part of a spot chain (Figure 3.16). In 2-DE separations, multiple *pI* variants of the same protein can be attributed to several factors, such as protein synthesis, protein degradation, or post-translational modification (PTM). Protein synthesis and degradation are not assumed to cause a *pI* shift resulting in spots located on a string horizontally over the gel like it is observed for AST-2, Aco-2 and UQCRC1. As

only distinct spots of these proteins exhibited abundance changes between experimental groups, the observed differential expression within the spot chain may be more likely due to PTMs such as phosphorylation, glycosylation or oxidative modification.

3.2.4 Post-translational modifications of protein spots in multiple *pI* variants

Feng *et al.* investigated the cardiac phosphoproteome of isoflurane-protected heart mitochondria, and identified numerous phosphorylated protein spots following anesthetic preconditioning (41). To determine whether DES-PC induced alterations in multiple spot isoforms result from phosphorylation changes we mapped respective 2-DE gels with ProQ Diamond Phosphoprotein stain. ProQ has been shown to directly detect phosphate groups attached to tyrosing, serine, or threonine residues and allowed selecting for proteins with high stable phosphorylation levels (133, 144).

Protein expression of spot #16/59 (AST-2) was significantly enhanced after the second desflurane administration (Des 2) (Figure 3.16). Comparing spot intensities at ctrl 0’ and Des 2 levels using ProQ, no increased phosphorylation was detected (Figure 3.17). The protein increase of spots #16/59 might therefore be independent of protein phosphorylation. Spot #49 of Aco-2 was found to be decreased 1.5-fold at treatment point Des 2, suggesting dephosphorylation during the DES-PC protocol. But neither control levels nor Des 2-treated hearts showed any phosphorylated protein spot of Aco-2 (Figure 3.17). Thus dephosphorylation seems not to be the reason for the specific alteration in spot #49 of Aco-2.

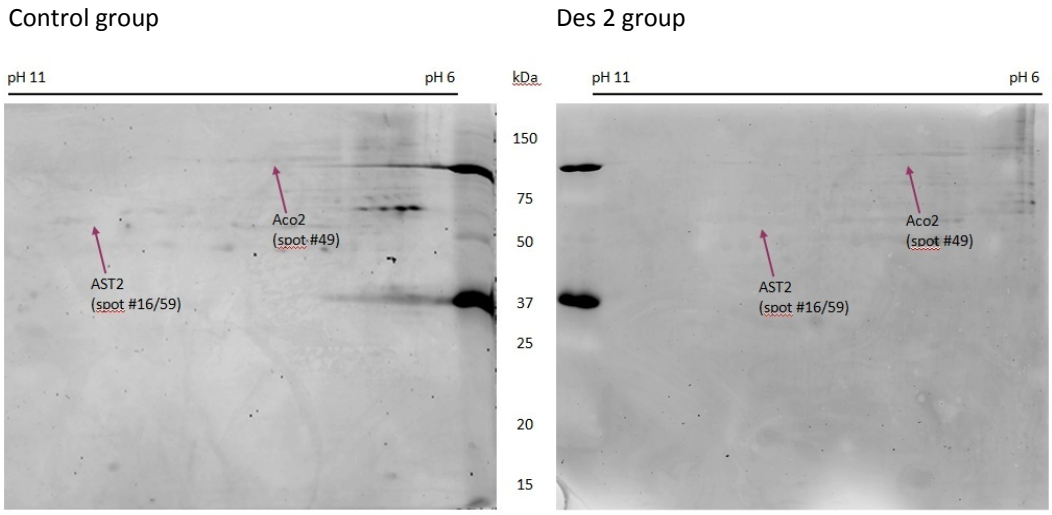

Figure 3.17: Multiple *pI* spot variants of Aco-2 and AST-2 are not phosphorylated. Post-translational phosphorylation of Aco-2 and AST-2 was investigated using ProQ Diamond stain. No differences in the phosphorylation pattern were observed during DES-PC.

UQCRC1 was significantly altered only at the most acidic protein spot (spot #501) which became completely absent after the first washout phase (Figure 3.16). Christian Schuh demonstrated in his experiments that spot #501 of UQCRC1 was phosphorylated in ctrl 0' hearts (132). Thus the decrease in abundance of spot #501 may reflect the result of dephosphorylation.

Resulting from these experiments, protein phosphorylation of Aco-2 and AST-2 during DES-PC seems to be unlikely. Besides phosphorylation, heterogeneous protein isoforms in a series of spots with the same molecular weight but different *pI* values might be due to protein oxidation. Recently, mitochondrial proteins were shown to be hot spots for oxidative modification (149). Especially Aco-2 was shown to be modified by oxidative modification at tryptophan residues (149, 60). For this reason, MS/MS analysis of spot #49, #16/59 and #501 was performed to identify peptides containing tryptophan residues and to determine possible oxidized amino acid sites by +32 atomic mass unit increase. Unfortunately, possible oxidative modifications to AST-2 could not be determined due to insufficient coverage of tryptophan native peptides. On the contrary, several peptide ions with unmodified and doubly oxidized tryptophan residues were retrieved for Aco-2 in control level and DES-PC treated hearts.

As indicated in the MS spectrum of spot #49 (Figure 3.18), the signals 493.27 $[M+2H]^{2+}$, 624.33 $[M+2H]^{2+}$ and 834.40 $[M+2H]^{2+}$ were attributed to tryptophan containing peptides of Aco-2. In the enlarged areas corresponding to respective

increments of 16 Da (atomic mass unit of two oxygen atoms in $[M+2H]^{2+}$ ions), appropriate signals at 509.30 $[M+2H]^{2+}$, 640.34 $[M+2H]^{2+}$ and 850.40 $[M+2H]^{2+}$ were located (Figure 3.19).

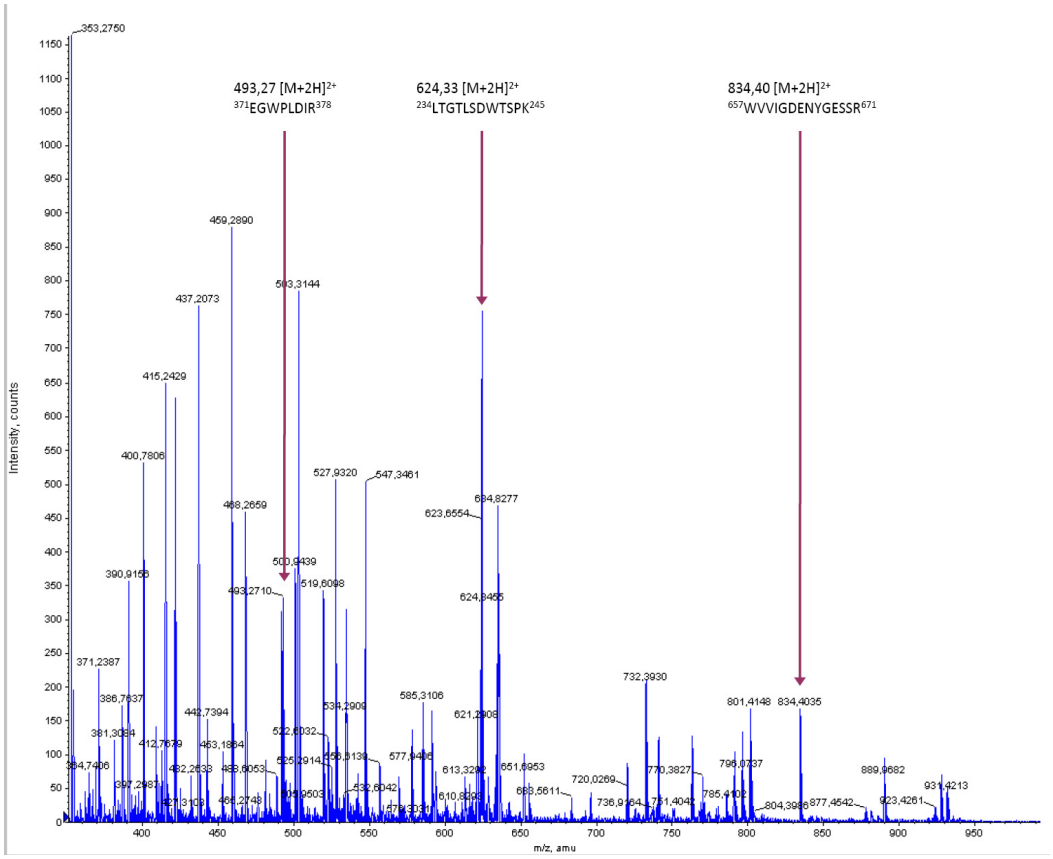

Figure 3.18: ESI-MS spectrum of proteolytic peptides of Aco-2. ESI-MS analysis revealed three tryptophan-containing peptides (indicated by arrows, peptide masses and amino acid sequence) .

It is well known that sample handling can induce oxidative modifications to amino acids, like for instance the oxidation of methionine. MS/MS analysis of protein spot #49 revealed no mono-oxidation of methionine- or tryptophan- containing peptides, indicating that tryptophan dioxidation was specific to the selected protein spot of Aco-2.

To substantiate tryptophan dioxidation (W_{2ox}), MS/MS fragmentation was used to identify the modified amino acid site(s). Fragment ions resulting from collision-induced dissociation of the tryptophan containing peptides aa 234-245, aa 371-378 and aa 657-671 revealed the respective mass shift due to dioxidation (W 186 Da $\rightarrow$ W_{2ox} 218 Da) at residue 241, 371 and 657 of Aco-2. Figure 3.19 shows the *de novo*

sequencing of the peptide at 640.34 $[M+2H]^{2+}$ Da with the amino acid sequence $^{234}LTGTLSGW_{2ox}TSPK^{245}$. The theoretical fragmentations of unmodified and oxidative modified peptides as well as the corresponding fragment spectra of the doubly oxidized peptides 509.30 $[M+2H]^{2+}$ and 850.40 $[M+2H]^{2+}$ are listed in the appendix (Figure A.2; Table A.4).

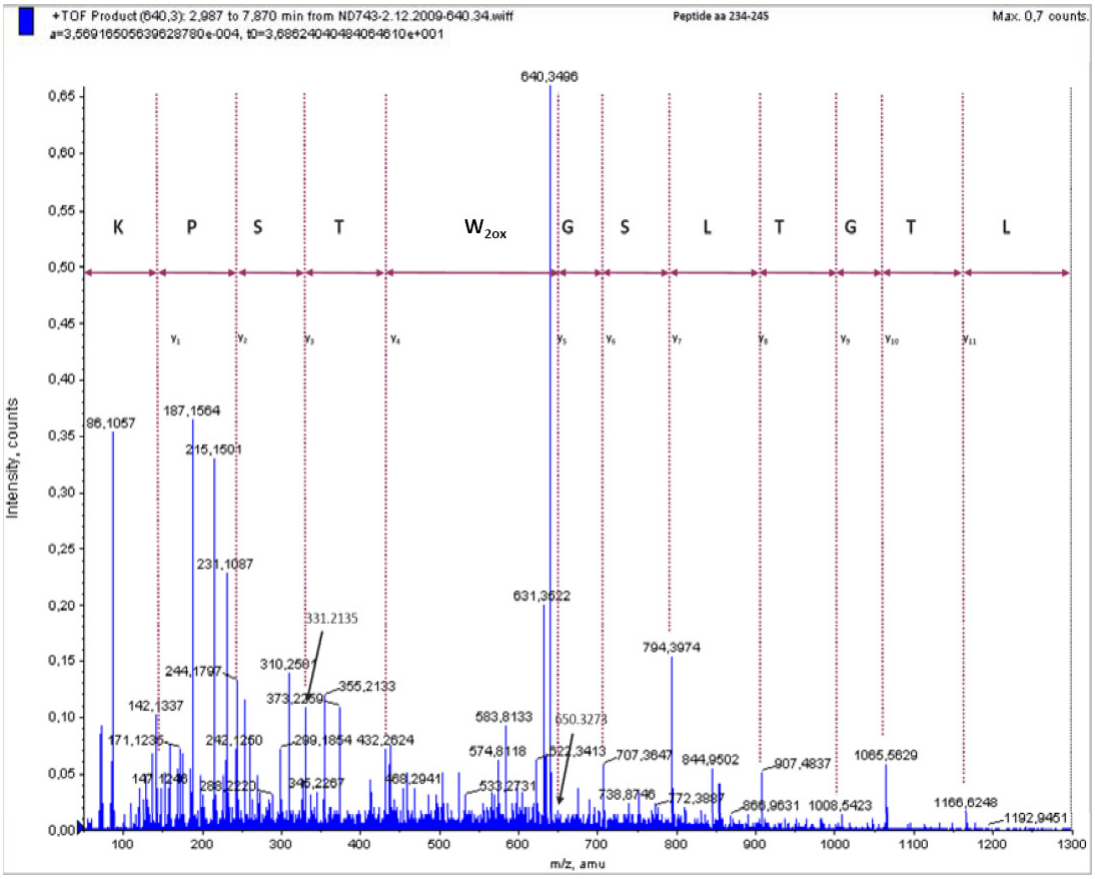

Figure 3.19: *De novo* sequencing of the Aco-2 peptide m/z 640.3434 $[M+2H]^{2+}$. Using collision induced fragmentation the complete y-ion series including the doubly oxidized tryptophan (W_{2ox}) of the Aco-2 peptide aa 234-245 was obtained from the MS/MS spectrum.

It is important to note that dioxidation of tryptophan residues was exclusively found in the spot of the control group (Figure 3.20 blue spectrum) but not in the Des 2 group (red spectrum). Oxidative modification thus seems to be abolished at least after the second desflurane preconditioning stimulus, and may hereby influence the expression ratio of Aco-2 spot #49.

aa 234-245 aa 371-378 aa 657-671

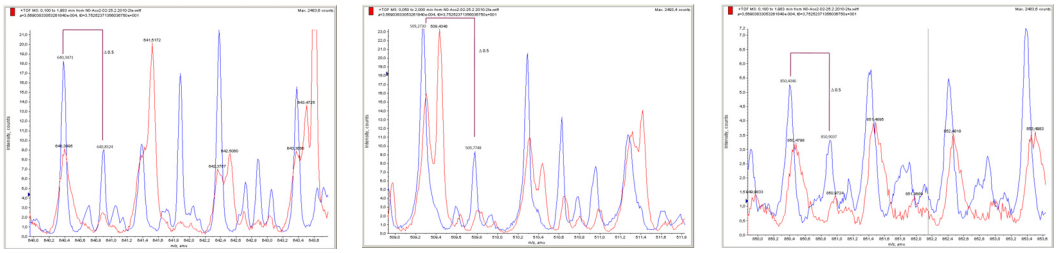

Figure 3.20: Oxidized tryptophan-containing peptides of Aco-2. The indicated peptides 640.34 $[M+2H]^{2+}$ (left), 509.30 $[M+2H]^{2+}$ (middle) and 850.40 $[M+2H]^{2+}$ (right) correspond to doubly oxidized peptides containing tryptophan. The overlay of MS spectra allow differentiating peptides from control spot (blue) and Des 2 spot (red).

The ratio between tryptophan native and oxidative modified peptides in the one and same spot (#49 of control group) was always > 0 indicating that tryptophan is predominantly non-modified. It will therefore be of interest to examine in further experiments the extent of oxidative modification in the other protein spots of Aco-2, both in control and preconditioned hearts.

3.2.5 Modulation of proteins differentially expressed during DES-PC

Comparison of the 12 proteins in the four experimental DES-PC groups revealed several clusters of related expression pattern (Figure 3.21). The significant changes in protein spot expression were not consistent for all spots at all four time points during DES-PC. Regarding the protein spots with increased abundances relative to the control group (#16, 59 and 160), all three spots show a uniform modulation over the course of DES-PC (Figure 3.21 A): a substantial increase after the first preconditioning stimulus (Des 1) with a maximum peak at condition Des 2, and a rapid drop down in expression following the second wash-out phase (Wash 2).

On the contrary, protein spots with decreased abundance during DES-PC do not have a characteristic phenotype (Figure3.21 B). The only thing in common is a more or less dramatic decrease in response to the first desflurane application (Des 1). Having a closer look at the modulation at certain treatment points, several different behavior patterns could be observed.

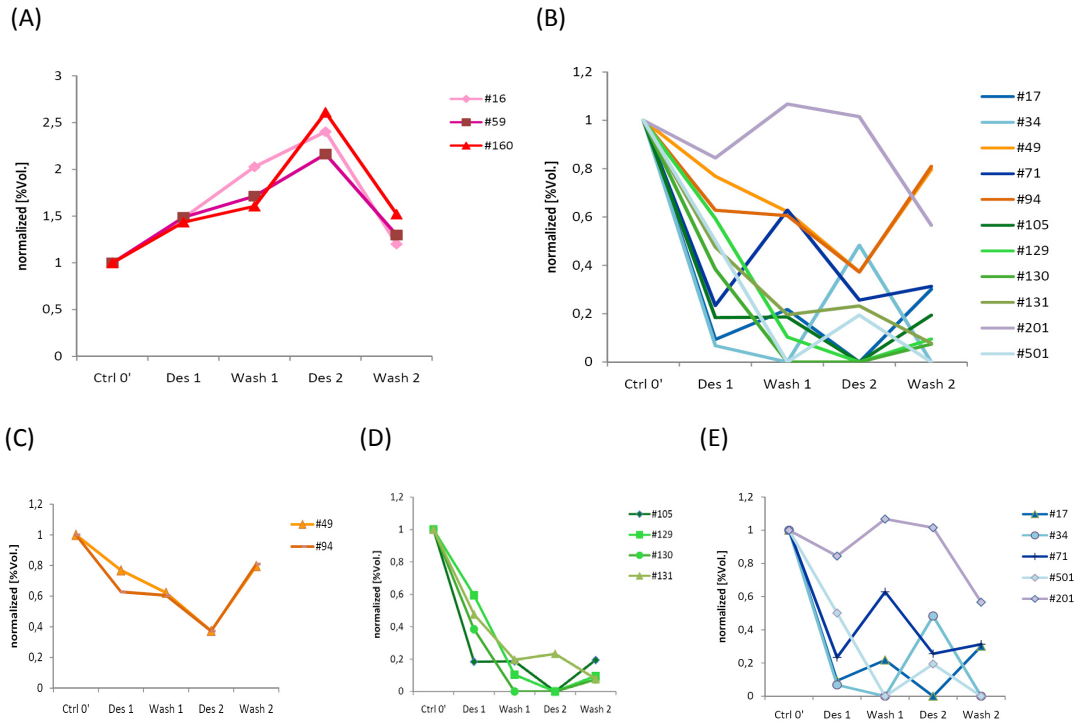

Figure 3.21: Treatment-dependent modulation of identified proteins during DES-PC. For the analysis of protein expression changes with respect to increased and decreased levels during DES-PC, individual %Vol. values of identified protein spots were normalized to the control level. (A) Protein spots that showed an increased abundance compared to control; (B) Protein spots with decreased abundance during DES-PC. (C-E) Graphs representing protein spots down-regulated in response to the desflurane preconditioning protocol sorted by similar distribution pattern.

Spot #49 and 94 show the same modulation as the increased spots but mirror-inverted: a continuous decline until Des 2 followed by an immediate increase up to expression level at condition Des 1 (Figure 3.21 C). It is noticeable that in both pattern (Figure 3.21 A+C) nearly all proteins seem to return to baseline levels of abundance.

Proteins identified from spot #105, 129 and 130 follow the same trend but totally vanish at Des 2 and reappear at Wash 2 to the same extend like at Wash 1. Spot #131 also matches to this set but its expression change at condition Des 2 is unaltered with respect to Wash 1 and Wash 2. In the end, all four spots have in common that their expression level remains significantly altered (Figure 3.21 D).

The third set of proteins consisting of spot #17, 34, 71, 201 and 501 looks quite cluttered at first sight (Figure 3.21 E). In comparison to control, the expression changes take a course up and down. However, spot 71 and 17 on the one hand and spot 34 and 501 on the other hand show a similar developing. And comparison

of these two groups reveals that spots 34 and 501 reflect the behavior of spots 17 and 71 but in a delayed manner.

All spots are present in moderate abundance except spot 201 which is highly abundant (0.5 Vol.% *vs.* 8 Vol.% in control gels). This might be the reason why its expression intensity does not considerably alter in comparison to the rest of the protein spots. Nevertheless, the appearance of spot 201 significantly declines about the half after the second washout phase (Wash 2).

3.2.6 Classifications of proteins involved in DES-PC

Based on the annotations of the NCBInr database, the 12 identified proteins were functionally classified into categories with regard to their molecular function and biological processes. Classification of proteins was based on the PANTHER (Protein ANalysis THrough Evolutionary Relationships) classification system (http://www.pantherdb.org/). Categorization on the basis of molecular function showed that 50% of identified myocardial proteins account for two classes: reductase and dehydratase (each 25%), followed by transaminases and dehydrogenases which make up each 17% (Figure 3.22 left). In turn, these proteins are involved in fundamental processes of the cardiac metabolism including the Krebs cycle, oxidative phosphorylation and electron transport (Figure 3.22 right). The remaining two proteins exhibit pyrophosphatase activity and carrier function, altogether 16%.

Among the distinct proteins, 11 out of 12 are metabolically active enzymes involved in aerobic metabolism or enzyme subunits with a wide spectrum of catalytic and regulatory activities. The majority of proteins is associated with the amino acid metabolism (AST-1 and AST-2, MMSDH), followed by electron transport proteins (NDUFS1 and UQCRC1) as well as the carboanhydrases (CAI and CAII) which participate in the metabolism of hydrocarbons and phenolic compounds that are not proteins or lipids. Other proteins belong in equal parts to the oxidative phosphorylation (NDUFV1), glycolysis (LDH-B), polyphosphate catabolism (PPA2) and Krebs cycle (Aco-2). The only non-metabolic protein is associated with transport (ALB).

Molecular function

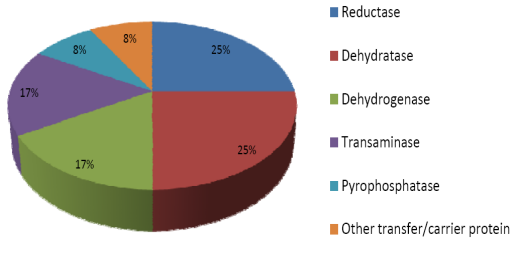

Biological process

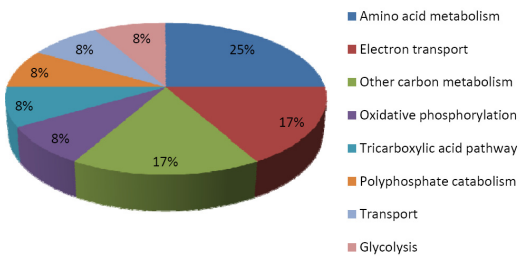

Figure 3.22: Function and biological process of identified proteins. The 12 distinct identified proteins were plotted in a pie chart relating to their function (left) and biological process (right). Categorizations were based on information provided by the online PANTHER classification system.

4 Discussion

The primary goal of this study was to identify alterations in the cardiac proteome which possibly enlighten the phenomenon of anesthetic preconditioning, using an experimental model of desflurane-induced preconditioning (DES-PC). In the field of anesthetic preconditioning this is the first proteomics approach using an *in vivo* model. Furthermore, this study is specifically focused on myocardial protein alterations *during* the preconditioning regimen with the aim to identify trigger molecules of the cardioprotective signaling pathway. In the context of anesthetic preconditioning there is only one previous proteomics study of isoflurane-induced preconditioning, analyzing protein phosphorylation in the mitochondria of isolated perfused hearts undergoing ischemia-reperfusion (41).

To investigate differential protein expression in the time course of DES-PC, heart tissue from untreated and desflurane preconditioned rats were examined by 2-DE, total protein staining, and mass spectrometric analysis. The comparative analysis of proteins with changed abundance revealed that:

- The cardiac proteomes of untreated and desflurane preconditioned rats were strikingly different even though they had similar hemodynamics and cardiac function
- DES-PC rats had significantly altered abundances especially in proteins involved in energy metabolism
- Differentially expressed protein spots showed various modulations in the time course of DES-PC
- Not all protein spot isoforms of the same protein show abundance changes indicating specific regulations during DES-PC
- Preliminary experiments investigating post-translational modifications of multiple spot isoforms reveal phosphorylation and oxidative modification as possible regulator

In order to judge the contribution of this study to the understanding of DES-PC it is necessary to be aware of the advantages and limitation of proteomic approaches. The greatest challenge in 2-DE based analyses is the right sample preparation strategy. Without reducing complex protein samples such as mammalian tissue the resulting 2-D gel is crowded with poorly resolved spots, making interpretation of

proteome profiles difficult. Optimizing the 2-DE procedure is therefore a fundamental step before performing comparative analyses.

4.1 Better proteome characterization using optimized 2-DE

In theory approximately 10.000 proteins are expressed in the human heart (93). In practice only a subset of proteins can be displayed on a wide-range (pH 3-10) 2-DE gel. But how much proteome resolution is necessary for a practical and meaningful 2-DE gel approach using comparative proteomics?

Li *et al.* tried to provide guidance for cardiac proteome analyses in terms of selection of the *pI* separating window, accurate quantitation of protein abundance, reduction of sample complexity and enrichment of low-abundant proteins (88). In their experiments they characterized the cardiac proteome in the pH range 3-10 as well as in narrow-range IPG strips for a deeper view on neutral proteins (pH 5-8 and 5.5-6.7). Spot quantitative comparison was performed between silver- and SYPRO Ruby- stained gels. To evaluate the separation power upon subcellular fractionation, they analyzed the effectiveness of commercially available kits for isolating protein fractions of cardiac tissue. Anyhow, the 2-DE gels observed in this study lack in well-focused protein pattern. For this reason, numerous procedures concerning sample preparation and isoelectric focusing were tested to provide maximal spot separation and proteome coverage. Particular attention was turned to the alkaline proteome to overcome spot streaking present by default 2-DE separations.

4.1.1 Establishment of a fundamental protein extraction procedure

Direct extraction of proteins in urea-containing sample buffer offers the advantage to perform only few interventions prior to IEF and concurrently introduce just little modifications to the proteins. For the use of solid tissue like the heart, only incomplete cell disruption and/or solubilization of proteins was achieved using this conventional buffer (Figure 3.1). The bad extraction efficiency might be amplified due to co-extraction of non-protein cellular components that interfere with protein migration. The occurrence of an intense precipitation streak at the acidic

end of the IPG strip supports this assumption. Several individual proteins actually show intense spots and cannot be resolved equally well with any of the other tested extraction methods.

TCA-acetone preparation, which is specifically recommended for samples from difficult protein sources with high levels of interfering substances like tissue, showed the worst extraction efficiency (Figure 3.1). The method is known to produce protein solutions substantially free of salts, nucleic acid and other contaminating substances which therefore cannot be the reason for the low amount of protein spots resolved on the 2-D gel. But during the precipitation procedure not only proteins of the ground tissue sediment but also particulate material which concomitantly disturbs isoelectric focusing of proteins.

In comparison to these two protocols, the best 2-DE result was obtained when using the physiological protein extraction method (Figure 3.1). In fact, a multitude of proteins was separated but due to compressed areas where high-abundant proteins mask spots of low-abundant proteins a considerable loss of resolution was the consequence. In order to reduce that complexity, sample prefractionation was an important aspect in the experiments. Protein extraction using sequential solubilization is reported to increase the overall number of proteins detected in a sample (97). In this work, step-wise increasing of the extraction power, using first an aqueous buffer for the extraction of cytosolic proteins followed by a detergent-based solution to recover matrix and membrane-associated proteins, provided a complementary way to achieve better proteome coverage (Figure 3.1). This observation is consistent with a study on the intracellular localization of murine heart and skeletal muscle proteins (124). They found out that cardiac proteins were largely derived from mitochondria, followed by multiple subcellular localization and cytosol. And only 6% of heart proteins are allocated to the nucleus. This implies that the same quantity of protein was distributed over a fewer number of proteins and thus individual protein spots have increased abundance whereas low-abundant proteins disappear.

4.1.2 Improving proteome coverage by the use of overlapping subproteomes

The use of partially overlapping pH gradients (pH 4-7 and pH 6-11) enhanced the number of proteins detectable in each 2-DE gel and allowed a suitable increase in resolution for acidic-neutral and alkaline proteins (Figures 3.5 and 3.6). In combination with sample prefractionation, proteome coverage was considerably improved. However, the representation of proteomes by 2-DE are restricted to those proteins that are soluble at every stage of analysis including tissue homogenization, isoelectric focusing and SDS-PAGE. In order to maximize the myocardial proteome observed by 2-DE, Stanley and colleagues examined the efficiency of different zwitterionic detergents in solubilizing proteins during tissue extraction as well as IEF (143). The results of this study demonstrate that the standard detergent CHAPS is a reasonable detergent for 2-DE but possesses a decreased ability to solubilize proteins compared to linear sulfobetaines like ASB-14 and SB 3-10. Unfortunately, ASB-14 in the focusing buffer seems to cause pronounced horizontal streaking towards the basic end of the IPG strip.

Due to different protein compositions in the accordant subproteomes (water-soluble *vs*. detergent-soluble, neutral-acidic *vs*. basic pIs), the effectiveness of different protein solubilization protocols for IEF were employed. Of particular interest was the observation that the choice of detergent allowed for the selective solubilization of proteins presumably based on their physiochemical properties. Whereas CHAPS alone was most suitable for the resolution of acidic-neutral proteins in pH 4-7 IPG strips, the combination of CHAPS and ASB-14 (each 2%) superiorly solubilized basic proteins (IPG 6-11). The addition of ASB-14 to CHAPS containing IEF buffers has also been reported to be superior for the analysis of ribosomal and nuclear proteins in very alkaline 2-DE gels (49). This highlights that buffers with individual detergent compositions are necessary for IEF of different protein fractions.

4.1.3 De-streak business of basic proteins

Whereas 2-DE optimization of acidic and neutral proteins was a generally quite uncomplicated procedure, the analysis of basic proteins in alkaline IPG strips is more challenging. Sample application via cup-loading is preferable to sample in-gel

rehydration when analyzing alkaline proteins (52). The choice of the sample application point further has a great impact on the gel quality. In general, anodic cup-loading sample application is recommended for separation in alkaline regions above pH 8 (28, 7, 81, 115). On the contrary, Corbett *et al.* showed that human cardiac proteins were preferably applied at the cathode (25). For the analysis of cardiac tissue proteins in alkaline pH regions, cup-loading as alternative sample application method was investigated. Comparison of cathodic and anodic sample application revealed that the latter one performed better in terms of improved protein coverage and enhanced spot intensity (Figure 3.8). Unfortunately, cup-loading is restricted to sample volumes of 100-150 µl, and a maximum protein concentration of 100 µg/ 100 µl (51). Larger sample loads can lead to protein aggregation and precipitation in the sample cup or at the interface between sample solution and the IPG strip gel. To overcome this restricted protein load a repetitive refilling of the cup was established (Figure 3.9). This trivial idea actually allows sample application of semi-preparative protein loads (at least 2-fold of the recommended sample loads).

The problem of non-specific oxidation, due to the fact that DTT migrates off the basic part of the IPG strip, can be overcome by a continuous influx of DTT from a paper wick reservoir at the cathode (59). A less pedestrian and more permanent strategy is the use of hydroxyethyl disulfide (HED) as de-streaking agent for first dimension separation (108). In the present study, replacing DTT by HED counteracts the phenomenon of pronounced streaking and the appearance of artificial spots in the alkaline pH range of IPG 6-11 strips (Figure 3.11). Thus, the analysis of basic proteins of the cardiac proteome was considerably improved by the use of IPG 6-11 zoom gels in combination with repetitive anodic cup-loading, and HED as reducing agent to prevent EOF as well as to preserve the reduced state of proteins during IEF.

4.2 In search of proteins that cause cardioprotection by anesthetic-preconditioning

4.2.1 Evaluation of intrinsic variability of 2-DE in *in vivo* experiments

The natural consequence of separating hundreds of proteins in 2-DE approaches is high gel-to-gel variability which strongly influences a comparative analysis. To judge the effect of sample preparation and system error across the different subproteomes investigated, scatter plot analysis was performed. Despite higher interventions due to cup-loading application and repetitive sample load, it is notable that the mean of the correlation coefficient (*Corr*) in the experiments for the basic subproteome was quite similar to the data obtained from the subproteomes investigated by in-gel rehydration (*Corr* 0.898 versus 0.961 and 0.995) (Table 3.2). The respective coefficients of variation (CV) values (26% and 27% for the subproteomes in pH 4-7, and 40% for pH 6-11) were also very favorable when compared to difference gel electrophoresis (DIGE) experiments. DIGE was developed to overcome limitations in reproducibility as two protein samples are separately labeled with different fluorescent dyes and then co-electrophoresed on the same 2-DE gel. A multi-laboratory assay using DIGE and other single stain experiments reported spots variations of <15% for DIGE, and 20-40% for Sypro Ruby and silver respectively (9).

As expected, sample-to-sample variation was determined to be greater than the experimental variance because it is the sum of experimental plus any animal-to-animal protein expression variations. The *Corr* and CV values for cup-loading experiments may appear high (Table 3.2) but to my knowledge there are no other studies which investigated the reproducibility of this sample application method. Regarding the analysis of pH 4-7 gels, the CV values were far better than reported in other studies dealing with myocardial tissue (88, 53). And in comparison with reports of cell culture experiments which show CV% values of 31.2% for bacterial cells, 26% for mammalian tissue cultures, and 46.6% for mammalian primary cell cultures (98), the *in vivo* experiments showed comparable reproducibility to *in vitro* studies. This highlights that optimizing the 2-DE procedure in comparative analyses is crucial for the reliability of the results obtained.

4.2.2 Implication of differentially expressed proteins for DES-PC

The present study aimed at identifying protein alterations in the myocardium of desflurane-preconditioned rats to contribute to the understanding of cardioprotection. Prior to introducing large-scale technologies as powerful tools for unraveling pathways of complex (patho-) physiology, hypothesis-driven research on a limited number of proteins was conducted, and the results were cumulated to answer the specific question. By contrast, the new *-omics* studies are more discovery-driven and generate a large amount of data that gives the researcher the opportunity to select targets of interest to be analyzed afterwards.

Application of the microarray technology to an *in vitro* model of anesthetic preconditioning (APC) has shown that isoflurane highly modulates gene expression in the heart (137). Among a huge number of commonly regulated genes (e.g. cell defense), a pool of protective and antiprotective genes was found to be differentially regulated in APC. Conversely, the same working group recently showed in a proteomics approach that isoflurane-preconditioning (ISO-PC) did not induce any significant changes in the protein expression levels of mitochondria, but instead evoked profound alterations in the phosphorylation pattern (41). This clearly demonstrates that a study of gene expression can not accurately predict the embodiment of the respective proteins (2).

Using an optimized gel-based approach for the analysis of proteomic alterations during DES-PC (summarized in chapter 3.1.5), 70 protein spots were found to be affected in the rat heart (Figure 3.15), indicating a highly general response to DES-PC. To ensure statistical significance analysis was restricted to those proteins which hold a $P<0.02$ in the ANOVA statistics. In the end, 40 protein spots showed significant expression changes during the DES-PC protocol (Table 3.3). Among the 12 identified non-redundant proteins, eleven were involved in various metabolic processes (Table 3.4, Figure 3.23). The myocardium is known to tolerate brief exposure to ischemia by preserving energy levels. The reversible inhibition of mainly mitochondrial metabolism can serve to prevent the pathologic cascade of events in ischemia-reperfusion injury. The proteome alterations found in this study may therefore account for the cardioprotective benefit of preconditioning.

4.2.2.1 Cardioprotective mechanism of preconditioning

APC and ischemic preconditioning (IPC) share many fundamental steps (Figure 4.1). Both are thought to be initially induced by stimulation of G-protein coupled receptors and subsequent activation of various types of interacting protein kinases, and by increased formation of nitric oxide and free oxygen radicals. Both preconditioning stimuli finally prime the opening of sarcolemmal and mitochondrial K_{ATP} channels, thereby constricting Ca^{2+} overload (for references see (156, 58)). Ca^{2+} overload results in mitochondrial dysfunction with depolarization of the mitochondrial membrane and uncoupling of respiration and oxidative phosphorylation (1, 35, 42), and the magnitude of these changes correlates with cell death (34). In this context, the identified proteins will be discussed in the following.

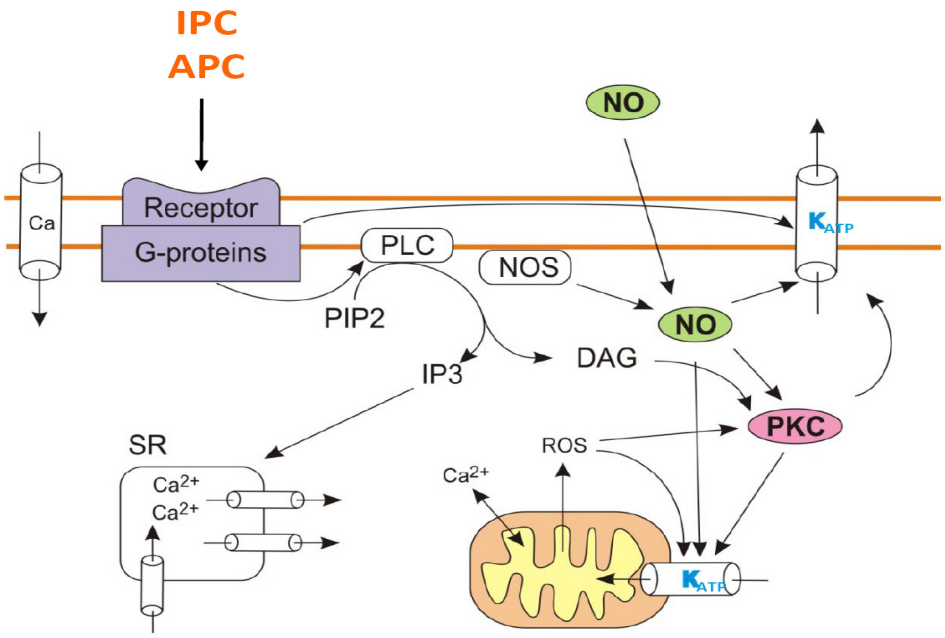

Figure 4.1: Preconditioning signaling in the early phase of cardioprotection. Simplified scheme of mechanisms involved in ischemic- and anesthetic-induced preconditioning. Ca, sarcolemmal L-type Ca^{2+}-channel; K_{ATP}, sarco-and mitochondrial K_{ATP} channels; PLC, phospholipase C; PIP2, phosphatidylinositol biphosphate; IP3, inositoltriphosphate; SR, sarcoplasmic reticulum; NO, nitric oxide; NOS, NO synthase; DAG, diacylglycerol; PKC, protein kinase C; ROS, reactive oxygen species. Figure was adapted from (168).

4.2.2.2 Metabolic inhibition as mechanism of anesthetic preconditioning

Aconitase-2

Aconitase-2 (Aco-2; EC 4.1.2.3) is an iron-sulfur protein that catalyses the stereo-specific isomerization of citrate to isocitrate via cis-aconitate in the Krebs cycle, a reaction essential to normal metabolic function. Aco-2 is particularly susceptible to oxidation at the Fe-S cluster in its active site. Oxidatively modified proteins are generally dysfunctional, losing catalytical or structural integrity. Inactivation by Fe-S oxidation may block normal electron flow to oxygen, leading to an accumulation of reduced metabolites such as NADH. Aco-2 has been implicated in oxidative stress regulation and cardiac ischemia-reperfusion injury (17).

Aco-2 is represented by multiple *pI* variants (Figure 3.18), whereby only one spot variant was found to be differentially regulated during DES-PC (Table 3.4). In an effort to understand this specific regulation, the possibility of post-translational modification (PTM) was investigated. Interestingly, Aco-2 did not show any phosphorylation pattern (Figure 3.19) but was doubly oxidized at tryptophan in control but not DES-PC hearts (Figure 3.21). No relationship was observed between the tryptophan modification and methionine oxidation, a known artifact of sample handling (120). The specificity of this response indicates that these changes are not random events that may arise from nonspecific oxidation, but rather are targeted effects. In any case the ratio between unmodified and tryptophan oxidized peptides was quite small, thus this oxidation may be not regulatory *per se*. We only investigated the protein spot which was differentially regulated during DES-PC, thus it would be of general interest if the other isoforms of Aco-2 show tryptophan modification to a greater extend.

Aspartate aminotransferases

The only protein isoforms with increased abundance during DES-PC were found to be aspartate aminotransferases (AST; EC 2.6.1.1) (Table 3.4). AST is a pyridoxal phosphate-dependent enzyme which exists in cytoplasmic and inner-membrane mitochondrial forms, AST-1 and AST-2, respectively. AST plays a role in amino acid metabolism and the urea and Krebs cycles where it catalyzes the conversion of aspartate and alpha-ketoglutarate to oxaloacetate and glutamate.

Cytosolic AST-1 participates in the malate-aspartate shuttle which exchanges cytoplasmic malate for mitochondrial aspartate and allows the transport of

reducing equivalents across the inner mitochondrial membrane. During ischemia reduced equivalents become accumulated and lead to intracellular acidosis. Enhanced AST-1 level during DES-PC may contribute to cardioprotection by triggering post-ischemic removal and oxidation of NADH. The increase of AST-1 seems to be specific for anesthetic preconditioning as neither IPC, nor pharmacological PC with resveratrol, adenosine or diazoxide reported changes in its expression so far (163, 12, 4). Regulation due to desflurane itself can be negated by the proteomic study of Kalenka *et al.* who did not document any changes of AST-1 expression after desflurane anesthesia (65).

During DES-PC, multiple *pI* variants of mitochondrial AST (AST-2) were detected in the cytosolic fraction (Figure 3.18). From the current data one cannot exclude that the high amount of AST-2 in the cytosolic fraction results from an inappropriate sample fractionation protocol as we did not finish the analysis of the alkaline pH region for the detergent-soluble fraction so far. However, in IR injury AST-2 was also found to be significantly increased in the cytosolic fraction, and dramatically decreased in heart mitochondria, respectively (110, 41). The protein abundance changes were only detected for the two spots at the acidic end of the chain. Both isoforms were found to be maximal expressed after the second desflurane administration, possibly indicating an increase in protein phosphorylation. But using ProQ Diamond phosphoprotein stain, no phosphorylation was detectable in protein spots of AST-2 in the time course of DES-PC (Figure 3.19). Due to the low sequence coverage of tryptophan-containing peptides we could not investigate oxidative modifications like found for Aco-2. At present it is therefore not possible to state any contribution of phosphorylation or oxidation to the multiple protein isoforms of AST-2, nor can be concluded that specific protein spot isoforms exclusively may affect the preconditioning effect.

Carbonic anhydrases

Carbonic anhydrases (CA; EC 4.2.1.1) are zinc-containing enzymes that catalyze the reversible reaction between carbon dioxide hydration and bicarbonate dehydration to maintain acid-base balance in blood and other tissues. They have essential roles in facilitating the transport of carbon dioxide and protons in the intracellular space, across biological membranes and in the layers of the extracellular space. By increasing the movement of protons, CA can dissipate pH gradients, thereby helping the cell to maintain a uniform intracellular pH. As a

result, the inhibition of CA will lead to intracellular acidosis that could reduce muscle contractility and calcium handling.

Two of the 15 mammalian CA isozymes (CAI and CAII) were found to be significantly reduced in the time course of DES-PC (Table 3.3), possibly provoking mild intracellular acidosis. DES-PC may thus induce an adaptive mechanism to maintain proper calcium homeostasis during upcoming severe periods of acidification, such as prolonged ischemia during myocardial infarction. In accordance with this hypothesis, hypoxic preconditioning was found to improve contractility, Ca^{2+} handling and cell recovery during subsequent hypoxic insult (77).

Intracellular acidosis was shown to activate p38 mitogen activated protein kinase (MAPK) that constitutes a mediator to deliver hypoxia-induced apoptotic signal in cardiomyocytes (169). Our group recently studied the regulation of different MAPKs during DES-PC but did not detect any significant increase in p38 MAPK phosphorylation in the course of the regimen (157). Da Silva and co-workers also could not demonstrate an involvement of p38 MAPK in isoflurane-induced preconditioning in the isolated rat heart (140). On the contrary, in hyperglycemia hearts where DES-PC is abolished, phosphorylation of p38 MAPK was significantly increased (157). These studies suggest that p38 MAPK inactivation may play a role in APC-induced cardioprotection. The reduced CAI and CAII abundances during DES-PC may therefore represent a cardioprotective action by establishing a mild acidosis that in turn renders the myocardium more resistant to ischemia-reperfusion injury.

Lactate dehydrogenase B

Lactate dehydrogenase B (LDH-B; EC 1.1.1.27) is an enzyme that participates in the final step of anaerobic glycolysis. During ischemia it converts pyruvate to lactate with concomitant interconversion of NADH and NAD^+ resulting in the production and intracellular accumulation of lactate and H^+. Lactate is exported with H^+ via the lactate/H^+ co-transporter. H^+ efflux also occurs via the Na^+/H^+ exchanger, resulting in high intracellular Na^+ concentrations that have been related to Ca^{2+} influx and ischemic damage. IPC was found to reduce post-ischemic lactate levels of the heart to ~70% of values in non-preconditioned hearts (165). During DES-PC we detected decreased LDH-B levels at the end of the preconditioning regimen (Table 3.3). As LDH can be inactivated by ROS (103), and ROS mediates DES-PC in the human heart (57), DES-PC might prepare for upcoming ischemic events by depressing

lactate levels in the cytosol. This probably regulates the lactate/pyruvate ratio which influences the NADH/NAD^+ ratio in the cytosol. In accordance with this hypothesis, metabolic modulation of the cytosolic NADH/NAD^+ ratio by pyruvate was shown to protect the heart from ischemia–reperfusion injury (112).

Methylmalonate-semialdehyde dehydrogenase

Methylmalonate-semialdehyde dehydrogenase (MMSDH; EC 1.2.1.27) belongs to the aldehyde dehydrogenases family of proteins. It is located in the mitochondrial matrix space and catalyzes the irreversible oxidative decarboxylation of malonate semialdehyde and methylmalonate semialdehyde to acetyl-CoA and propionyl-CoA, respectively (69). Acetyl-CoA is a central metabolic intermediate in the Krebs cycle and a substrate of fatty acyl-CoA in fatty acid synthesis. Propionyl-CoA is also fed into the Krebs cycle after conversion to succinyl-CoA. Suppressed MMSDH expression was demonstrated to alter the concentration of Krebs cycle metabolites in rice, suggesting that acetyl-CoA was reduced by decreased amounts of MMSDH (148).

During DES-PC, MMSDH was found to be decreased in abundance (Table 3.3). MMSDH was demonstrated to decrease dramatically under oxidative stress (145). Furthermore, MMSDH was found to be oxidized following hepatic ischemia-reperfusion injury (99). Thus increased degradation of oxidatively modified MMSDH may contribute to the reduced level of MMSDH during ischemia.

During ischemia, NADH increases because O_2 shortage limits NADH oxidation at the electron transport chain. MMSDH is quite sensitive to inhibition by NADH (47), thus an increase in the mitochondrial NADH/NAD^+ ratio may inhibit MMSDH. Interestingly, both IPC and SEVO-PC have been shown to reversibly increase NADH (127). DES-PC may mimic ischemic metabolic responses by enhancing NADH/NAD^+ ratio and therefore inhibit MMSDH. But enzyme inhibition does not necessarily correlate with decreased protein expression.

Inorganic pyrophosphatase

Inorganic pyrophosphatase (PPA2; EC 3.6.1.1) catalyzes the hydrolysis of inorganic pyrophosphate (PP_i) to two orthophosphates, and can be considered to be the simplest possible model of biological utilization of high-energy phosphates. Compared to control levels, PPA2 was significantly decreased during the whole preconditioning protocol (Table 3.3), possibly leading to accumulation of PP_i in the

cytosol. During ischemia, when cellular ATP pools become diminished and enhance the open probability of the sarcolemmal K_{ATP} channel, the preferential utilization of inorganic pyrophosphate (PP_i) as an energy donor may then counteract Ca^{2+} overload. Thus accumulated PP_i may be a metabolic adaptation of the preconditioned myocardium to subsequent environmental extremes like ischemia that cause depressed ATP pools.

Complex I and III subunits of the respiratory chain

Previous studies reported a profound attenuation of the mitochondrial electron transport by volatile anesthetics. The inhibition of the electron transfer leads to an increased generation of ROS. ROS participate in the process of APC, which in turn trigger the opening of K_{ATP} channels and prevent Ca^{2+} overload in the mitochondria (146, 100, 105, 136). In accordance with that, a down-regulation of several proteins involved in electron transport chain was found (Table 3.4), including NADH-ubiquinone oxidoreductase 75 kDa subunit (NDUFS1) and NADH-dehydrogenase ubiquinone flavoprotein 1 (NDUFV1) of complex I (EC 1.6.5.3), and ubiquinol-cytochrome c reductase core protein 1 (UQCRC1) of complex III (EC 1.10.2.2). All three enzymes showed the same modulation during DES-PC, namely a dramatic decrease directly after the onset of the preconditioning protocol. Decrease in the level of NDUFS1 has been found to result in reduced electron transport and ROS generation (62).

Reduction of complex I would be expected to decrease the rates of NADH oxidation in the mitochondria. During DES-PC, the soluble complex I subunits NDUFS1 and NDUFV1 showed decrease levels, possibly contributing to cardioprotection by regulating NADH/NAD^+ redox balance. NDUFS1 showed divergent values for both Mr and *pI* compared to the calculated values (Table 3.4), suggesting a shift due to protein degradation or post-translational modification. Studying the impact of oxidative stress on mitochondria, NDUFS1 was found to be decreased in cells exposed to H_20_2 (145). Recently, NDUFS1 was demonstrated to undergo dioxidation of tryptophan (96). The flavoprotein NDUFV1 was also found to be oxidatively modified (159). Protein oxidation can lead to proteolytic breakdown of the modified protein (32). Thus NDUFS1 and NDUFV1 possibly did here undergo oxidative modification that in turn evoked their degradation during DES-PC. This observation supports the hypothesis that cardioprotection is mediated by reversible metabolic shut-down (18).

Complex III of the respiratory chain represents the convergence point for electrons entering the Q cycle. Its partial inhibition is discussed to account for the cardioprotective properties of volatile anesthetics. In the present study we identified differential expression of the subunit UQCRC1 which is represented by multiple *pI* variants in the 2-DE pattern (Figure 3.18). During DES-PC, UQCRC1 was only altered at the most acidic protein spot, showing a decreased abundance after the onset of the preconditioning protocol. As an acidic shift in *pI* often is consistent with protein phosphorylation we investigated the phosphorylation status of UQCRC1 using a phosphospecific protein stain (ProQ Diamond). Preliminary results indicated different phosphorylation pattern for its spot chain (132). Interestingly, the changes in protein abundance of the most acidic *pI* variant of UQCRC1 (spot #501) seem to occur with concomitant changes in phosphorylation. This selective dephosphorylation may contribute to a mild reversible suppression of the respiratory chain that possibly attenuates oxygen consumption. This mimicry of an ischemic situation during the trigger phase of DES-PC may account for the cardioprotective benefit of desflurane during severe ischemia-reperfusion (IR) events.

Albumin

Albumin is a highly abundant protein and produces profound spots in 2-DE gels but was just identified as a faint spot at a position on the gel that does not fit to its theoretical *pI* and M_r (Table 3.4). Like postulated for NDUFS1, this modification might be the result of protein degradation. According to that, Albumin was found to be decreased during DES-PC. Interestingly, ischemia-modified albumin (IMA) has been shown to be a marker of myocardial ischemia (6). In the presence of myocardial ischemia, structural changes take place in the N-terminus of the protein which reduces its binding capacity, possibly, in part, as a result of exposure to ROS. As DES-PC is mediated by ROS, this truncated isoform of albumin possibly represents IMA. As no sequence data entry is available for IMA so far, no alignment of peptide sequences can clarify this question.

4.2.3 Proteome profiles during DES-PC reveal different expression trends

The experiments in this thesis were especially designed to analyze rapid proteomic alterations at different time/treatment points *during* the preconditioning regimen (Figure 2.1). Within 30 minutes of the preconditioning protocol, four different treatment samples were taken to track possible cardioprotective protein isoforms. In general most proteins seem to have a uniform response to the DES-PC protocol, being most distinctive after the second desflurane administration (Table 3.3). This is in accordance with the observation that DES-PC against ischemia-reperfusion injury in rabbits depends on timing and the threshold of repetitive application (84, 141). This evidence may explain why Feng *et al.* (2008) were not able to detect any protein expression change after one-time isoflurane exposure for preconditioning (41).

Despite the fact that the second administration of desflurane evokes greater effects on the cardiac proteome (Table 3.3), several different modulation patterns were observed for the identified proteins (Figure 3.22). Like it is expected during bioenergetics disturbances, metabolic enzymes were mainly decreased following DES-PC. It is possible that the down-regulation of proteins related to energy-dependant cellular functions results in a favorable change in the myocardial oxygen supply and demand relation. Of these, three replied directly after one-time desflurane exposure (NDUFV1, CAI and CAII) and two showed an exclusive response to the repetitive administration of desflurane (Aco-2 and MMSDH). The remaining protein isoforms with decreased abundance (NDUFS1, PPA2, UQCRC1, LDH-B and ALB) show random alterations during the DES-PC protocol. The increase in protein isoforms of AST was nearly to the same extend (determined by their expression ratios), possibly indicating a regulation by a shared signaling pathway.

Interestingly, protein differences appeared to be the result of isoelectric point shifts most probably resulting from chemical modifications, and molecular mass shifts resulting from proteolytic or physical fragmentation. This is consistent with the hypothesis that the time course for the onset of preconditioning associated with cardioprotection is too brief to be mediated by large changes to gene/protein expression, but rather that more subtle, rapid and potentially transient changes are occurring to the proteome

It is not remarkable that early alterations in protein abundance (within 30 minutes of preconditioning) were mainly observed for proteins associated with metabolic mechanisms (11/12 identified proteins). Since the mammalian heart has high energy requirements physiological disturbances evoked by preconditioning would induce a fast series of alterations in metabolic active proteins which finally may contribute to the ischemic tolerance during myocardial infarction. But the results of the present study clearly demonstrate that DES-PC associated proteins are not exclusively altered in their expression level but also reflect changes in protein isoforms due to post-translational modifications and degradation. But not all protein modifications will have detrimental or measurable effects on function. In summary, DES-PC seems to be a complex and dynamic process that exhibits manifold proteomic changes.

4.3 Challenges in interpreting data from proteomic studies

In recent years a large number of proteomics studies for various diseases were conducted such as for cancer, neurodegenerative and cardiovascular disorders. A typical 2-DE based proteomics study investigating differential expression features 400-1500 spots and reports between 10 and 40 identified up- and down-regulated proteins. The availability of these huge data sets with a large number of differentially expressed proteins now reveals the existence of a hit parade of repeatedly identified differentially expressed proteins (116). To explore this phenomenon the occurrence of individual differentially expressed proteins in 2-DE experiment reports were quantified performing a meta-analysis. Compiling proteins identified from human, mouse and rat tissues published in the years 2004-2006 in the journal *Proteomics* revealed a TOP 15 list that includes mostly glycolytic enzymes, heat shock, and stress proteins as well as cytoskeletal components. Studying the literature for cardiovascular proteomics, one also stumbles over nearly the same protein expression changes. Thus when interpreting the results of the current proteomics experiment in the context of the literature, the question arose: “Are these the key protein changes in metabolic enzymes responsible for cardioprotection, or are they compensatory changes which help the mitochondrion to survive?” In context to Darwin’s theory, these

protein changes are probably less specific but rather demonstrate a synergistic effect of cellular and molecular targets to adapt to metabolic stress. As such, understanding the protein (isoform) change of the different members of a given pathway is of major importance.

In the present study, several proteins appeared as multiple *pI* isoforms (Aco-2, AST-2, UQCRC1) likely due to PTMs, or were located at different positions in the gel (NDUFS1, ALB) possibly induced by protein degradation. Although all spots are isoforms of the same protein, PTMs or degradations can alter the function or localization of the protein. The protein modifications found in this study may contribute to the triggering phase of DES-PC by altering the proteins function. Thus protein modifications may play a more important role in the triggering phase than cellular protein turnover. It can be expected that further studies of post-translational isoforms of certain proteins will provide important information to expand the understanding of the mechanisms of cardiac preconditioning.

Some limitations of current proteomic methodology reflect on the ability of gel-based approaches to aid in understanding a complex physiological issue. First, to detect proteins on gels and to identify them by mass spectrometry, a minimum amount of protein is required. It has been estimated that abundant proteins, including structural proteins and metabolic enzymes, are expressed in the range of from 10^5 to 10^6 molecules per cell, while lower abundant proteins like protein kinases and transcription factors may be expressed with less than 100 molecules per cell. Thus we were not able to detect any targets known to contribute to the cardioprotection by DES-PC, like protein kinase C epsilon or extracellular signal-regulated kinase 1/2 (152). Secondly, there are also considerable difficulties in separating and identifying membrane proteins by 2-DE. Despite the efforts to optimize sample preparation and IEF, we probably did not fully solubilize highly hydrophobic membrane proteins. This may explain why the two prominent targets of the current preconditioning model, the mitochondrial K_{ATP} channel and the permeability transition pore, have not been identified in this approach. Third, many of the proteins in this study that were not evaluated due to the strict selection made for differential expression, are likely to play an unforeseen role in the mechanisms of APC. Thus we cannot exclude that the search for proteins that is based on all- or nonexpression differences yields an incomplete picture.

4.4 Conclusion

Like other proteins, Aco-2, complex I and III proteins and ASTs function in the context of complex networks; therefore, the functional impact of metabolic active enzymes stretches well beyond the scope of the current study. It should therefore be reminded that extrapolation from alterations in protein concentration to changes in enzyme activities have to be considered with great care. However, the results of the current study emphasize the extent of what remains to be discovered about the widespread effects of APC on the cardiac proteome. As such, proteomic analyses have the potential to identify previously uncharacterized effectors of such pathways and, as demonstrated in the current study, they can lead to new information about how those effectors might contribute to physiologically important phenotypes.

To be sure that the "sets of changes" provide a true description of the mechanism taking place during DES-PC, any candidate of this proteomics approach will need to be confirmed by several independent experiments. Classical biochemical methods like Western Blot or immunohistochemistry are the first choice to prove protein expression changes. To further investigate differential protein abundance, other PTMs like glycosylation, acetylation, deamidation and S-nitrosylation have to be considered. Experiments investigating protein-protein interactions will bring the identified proteins into relation, and possibly differentiate the candidates into potential triggers or secondary effectors of anesthetic preconditioning. To turn data into evidence functional verification will be necessary, i.e. by the use of inhibitor studies or transgenic animals. Finally, *in vivo* experiments with animals of cardiovascular disorders have to be carried out to address clinically relevant situations.

In summary, initial data obtained by broad-based proteomics are the framework upon which downstream experimental decisions are based. The next level of analysis already focuses on the apparent key role of the mitochondria in preconditioning, and special emphasis is placed on the analysis of post-translational modifications of protein spot isoforms.

5 Literature

1. **Altschuld R. A. 1996.** Intracellular calcium regulatory systems during ischemia and reperfusion. *EXS* **76**:87-97.
2. **Anderson L., and J. Seilhamer. 1997.** A comparison of selected mRNA and protein abundances in human liver. *Electrophoresis* **18**:533-537.
3. **Anderson N. G. 2010.** Adventures in clinical chemistry and proteomics: a personal account. *Clin. Chem* **56**:154-160.
4. **Arrell D. K., S. T. Elliott, L. A. Kane, Y. Guo, Y. H. Ko, P. L. Pedersen, J. Robinson, M. Murata, A. M. Murphy, E. Marbán, and J. E. Van Eyk**. 2006. Proteomic analysis of pharmacological preconditioning: novel protein targets converge to mitochondrial metabolism pathways. *Circ. Res* **99**:706-714.
5. **Bak-Jensen K. S., S. Laugesen, P. Roepstorff, and B. Svensson**. 2004. Two-dimensional gel electrophoresis pattern (pH 6-11) and identification of water-soluble barley seed and malt proteins by mass spectrometry. *Proteomics* **4**:728-742.
6. **Bar-Or D., E. Lau, and J. V. Winkler**. 2000. A novel assay for cobalt-albumin binding and its potential as a marker for myocardial ischemia-a preliminary report. *J Emerg Med* **19**:311-315.
7. **Barry R. C., B. L. Alsaker, J. F. Robison-Cox, and E. A. Dratz**. 2003. Quantitative evaluation of sample application methods for semipreparative separations of basic proteins by two-dimensional gel electrophoresis. *Electrophoresis* **24**:3390-3404.
8. **Baxter G. F., M. S. Marber, V. C. Patel, and D. M. Yellon**. 1994. Adenosine receptor involvement in a delayed phase of myocardial protection 24 hours after ischemic preconditioning. *Circulation* **90**:2993-3000.
9. **Bech-Serra J., A. Borthwick, N. Colomé, P. Consortium, J. Albar, M. Wells, M. Sánchez del Pino, and F. Canals**. 2009. A Multi-Laboratory Study Assessing Reproducibility of a 2D-DIGE Differential Proteomic Experiment. *J Biomol Tech* **20**:293-296.
10. **Bein B., J. Renner, D. Caliebe, R. Hanss, M. Bauer, S. Fraund, and J. Scholz**. 2008. The effects of interrupted or continuous administration of sevoflurane on preconditioning before cardio-pulmonary bypass in coronary artery surgery: comparison with continuous propofol. *Anaesthesia* **63**:1046-1055.
11. **Belhomme D., J. Peynet, M. Louzy, J. M. Launay, M. Kitakaze, and P. Menasché**. 1999. Evidence for preconditioning by isoflurane in coronary artery bypass graft surgery. *Circulation* **100**:340-344.
12. **Bezstarosti K., S. Das, J. M. J. Lamers, and D. K. Das**. 2006. Differential proteomic profiling to study the mechanism of cardiac pharmacological preconditioning by resveratrol. *J. Cell. Mol. Med* **10**:896-907.
13. **Bradford M. M.** 1976. A rapid and sensitive method for the quantitation of microgram quantities of protein utilizing the principle of protein-dye binding. *Anal. Biochem* **72**:248-254.
14. **Bukhari E. A., I. B. Krukenkamp, P. G. Burns, G. R. Gaudette, J. J. Schulman, M. R. al-Fagih, and S. Levitsky**. 1995. Does aprotinin increase the myocardial damage in the setting of ischemia and preconditioning? *Ann. Thorac. Surg* **60**:307-310.
15. **Buljubasic N., J. Marijic, D. F. Stowe, J. P. Kampine, and Z. J. Bosnjak**. 1992. Halothane reduces dysrhythmias and improves contractile function after global hypoperfusion in isolated hearts. *Anesth. Analg* **74**:384-394.
16. **Buljubasic N., D. F. Stowe, J. Marijic, D. L. Roerig, J. P. Kampine, and Z. J. Bosnjak**. 1993. Halothane reduces release of adenosine, inosine, and lactate with ischemia and reperfusion in isolated hearts. *Anesth. Analg* **76**:54-62.
17. **Bulteau A., K. C. Lundberg, M. Ikeda-Saito, G. Isaya, and L. I. Szweda**. 2005. Reversible redox-dependent modulation of mitochondrial aconitase and proteolytic

activity during in vivo cardiac ischemia/reperfusion. *Proc. Natl. Acad. Sci. U.S.A* **102**:5987-5991.

18. **Burwell L. S., S. M. Nadtochiy, and P. S. Brookes**. 2009. Cardioprotection by metabolic shut-down and gradual wake-up. *Journal of Molecular and Cellular Cardiology* **46**:804-810.
19. **Cason B. A., A. K. Gamperl, R. E. Slocum, and R. F. Hickey**. 1997. Anesthetic-induced preconditioning: previous administration of isoflurane decreases myocardial infarct size in rabbits. *Anesthesiology* **87**:1182-1190.
20. **Chen C., G. R. Budas, E. N. Churchill, M. Disatnik, T. D. Hurley, and D. Mochly-Rosen**. 2008. Activation of aldehyde dehydrogenase-2 reduces ischemic damage to the heart. *Science* **321**:1493-1495.
21. **Chinnasamy G., and C. Rampitsch**. 2006. Efficient solubilization buffers for two-dimensional gel electrophoresis of acidic and basic proteins extracted from wheat seeds. *Biochim. Biophys. Acta* **1764**:641-644.
22. **Clark B. N., and H. B. Gutstein**. 2008. The myth of automated, high-throughput two-dimensional gel analysis. *Proteomics* **8**:1197-1203.
23. **Clarke S. J., I. Khaliulin, M. Das, J. E. Parker, K. J. Heesom, and A. P. Halestrap**. 2008. Inhibition of mitochondrial permeability transition pore opening by ischemic preconditioning is probably mediated by reduction of oxidative stress rather than mitochondrial protein phosphorylation. *Circ. Res* **102**:1082-1090.
24. **Cope D. K., W. K. Impastato, M. V. Cohen, and J. M. Downey**. 1997. Volatile anesthetics protect the ischemic rabbit myocardium from infarction. *Anesthesiology* **86**:699-709.
25. **Corbett J. M., M. J. Dunn, A. Posch, and A. Görg**. 1994. Positional reproducibility of protein spots in two-dimensional polyacrylamide gel electrophoresis using immobilised pH gradient isoelectric focusing in the first dimension: an interlaboratory comparison. *Electrophoresis* **15**:1205-1211.
26. **Cordwell S. J., D. J. Basseal, B. Bjellqvist, D. C. Shaw, and I. Humphery-Smith**. 1997. Characterisation of basic proteins from Spiroplasma melliferum using novel immobilised pH gradients. *Electrophoresis* **18**:1393-1398.
27. **Corthals G. L., V. C. Wasinger, D. F. Hochstrasser, and J. C. Sanchez**. 2000. The dynamic range of protein expression: a challenge for proteomic research. *Electrophoresis* **21**:1104-1115.
28. **Cortón M., G. Villuendas, J. I. Botella, J. L. San Millán, H. F. Escobar-Morreale, and B. Peral**. 2004. Improved resolution of the human adipose tissue proteome at alkaline and wide range pH by the addition of hydroxyethyl disulfide. *Proteomics* **4**:438-441.
29. **Cribier A., L. Korsatz, R. Koning, P. Rath, H. Gamra, G. Stix, S. Merchant, C. Chan, and B. Letac**. 1992. Improved myocardial ischemic response and enhanced collateral circulation with long repetitive coronary occlusion during angioplasty: a prospective study. *J. Am. Coll. Cardiol* **20**:578-586.
30. **De Hert S. G., S. Cromheecke, P. W. ten Broecke, E. Mertens, I. G. De Blier, B. A. Stockman, I. E. Rodrigus, and P. J. Van der Linden**. 2003. Effects of propofol, desflurane, and sevoflurane on recovery of myocardial function after coronary surgery in elderly high-risk patients. *Anesthesiology* **99**:314-323.
31. **De Hert S. G., B. Preckel, M. W. Hollmann, and W. S. Schlack**. 2009. Drugs mediating myocardial protection. *Eur J Anaesthesiol* **26**:985-995.
32. **Dean R. T., S. Fu, R. Stocker, and M. J. Davies**. 1997. Biochemistry and pathology of radical-mediated protein oxidation. *Biochem. J* **324 (Pt 1)**:1-18.
33. **Deutsch E., M. Berger, W. G. Kussmaul, J. W. Hirshfeld, H. C. Herrmann, and W. K.**

Laskey. 1990. Adaptation to ischemia during percutaneous transluminal coronary angioplasty. Clinical, hemodynamic, and metabolic features. *Circulation* **82**:2044-2051.

34. **Di Lisa F., and P. Bernardi**. 1998. Mitochondrial function as a determinant of recovery or death in cell response to injury. *Mol. Cell. Biochem* **184**:379-391.
35. **Doliba N. M., N. M. Doliba, Q. Chang, A. M. Babsky, K. Wroblewski, B. H. Natelson, and M. D. Osbakken**. 1999. Mitochondrial oxidative phosphorylation in heart from stressed cardiomyopathic hamsters. *J. Mol. Cell. Cardiol* **31**:543-553.
36. **Dunn M.** Detection of proteins in polyacrylamide gels by silver staining. *In* The Protein Protocols Handbook, 2nd ed. *Humana Press Inc.*
37. **Dyballa N., and S. Metzger**. 2009. Fast and sensitive colloidal coomassie G-250 staining for proteins in polyacrylamide gels. *J Vis Exp*.
38. **Ebel D., J. Müllenheim, H. Südkamp, T. Bohlen, J. Ferrari, R. Huhn, B. Preckel, and W. Schlack**. 2004. Role of tyrosine kinase in desflurane-induced preconditioning. *Anesthesiology* **100**:555-561.
39. **Eisen A., E. Z. Fisman, M. Rubenfire, D. Freimark, R. McKechnie, A. Tenenbaum, M. Motro, and Y. Adler**. 2004. Ischemic preconditioning: nearly two decades of research. A comprehensive review. *Atherosclerosis* **172**:201-210.
40. **Evans G., C. H. Wheeler, J. M. Corbett, and M. J. Dunn**. 1997. Construction of HSC-2DPAGE: a two-dimensional gel electrophoresis database of heart proteins. *Electrophoresis* **18**:471-479.
41. **Feng J., M. Zhu, M. C. Schaub, P. Gehrig, B. Roschitzki, E. Lucchinetti, and M. Zaugg**. 2008. Phosphoproteome analysis of isoflurane-protected heart mitochondria: phosphorylation of adenine nucleotide translocator-1 on Tyr194 regulates mitochondrial function. *Cardiovasc. Res* **80**:20-29.
42. **Ferrari R.** 1996. The role of mitochondria in ischemic heart disease. *J. Cardiovasc. Pharmacol* **28 Suppl 1**:S1-10.
43. **Fert-Bober J., R. S. Basran, J. Sawicka, and G. Sawicki**. 2008. Effect of duration of ischemia on myocardial proteome in ischemia/reperfusion injury. *Proteomics* **8**:2543-2555.
44. **Fleisher L. A., J. A. Beckman, K. A. Brown, H. Calkins, E. L. Chaikof, E. Chaikof, K. E. Fleischmann, W. K. Freeman, J. B. Froehlich, E. K. Kasper, J. R. Kersten, B. Riegel, J. F. Robb, S. C. Smith, A. K. Jacobs, C. D. Adams, J. L. Anderson, E. M. Antman, C. E. Buller, M. A. Creager, S. M. Ettinger, D. P. Faxon, V. Fuster, J. L. Halperin, L. F. Hiratzka, S. A. Hunt, B. W. Lytle, R. Nishimura, J. P. Ornato, R. L. Page, B. Riegel, L. G. Tarkington, and C. W. Yancy**. 2007. ACC/AHA 2007 Guidelines on Perioperative Cardiovascular Evaluation and Care for Noncardiac Surgery: Executive Summary: A Report of the American College of Cardiology/American Heart Association Task Force on Practice Guidelines (Writing Committee to Revise the 2002 Guidelines on Perioperative Cardiovascular Evaluation for Noncardiac Surgery) Developed in Collaboration With the American Society of Echocardiography, American Society of Nuclear Cardiology, Heart Rhythm Society, Society of Cardiovascular Anesthesiologists, Society for Cardiovascular Angiography and Interventions, Society for Vascular Medicine and Biology, and Society for Vascular Surgery. *J. Am. Coll. Cardiol* **50**:1707-1732.
45. **Fountoulakis M., B. Takács, and H. Langen**. 1998. Two-dimensional map of basic proteins of Haemophilus influenzae. *Electrophoresis* **19**:761-766.
46. **Frässdorf J., A. Borowski, D. Ebel, P. Feindt, M. Hermes, T. Meemann, R. Weber, J. Müllenheim, N. C. Weber, B. Preckel, and W. Schlack**. 2009. Impact of preconditioning protocol on anesthetic-induced cardioprotection in patients having

coronary artery bypass surgery. *J. Thorac. Cardiovasc. Surg* **137**:1436-1442, 1442.e1-2.

47. **Goodwin G. W., P. M. Rougraff, E. J. Davis, and R. A. Harris**. 1989. Purification and characterization of methylmalonate-semialdehyde dehydrogenase from rat liver. Identity to malonate-semialdehyde dehydrogenase. *J. Biol. Chem* **264**:14965-14971.
48. **Görg A., G. Boguth, C. Obermaier, and W. Weiss**. 1998. Two-dimensional electrophoresis of proteins in an immobilized pH 4-12 gradient. *Electrophoresis* **19**:1516-1519.
49. **Görg A., C. Obermaier, G. Boguth, A. Csordas, J. J. Diaz, and J. J. Madjar**. 1997. Very alkaline immobilized pH gradients for two-dimensional electrophoresis of ribosomal and nuclear proteins. *Electrophoresis* **18**:328-337.
50. **Görg A., C. Obermaier, G. Boguth, and W. Weiss**. 1999. Recent developments in two-dimensional gel electrophoresis with immobilized pH gradients: wide pH gradients up to pH 12, longer separation distances and simplified procedures. *Electrophoresis* **20**:712-717.
51. **Görg A.** 2004. 2-D Electrophoresis, Principles and Methods, 3rd ed. GE Healthcare Limited.
52. **Görg A., W. Weiss, and M. J. Dunn**. 2004. Current two-dimensional electrophoresis technology for proteomics. *Proteomics* **4**:3665-3685.
53. **Grussenmeyer T., S. Meili-Butz, T. Dieterle, E. Traunecker, T. P. Carrel, and I. Lefkovits**. 2008. Quantitative proteome analysis in cardiovascular physiology and pathology. I. Data processing. *J. Proteome Res* **7**:5211-5220.
54. **Guillonneau F., V. Labas, C. Auvin, and D. Praseuth**. 2001. A reliable and simple method for two-dimensional electrophoresis and identification of HeLa nuclear alkaline nucleic acid-binding proteins using immobilized pH gradient. *Electrophoresis* **22**:4391-4403.
55. **Guo Y., W. J. Wu, Y. Qiu, X. L. Tang, Z. Yang, and R. Bolli**. 1998. Demonstration of an early and a late phase of ischemic preconditioning in mice. *Am. J. Physiol* **275**:H1375-1387.
56. **Hanouz J., A. Yvon, M. Massetti, O. Lepage, G. Babatasi, A. Khayat, H. Bricard, and J. Gérard**. 2002. Mechanisms of desflurane-induced preconditioning in isolated human right atria in vitro. *Anesthesiology* **97**:33-41.
57. **Hanouz J., L. Zhu, S. Lemoine, C. Durand, O. Lepage, M. Massetti, A. Khayat, B. Plaud, and J. Gérard**. 2007. Reactive oxygen species mediate sevoflurane- and desflurane-induced preconditioning in isolated human right atria in vitro. *Anesth. Analg* **105**:1534-1539.
58. **Hausenloy D. J., and D. M. Yellon**. 2009. Preconditioning and postconditioning: underlying mechanisms and clinical application. *Atherosclerosis* **204**:334-341.
59. **Hoving S., B. Gerrits, H. Voshol, D. Müller, R. C. Roberts, and J. van Oostrum**. 2002. Preparative two-dimensional gel electrophoresis at alkaline pH using narrow range immobilized pH gradients. *Proteomics* **2**:127-134.
60. **Hunzinger C., W. Wozny, G. P. Schwall, S. Poznanović, W. Stegmann, H. Zengerling, R. Schoepf, K. Groebe, M. A. Cahill, H. D. Osiewacz, N. Jägemann, M. Bloch, N. A. Dencher, F. Krause, and A. Schrattenholz**. 2006. Comparative profiling of the mammalian mitochondrial proteome: multiple aconitase-2 isoforms including N-formylkynurenine modifications as part of a protein biomarker signature for reactive oxidative species. *J. Proteome Res* **5**:625-633.
61. **Islam C. F., R. T. Mathie, M. D. Dinneen, E. A. Kiely, A. M. Peters, and P. A. Grace**. 1997. Ischaemia-reperfusion injury in the rat kidney: the effect of preconditioning. *Br J Urol* **79**:842-847.

62. **Iuso A., S. Scacco, C. Piccoli, F. Bellomo, V. Petruzzella, R. Trentadue, M. Minuto, M. Ripoli, N. Capitanio, M. Zeviani, and S. Papa**. 2006. Dysfunctions of Cellular Oxidative Metabolism in Patients with Mutations in the NDUFS1 and NDUFS4 Genes of Complex I. *Journal of Biological Chemistry* **281**:10374-10380.
63. **Julier K., R. da Silva, C. Garcia, L. Bestmann, P. Frascarolo, A. Zollinger, P. Chassot, E. R. Schmid, M. I. Turina, L. K. von Segesser, T. Pasch, D. R. Spahn, and M. Zaugg**. 2003. Preconditioning by sevoflurane decreases biochemical markers for myocardial and renal dysfunction in coronary artery bypass graft surgery: a double-blinded, placebo-controlled, multicenter study. *Anesthesiology* **98**:1315-1327.
64. **Jungblut P., A. Otto, E. Zeindl-Eberhart, K. P. Plessner, M. Knecht, V. Regitz-Zagrosek, E. Fleck, and B. Wittmann-Liebold**. 1994. Protein composition of the human heart: the construction of a myocardial two-dimensional electrophoresis database. *Electrophoresis* **15**:685-707.
65. **Kalenka A., M. H. Maurer, R. E. Feldmann, W. Kuschinsky, and K. F. Waschke**. 2006. Volatile anesthetics evoke prolonged changes in the proteome of the left ventricule myocardium: defining a molecular basis of cardioprotection? *Acta Anaesthesiol Scand* **50**:414-427.
66. **Kane L. A., C. K. Yung, G. Agnetti, I. Neverova, and J. E. Van Eyk**. 2006. Optimization of paper bridge loading for 2-DE analysis in the basic pH region: application to the mitochondrial subproteome. *Proteomics* **6**:5683-5687.
67. **Kang D., Y. S. Gho, M. Suh, and C. Kang**. 2002. Highly sensitive and fast protein detection with Coomassie Brilliant Blue in sodium dodecyl sulfate-polyacrylamide gel electrophoresis. *Bull. Korean Chem. Soc.* **23**:1511-1512.
68. **Karas M., and F. Hillenkamp**. 1988. Laser desorption ionization of proteins with molecular masses exceeding 10,000 daltons. *Anal. Chem* **60**:2299-2301.
69. **Kedishvili N. Y., K. M. Popov, P. M. Rougraff, Y. Zhao, D. W. Crabb, and R. A. Harris**. 1992. CoA-dependent methylmalonate-semialdehyde dehydrogenase, a unique member of the aldehyde dehydrogenase superfamily. cDNA cloning, evolutionary relationships, and tissue distribution. *J. Biol. Chem* **267**:19724-19729.
70. **Kenrick K. G., and J. Margolis**. 1970. Isoelectric focusing and gradient gel electrophoresis: a two-dimensional technique. *Anal. Biochem* **33**:204-207.
71. **Kersten J. R., T. J. Schmeling, P. S. Pagel, G. J. Gross, and D. C. Warltier**. 1997. Isoflurane mimics ischemic preconditioning via activation of K(ATP) channels: reduction of myocardial infarct size with an acute memory phase. *Anesthesiology* **87**:361-370.
72. **Kim N., Y. Lee, H. Kim, H. Joo, J. B. Youm, W. S. Park, M. Warda, D. V. Cuong, and J. Han**. 2006. Potential biomarkers for ischemic heart damage identified in mitochondrial proteins by comparative proteomics. *Proteomics* **6**:1237-1249.
73. **Kloner R. A., and R. B. Jennings**. 2001. Consequences of brief ischemia: stunning, preconditioning, and their clinical implications: part 1. *Circulation* **104**:2981-2989.
74. **Kloner R. A., and R. B. Jennings**. 2001. Consequences of brief ischemia: stunning, preconditioning, and their clinical implications: part 2. *Circulation* **104**:3158-3167.
75. **Klose J.** 1975. Protein mapping by combined isoelectric focusing and electrophoresis of mouse tissues. A novel approach to testing for induced point mutations in mammals. *Humangenetik* **26**:231-243.
76. **Klose J., and U. Kobalz**. 1995. Two-dimensional electrophoresis of proteins: an updated protocol and implications for a functional analysis of the genome. *Electrophoresis* **16**:1034-1059.
77. **Kohin S., C. M. Stary, R. A. Howlett, and M. C. Hogan**. 2001. Preconditioning improves function and recovery of single muscle fibers during severe hypoxia and

reoxygenation. *Am. J. Physiol., Cell Physiol* **281**:C142-146.

78. **Korzick D. H., J. C. Kostyak, J. C. Hunter, and K. W. Saupe**. 2007. Local delivery of PKCepsilon-activating peptide mimics ischemic preconditioning in aged hearts through GSK-3beta but not F1-ATPase inactivation. *Am. J. Physiol. Heart Circ. Physiol* **293**:H2056-2063.
79. **Kume M., Y. Yamamoto, S. Saad, T. Gomi, S. Kimoto, T. Shimabukuro, T. Yagi, M. Nakagami, Y. Takada, T. Morimoto, and Y. Yamaoka**. 1996. Ischemic preconditioning of the liver in rats: implications of heat shock protein induction to increase tolerance of ischemia-reperfusion injury. *J. Lab. Clin. Med* **128**:251-258.
80. **Kuzuya T., S. Hoshida, N. Yamashita, H. Fuji, H. Oe, M. Hori, T. Kamada, and M. Tada**. 1993. Delayed effects of sublethal ischemia on the acquisition of tolerance to ischemia. *Circ. Res* **72**:1293-1299.
81. **Lamberti C., E. Pessione, M. G. Giuffrida, R. Mazzoli, C. Barello, A. Conti, and C. Giunta**. 2007. Combined cup loading, bis(2-hydroxyethyl) disulfide, and protein precipitation protocols to improve the alkaline proteome of Lactobacillus hilgardii. *Electrophoresis* **28**:1633-1638.
82. **Landoni G., G. G. L. Biondi-Zoccai, A. Zangrillo, E. Bignami, S. D'Avolio, C. Marchetti, M. G. Calabrò, O. Fochi, F. Guarracino, L. Tritapepe, S. De Hert, and G. Torri**. 2007. Desflurane and sevoflurane in cardiac surgery: a meta-analysis of randomized clinical trials. *J. Cardiothorac. Vasc. Anesth* **21**:502-511.
83. **Lang S. C., A. Elsässer, C. Scheler, S. Vetter, C. P. Tiefenbacher, W. Kübler, H. A. Katus, and A. M. Vogt**. 2006. Myocardial preconditioning and remote renal preconditioning--identifying a protective factor using proteomic methods? *Basic Res. Cardiol* **101**:149-158.
84. **Lange M., A. Redel, T. M. Smul, C. Lotz, T. Nefzger, J. Stumpner, C. Blomeyer, F. Gao, N. Roewer, and F. Kehl**. 2009. Desflurane-induced preconditioning has a threshold that is lowered by repetitive application and is mediated by beta(2)-adrenergic receptors. *J. Cardiothorac. Vasc. Anesth* **23**:607-613.
85. **Lescuyer P., J. Strub, S. Luche, H. Diemer, P. Martinez, A. Van Dorsselaer, J. Lunardi, and T. Rabilloud**. 2003. Progress in the definition of a reference human mitochondrial proteome. *Proteomics* **3**:157-167.
86. **Li H., Y. Xiao, Y. Gao, and T. Yang**. 2006. Comparative proteomics analysis of differentially expressed phosphoproteins in adult rat ventricular myocytes subjected to diazoxide preconditioning. *Drug Metabol Drug Interact* **21**:245-258.
87. **Li X., B. B. Patel, E. L. Blagoi, M. D. Patterson, S. H. Seeholzer, S. H. Seehozer, T. Zhang, S. Damle, Z. Gao, B. Boman, and A. T. Yeung**. 2004. Analyzing alkaline proteins in human colon crypt proteome. *J. Proteome Res* **3**:821-833.
88. **Li Z. B., P. W. Flint, and M. O. Boluyt**. 2005. Evaluation of several two-dimensional gel electrophoresis techniques in cardiac proteomics. *Electrophoresis* **26**:3572-3585.
89. **Liu Y., and J. M. Downey**. 1992. Ischemic preconditioning protects against infarction in rat heart. *Am. J. Physiol* **263**:H1107-1112.
90. **Liu Y., H. Kato, N. Nakata, and K. Kogure**. 1992. Protection of rat hippocampus against ischemic neuronal damage by pretreatment with sublethal ischemia. *Brain Res* **586**:121-124.
91. **Lowry O. H., N. J. Rosebrough, A. L. Farr, and R. J. Randall**. 1951. Protein measurement with the Folin phenol reagent. *J. Biol. Chem* **193**:265-275.
92. **Magalhães A. D., S. Charneau, J. Paba, R. A. Guércio, A. R. Teixeira, J. M. Santana, M. V. Sousa, and C. A. Ricart**. 2008. Trypanosoma cruzi alkaline 2-DE: Optimization and application to comparative proteome analysis of flagellate life stages. *Proteome Sci* **6**:24.

93. **McGregor E., and M. J. Dunn**. 2003. Proteomics of heart disease. *Hum. Mol. Genet.* **12**:R135-144.
94. **Meco M., S. Cirri, C. Gallazzi, G. Magnani, and D. Cosseta**. 2007. Desflurane preconditioning in coronary artery bypass graft surgery: a double-blinded, randomised and placebo-controlled study. *Eur J Cardiothorac Surg* **32**:319-325.
95. **Miyawaki H., X. Zhou, and M. Ashraf**. 1996. Calcium preconditioning elicits strong protection against ischemic injury via protein kinase C signaling pathway. *Circ. Res* **79**:137-146.
96. **Møller I. M., and B. K. Kristensen**. 2006. Protein oxidation in plant mitochondria detected as oxidized tryptophan. *Free Radic. Biol. Med* **40**:430-435.
97. **Molloy M. P., B. R. Herbert, B. J. Walsh, M. I. Tyler, M. Traini, J. C. Sanchez, D. F. Hochstrasser, K. L. Williams, and A. A. Gooley**. 1998. Extraction of membrane proteins by differential solubilization for separation using two-dimensional gel electrophoresis. *Electrophoresis* **19**:837-844.
98. **Molloy M. P., E. E. Brzezinski, J. Hang, M. T. McDowell, and R. A. VanBogelen**. 2003. Overcoming technical variation and biological variation in quantitative proteomics. *Proteomics* **3**:1912-1919.
99. **Moon K., B. L. Hood, P. Mukhopadhyay, M. Rajesh, M. A. Abdelmegeed, Y. Kwon, T. P. Conrads, T. D. Veenstra, B. Song, and P. Pacher**. 2008. Oxidative inactivation of key mitochondrial proteins leads to dysfunction and injury in hepatic ischemia reperfusion. *Gastroenterology* **135**:1344-1357.
100. **Müllenheim J., D. Ebel, J. Frässdorf, B. Preckel, V. Thämer, and W. Schlack**. 2002. Isoflurane preconditions myocardium against infarction via release of free radicals. *Anesthesiology* **96**:934-940.
101. **Murry C. E., R. B. Jennings, and K. A. Reimer**. 1986. Preconditioning with ischemia: a delay of lethal cell injury in ischemic myocardium. *Circulation* **74**:1124-1136.
102. **Neely C. F., and I. M. Keith**. 1995. A1 adenosine receptor antagonists block ischemia-reperfusion injury of the lung. *Am. J. Physiol* **268**:L1036-1046.
103. **Nelson S. R., T. L. Pazdernik, and F. E. Samson**. 1992. Copper plus ascorbate inactivates lactate dehydrogenase: are oxygen radicals involved? *Proc. West. Pharmacol. Soc* **35**:37-41.
104. **Neuhoff V., N. Arold, D. Taube, and W. Ehrhardt**. 1988. Improved staining of proteins in polyacrylamide gels including isoelectric focusing gels with clear background at nanogram sensitivity using Coomassie Brilliant Blue G-250 and R-250. *Electrophoresis* **9**:255-262.
105. **Novalija E., S. G. Varadarajan, A. K. S. Camara, J. An, Q. Chen, M. L. Riess, N. Hogg, and D. F. Stowe**. 2002. Anesthetic preconditioning: triggering role of reactive oxygen and nitrogen species in isolated hearts. *Am. J. Physiol. Heart Circ. Physiol* **283**:H44-52.
106. **O'Farrell P. H.** 1975. High resolution two-dimensional electrophoresis of proteins. *J. Biol. Chem* **250**:4007-4021.
107. **Ohlmeier S., C. Scharf, and M. Hecker**. 2000. Alkaline proteins of Bacillus subtilis: first steps towards a two-dimensional alkaline master gel. *Electrophoresis* **21**:3701-3709.
108. **Olsson I., K. Larsson, R. Palmgren, and B. Bjellqvist**. 2002. Organic disulfides as a means to generate streak-free two-dimensional maps with narrow range basic immobilized pH gradient strips as first dimension. *Proteomics* **2**:1630-1632.
109. **Osborne D. L., T. Y. Aw, G. Cepinskas, and P. R. Kvietys**. 1994. Development of ischemia/reperfusion tolerance in the rat small intestine. An epithelium-independent event. *J. Clin. Invest* **94**:1910-1918.

110. **Ouyang Y., S. Kuroda, T. Kristián, and B. K. Siesjö**. 1997. Release of mitochondrial aspartate aminotransferase (mAST) following transient focal cerebral ischemia suggests the opening of a mitochondrial permeability transition pore. *Neuroscience Research Communications* **20**:167-173.
111. **Ovize M., R. A. Kloner, and K. Przyklenk**. 1994. Stretch preconditions canine myocardium. *Am. J. Physiol* **266**:H137-146.
112. **Park J., Y. Chun, M. Kim, Y. Park, S. J. Kwak, and S. C. Park**. 1998. Metabolic modulation of cellular redox potential can improve cardiac recovery from ischemia-reperfusion injury. *International Journal of Cardiology* **65**:139-147.
113. **Patton W. F.** 2002. Detection technologies in proteome analysis. *J. Chromatogr. B Analyt. Technol. Biomed. Life Sci* **771**:3-31.
114. **Pearte C. A., C. D. Furberg, E. S. O'Meara, B. M. Psaty, L. Kuller, N. R. Powe, and T. Manolio**. 2006. Characteristics and Baseline Clinical Predictors of Future Fatal Versus Nonfatal Coronary Heart Disease Events in Older Adults: The Cardiovascular Health Study. *Circulation* **113**:2177-2185.
115. **Pennington K., E. McGregor, C. L. Beasley, I. Everall, D. Cotter, and M. J. Dunn**. 2004. Optimization of the first dimension for separation by two-dimensional gel electrophoresis of basic proteins from human brain tissue. *Proteomics* **4**:27-30.
116. **Petrak J., R. Ivanek, O. Toman, R. Cmejla, J. Cmejlova, D. Vyoral, J. Zivny, and C. D. Vulpe**. 2008. Déjà vu in proteomics. A hit parade of repeatedly identified differentially expressed proteins. *Proteomics* **8**:1744-1749.
117. **Piriou V., P. Chiari, F. Lhuillier, O. Bastien, J. Loufoua, O. Raisky, J. S. David, M. Ovize, and J. J. Lehot**. 2002. Pharmacological preconditioning: comparison of desflurane, sevoflurane, isoflurane and halothane in rabbit myocardium. *Br J Anaesth* **89**:486-491.
118. **Piriou V., J. Mantz, G. Goldfarb, M. Kitakaze, P. Chiari, S. Paquin, C. Cornu, J. Lecharny, P. Aussage, E. Vicaut, A. Pons, and J. Lehot**. 2007. Sevoflurane preconditioning at 1 MAC only provides limited protection in patients undergoing coronary artery bypass surgery: a randomized bi-centre trial. *Br J Anaesth* **99**:624-631.
119. **Pleissner K. P., S. Sander, H. Oswald, V. Regitz-Zagrosek, and E. Fleck**. 1996. The construction of the World Wide Web-accessible myocardial two-dimensional gel electrophoresis protein database "HEART-2DPAGE": a practical approach. *Electrophoresis* **17**:1386-1392.
120. **Potgieter H. C., J. B. Ubbink, S. Bissbort, M. J. Bester, J. H. Spies, and W. J. Vermaak**. 1997. Spontaneous oxidation of methionine: effect on the quantification of plasma methionine levels. *Anal. Biochem* **248**:86-93.
121. **Przyklenk K., B. Bauer, M. Ovize, R. A. Kloner, and P. Whittaker**. 1993. Regional ischemic 'preconditioning' protects remote virgin myocardium from subsequent sustained coronary occlusion. *Circulation* **87**:893-899.
122. **Rabilloud T.** 1998. Use of thiourea to increase the solubility of membrane proteins in two-dimensional electrophoresis. *Electrophoresis* **19**:758-760.
123. **Rabilloud T., C. Adessi, A. Giraudel, and J. Lunardi**. 1997. Improvement of the solubilization of proteins in two-dimensional electrophoresis with immobilized pH gradients. *Electrophoresis* **18**:307-316.
124. **Raddatz K., D. Albrecht, F. Hochgräfe, M. Hecker, and M. Gotthardt**. 2008. A proteome map of murine heart and skeletal muscle. *Proteomics* **8**:1885-1897.
125. **Redel A., M. Lange, V. Jazbutyte, C. Lotz, T. M. Smul, N. Roewer, and F. Kehl**. 2008. Activation of mitochondrial large-conductance calcium-activated K+ channels via protein kinase A mediates desflurane-induced preconditioning. *Anesth. Analg*

106:384-391

126. **Riess M. L., A. K. S. Camara, L. G. Kevin, J. An, and D. F. Stowe**. 2004. Reduced reactive O2 species formation and preserved mitochondrial NADH and [Ca2+] levels during short-term 17 degrees C ischemia in intact hearts. *Cardiovasc. Res* **61**:580-590.
127. **Riess M. L., A. K. S. Camara, Q. Chen, E. Novalija, S. S. Rhodes, and D. F. Stowe**. 2002. Altered NADH and improved function by anesthetic and ischemic preconditioning in guinea pig intact hearts. *Am J Physiol Heart Circ Physiol* **283**:H53-60.
128. **Roepstorff P., and J. Fohlman**. 1984. Proposal for a common nomenclature for sequence ions in mass spectra of peptides. *Biomed. Mass Spectrom* **11**:601.
129. **Sakai J., H. Ishikawa, S. Kojima, H. Satoh, S. Yamamoto, and M. Kanaoka**. 2003. Proteomic analysis of rat heart in ischemia and ischemia-reperfusion using fluorescence two-dimensional difference gel electrophoresis. *Proteomics* **3**:1318-1324.
130. **Sawicki G., and B. I. Jugdutt**. 2004. Detection of regional changes in protein levels in the in vivo canine model of acute heart failure following ischemia-reperfusion injury: functional proteomics studies. *Proteomics* **4**:2195-2202.
131. **Schott R. J., S. Rohmann, E. R. Braun, and W. Schaper**. 1990. Ischemic preconditioning reduces infarct size in swine myocardium. *Circ. Res* **66**:1133-1142.
132. **Schuh C.** 2008. Kardioprotektive Wirkung volatiler Anästhetika (Poster). Deutscher Anästhesiecongress, Nürnberg.
133. **Schulenberg B., T. N. Goodman, R. Aggeler, R. A. Capaldi, and W. F. Patton**. 2004. Characterization of dynamic and steady-state protein phosphorylation using a fluorescent phosphoprotein gel stain and mass spectrometry. *Electrophoresis* **25**:2526-2532.
134. **Schwertz H., T. Längin, H. Platsch, J. Richert, S. Bomm, M. Schmidt, H. Hillen, G. Blaschke, J. Meyer, H. Darius, and M. Buerke**. 2002. Two-dimensional analysis of myocardial protein expression following myocardial ischemia and reperfusion in rabbits. *Proteomics* **2**:988-995.
135. **Sedlic F., D. Pravdic, M. Ljubkovic, J. Marinovic, A. Stadnicka, and Z. J. Bosnjak**. 2009. Differences in production of reactive oxygen species and mitochondrial uncoupling as events in the preconditioning signaling cascade between desflurane and sevoflurane. *Anesth. Analg* **109**:405-411.
136. **Sedlic F., D. Pravdic, M. Ljubkovic, J. Marinovic, A. Stadnicka, and Z. J. Bosnjak**. 2009. Differences in production of reactive oxygen species and mitochondrial uncoupling as events in the preconditioning signaling cascade between desflurane and sevoflurane.
137. **Sergeev P., R. da Silva, E. Lucchinetti, K. Zaugg, T. Pasch, M. C. Schaub, and M. Zaugg**. 2004. Trigger-dependent gene expression profiles in cardiac preconditioning: evidence for distinct genetic programs in ischemic and anesthetic preconditioning. *Anesthesiology* **100**:474-488.
138. **Shevchenko A., M. Wilm, O. Vorm, and M. Mann**. 1996. Mass spectrometric sequencing of proteins silver-stained polyacrylamide gels. *Anal. Chem* **68**:850-858.
139. **Shizukuda Y., R. T. Mallet, S. C. Lee, and H. F. Downey**. 1992. Hypoxic preconditioning of ischaemic canine myocardium. *Cardiovasc. Res* **26**:534-542.
140. **da Silva R., T. Grampp, T. Pasch, M. C. Schaub, and M. Zaugg**. 2004. Differential activation of mitogen-activated protein kinases in ischemic and anesthetic preconditioning. *Anesthesiology* **100**:59-69.
141. **Smul T. M., M. Lange, A. Redel, N. Burkhard, N. Roewer, and F. Kehl**. 2006.

Desflurane-induced preconditioning against myocardial infarction is mediated by nitric oxide. *Anesthesiology* **105**:719-725.

142. **Spiekermann P., J. Brückner, and W. Kübler**. 1969. Präischämische Belastung und Wiederbelebungszeiten des Herzens. *Verh Dtsch Ges Kreislaufforsch* **33**:358-64.
143. **Stanley B. A., I. Neverova, H. A. Brown, and J. E. Van Eyk**. 2003. Optimizing protein solubility for two-dimensional gel electrophoresis analysis of human myocardium. *Proteomics* **3**:815-820.
144. **Steinberg T. H., B. J. Agnew, K. R. Gee, W. Leung, T. Goodman, B. Schulenberg, J. Hendrickson, J. M. Beechem, R. P. Haugland, and W. F. Patton**. 2003. Global quantitative phosphoprotein analysis using Multiplexed Proteomics technology. *Proteomics* **3**:1128-1144.
145. **Sweetlove L. J., J. L. Heazlewood, V. Herald, R. Holtzapffel, D. A. Day, C. J. Leaver, and A. H. Millar**. 2002. The impact of oxidative stress on Arabidopsis mitochondria. *Plant J* **32**:891-904.
146. **Tanaka K., D. Weihrauch, F. Kehl, L. M. Ludwig, J. F. LaDisa, J. R. Kersten, P. S. Pagel, and D. C. Warltier**. 2002. Mechanism of preconditioning by isoflurane in rabbits: a direct role for reactive oxygen species. *Anesthesiology* **97**:1485-1490.
147. **Tanaka K., H. Waki, Y. Ido, S. Akita, Y. Yoshida, T. Yoshida, and T. Matsuo**. 1988. Protein and polymer analyses up to <I>m/z</I> 100 000 by laser ionization time-of-flight mass spectrometry. *Rapid Communications in Mass Spectrometry* **2**:151-153.
148. **Tanaka N., H. Takahashi, H. Kitano, M. Matsuoka, S. Akao, H. Uchimiya, and S. Komatsu**. 2005. Proteome approach to characterize the methylmalonate-semialdehyde dehydrogenase that is regulated by gibberellin. *J. Proteome Res* **4**:1575-1582.
149. **Taylor S. W., E. Fahy, J. Murray, R. A. Capaldi, and S. S. Ghosh**. 2003. Oxidative post-translational modification of tryptophan residues in cardiac mitochondrial proteins. *J. Biol. Chem* **278**:19587-19590.
150. **Thornton J., S. Striplin, G. S. Liu, A. Swafford, A. W. Stanley, D. M. Van Winkle, and J. M. Downey**. 1990. Inhibition of protein synthesis does not block myocardial protection afforded by preconditioning. *Am. J. Physiol* **259**:H1822-1825.
151. **Toller W. G., E. R. Gross, J. R. Kersten, P. S. Pagel, G. J. Gross, and D. C. Warltier**. 2000. Sarcolemmal and mitochondrial adenosine triphosphate- dependent potassium channels: mechanism of desflurane-induced cardioprotection. *Anesthesiology* **92**:1731-1739.
152. **Toma O., N. C. Weber, J. I. Wolter, D. Obal, B. Preckel, and W. Schlack**. 2004. Desflurane preconditioning induces time-dependent activation of protein kinase C epsilon and extracellular signal-regulated kinase 1 and 2 in the rat heart in vivo. *Anesthesiology* **101**:1372-1380.
153. **Vegh A., L. Szekeres, and J. R. Parratt**. 1991. Transient ischaemia induced by rapid cardiac pacing results in myocardial preconditioning. *Cardiovasc. Res* **25**:1051-1053.
154. **Wang S., R. Zhu, B. Peng, M. Liu, Y. Lou, X. Ye, Z. Xu, D. Liu, and X. Peng**. 2006. Identification of alkaline proteins that are differentially expressed in an overgrowth-mediated growth arrest and cell death of Escherichia coli by proteomic methodologies. *Proteomics* **6**:5212-5220.
155. **Warltier D. C., M. H. al-Wathiqui, J. P. Kampine, and W. T. Schmeling**. 1988. Recovery of contractile function of stunned myocardium in chronically instrumented dogs is enhanced by halothane or isoflurane. *Anesthesiology* **69**:552-565.
156. **Weber N. C., and W. Schlack**. 2008. Inhalational anaesthetics and cardioprotection. *Handb Exp Pharmacol* 187-207.
157. **Weber N. C., C. Goletz, R. Huhn, Y. Grueber, B. Preckel, W. Schlack, and D. Ebel**.

2008. Blockade of anaesthetic-induced preconditioning in the hyperglycaemic myocardium: the regulation of different mitogen-activated protein kinases. *Eur. J. Pharmacol* **592**:48-54.

158. **Weber N. C., O. Toma, J. I. Wolter, D. Obal, J. Müllenheim, B. Preckel, and W. Schlack**. 2005. The noble gas xenon induces pharmacological preconditioning in the rat heart in vivo via induction of PKC-epsilon and p38 MAPK. *Br. J. Pharmacol* **144**:123-132.
159. **Wen J., and N. Garg**. 2004. Oxidative modification of mitochondrial respiratory complexes in response to the stress of Trypanosoma cruzi infection. *Free Radic. Biol. Med* **37**:2072-2081.
160. **Westbrook J. A., J. X. Wheeler, R. Wait, S. Y. Welson, and M. J. Dunn**. 2006. The human heart proteome: Two-dimensional maps using narrow-range immobilised pH gradients. *Electrophoresis* **27**:1547-1555.
161. **White M. Y., S. J. Cordwell, H. C. K. McCarron, A. M. Prasan, G. Craft, B. D. Hambly, and R. W. Jeremy**. 2005. Proteomics of ischemia/reperfusion injury in rabbit myocardium reveals alterations to proteins of essential functional systems. *Proteomics* **5**:1395-1410.
162. **Whitehouse C. M., R. N. Dreyer, M. Yamashita, and J. B. Fenn**. 1985. Electrospray interface for liquid chromatographs and mass spectrometers. *Anal. Chem* **57**:675-679.
163. **Wong R., A. M. Aponte, C. Steenbergen, and E. Murphy**. 2010. Cardioprotection leads to novel changes in the mitochondrial proteome. *Am. J. Physiol. Heart Circ. Physiol* **298**:H75-91.
164. **Wu S., P. Wan, J. Li, D. Li, Y. Zhu, and F. He**. 2006. Multi-modality of pI distribution in whole proteome. *Proteomics* **6**:449-455.
165. **Yabe K., and S. Takeo**. 1997. Does glycogen depletion play an important role in ischemic preconditioning? Heart Vessels **12**:136-142.
166. **Yan L., D. E. Vatner, S. Kim, H. Ge, M. Masurekar, W. H. Massover, G. Yang, Y. Matsui, J. Sadoshima, and S. F. Vatner**. 2005. Autophagy in chronically ischemic myocardium. *Proc. Natl. Acad. Sci. U.S.A* **102**:13807-13812.
167. **Yellon D. M., A. M. Alkhulaifi, and W. B. Pugsley**. 1993. Preconditioning the human myocardium. *Lancet* **342**:276-277.
168. **Zaugg M., and M. C. Schaub**. 2003. Signaling and cellular mechanisms in cardiac protection by ischemic and pharmacological preconditioning. *J. Muscle Res. Cell. Motil* **24**:219-249.
169. **Zheng M., C. Reynolds, S. Jo, R. Wersto, Q. Han, and R. Xiao**. 2005. Intracellular acidosis-activated p38 MAPK signaling and its essential role in cardiomyocyte hypoxic injury. *FASEB J.* **19**:109-111.

6 Appendix

A. Supplementary data

Table A.1: Buffer combinations for improving protein solubility resolution during IEF[1].

	IEF buffer stock solution (including CHAPS)			Reducing agents		Solvents
IEF strip	**U**	**TU**	**TU-ASB**	**DTT**	**HED**	**glycerol/isopropanol**
a/A	✓			✓		
b/B	✓			✓		✓
c/C	✓				✓	
d/D	✓				✓	✓
e/E		✓		✓		
f/F		✓		✓		✓
g/G		✓			✓	
h/H		✓			✓	✓
i/I			✓	✓		
j/J			✓	✓		✓
k/K			✓		✓	
l/L			✓		✓	✓

[1] In support of the multiple subproteomic analyses to be conducted, the 2-DE experiments on the neutral-acidic subproteomes were carried out by MD students Christian Schuh and Hendrik Vogt.

(A) Water-soluble proteins

Figure A.1a: Optimal IEF separation by mix and matching buffer compositions.

(B) Detergent-soluble proteins

Figure A.1b: Optimal IEF separation by mix and matching buffer composition. 250 µg protein was solubilized in the different IEF buffers mentioned in Table A.1, applied by in-gel rehydration on 13 cm IPG strips pH 4-7, and focused according to the standard IEF protocol (chapter 2.5). Panel (A) shows the effect of the buffer compositions for water-soluble proteins, panel (B) demonstrates the effect for detergent-soluble proteins.

Table A.2: Amino acid sequences of differentially expressed proteins during DES-PC. Red amino acid sequences were identified by MS/MS fragmentation; underlined peptides account for PMF data.

Spot ID	Accession No.	Entry name
# 16/59 AST-2	NP_037309	aspartate aminotransferase, mitochondrial [Rattus norvegicus]

```
  1 MALLHSGRVL SGMAAAFHPG LAAAASARAS SWWTHVEMGP PDPILGVTEA FKRDTNSKKM
 61 NLGVGAYRDD NGKPYVLPSV RKAEAQIAGK NLDKEYLPIG GLADFCKASA ELALGENSEV
121 LKSGRFVTVQ TISGTGALRV GASFLQRFFK FSRDVFLPKP SWGNHTPIFR DAGMQLQGYR
181 YYDPKTCGFD FSGALEDISK IPEQSVLLLH ACAHNPTGVD PRPEQWKEMA AVVKKKNLFA
241 FFDMAYQGFA SGDGDKDAWA VRHFIEQGIN VCLCQSYAKN MGLYGERVGA FTVVCKDAEE
301 AKRVESQLKI LIRPLYSNPP LNGARIAATI LTSPDLRKQW LQEVKGMADR IISMRTQLVS
361 NLKKEGSSHN WQHITDQIGM FCFTGLKPEQ VERLTKEFSV YMTKDGRISV AGVTSGNVGY
421 LAHAIHQVTK
```

# 17 NDUFS1	NP_001005550	NADH-ubiquinone oxidoreductase 75 kDa subunit, mitochondrial precursor [Rattus norvegicus]

```
  1 MLRIPVKRAL IGLSKSPKGY VRSTGTAASN LIEVFVDGQS VMVEPGTTVL QACEKVGMQI
 61 PRFCYHERLS VAGNCRMCLV EIEKAPKVVA ACAMPVMKGW NILTNSEKSK KAREGVMEFL
121 LANHPLDCPI CDQGGECDLQ DQSMMFGSDR SRFLEGKRAV EDKNIGPLVK TIMTRCIQCT
181 RCIRFASEIA GVDDLGTTGR GNDMQVGTYI EKMFMSELSG NIIDICPVGA LTSKPYAFTA
241 RPWETRKTES IDVMDAVGSN IVVSTRTGEV MRILPRMHED INEEWISDKT RFAYDGLKRQ
301 RLTEPMVRNE KGLLTYTSWE DALSRVAGML QSFEGKAVAA IAGGLVDAEA LVALKDLLNK
361 VDSDTLCTEE IFPNEGAGTD LRSNYLLNTT IAGVEEADVV LLVGTNPRFE APLFNARIRK
421 SWLHNDLKVA LIGSPVDLTY RYDHLGDSPK ILQDIASGNH EFSKVLNAAK KPMVVLGSSA
481 LQRDDGAAIL AAVSSIAQKI RVASGAAAEW KVMNILHRIA SQVAALDLGY KPGVEAIRKN
541 PPKLLFLLGA DGGCITRQDL PKDCFIVYQG HHGDVGAPIA DVILPGAAYT EKSATYVNTE
601 GRAQQTKVAV TPPGLAREDW KIIRALSEIA GITLPYDTLD QVRNRLGEVS PNLVRYDDVE
661 EANYFQQASE LAKLVDQEFL ADPLVPPQLT IKDFYMTDSI SRASQTMAKC VKAVTEGAQA
721 VEEPSIC
```

Table A.2continued: Amino acid sequences of differentially expressed proteins during DES-PC.

# 34 PPA2	NP_001129343	inorganic pyrophosphatase 2, mitochondrial [Rattus norvegicus]

```
  1 MRALLPLLSV GRGWRVGAAA LPPRRVMSLY RTEELGHPRS KDYRLFFKHV AGHYISPFHD
 61 IPLKADCEEE HGIPRKKARN DEYKASFNMV VEIPRWTNAK MEIATEEPLN PIKQDTKNGR
121 LRYTPNIFPH KGYIWNYGAL PQTWEDPHLK DKSTNCCGDN DPIDVCEIGS KVLSRGDVVH
181 VKILGTLALI DQSETDWKII AINVNDPEAE KFHDIDDVKK FKPGYLEATV NWFRLYKVPD
241 GKPENKFAFN GEFKNKAFAL EVINSAHEHW KEMVMKKCDK GAISCVNVHI CDSPFHCTTE
301 EARSLVESIP TPSMSKESSV EEEVWHFLRN
```

# 49 Aco-2	NP_077374	aconitate hydratase, mitochondrial precursor [Rattus norvegicus]

```
  1 MAPYSLLVTR LQKALGVRQY HVASALCQRA KVAMSHFEPS EYIRYDLLEK NINIVRKRLN
 61 RPLTLSEKIV YGHLDDPANQ EIERGKTYLR LRPDRVAMQD ATAQMAMLQF ISSGLPKVAV
121 PSTIHCDHLI EAQLGGEKDL RRAKDINQEV YNFLATAGAK YGVGFWRPGS GIIHQIILEN
181 YAYPGVLLIG TDSHTPNGGG LGGICIGVGG ADAVDVMAGI PWELKCPKVI GVKLTGTLSG
241 WTSPKDVILK VAGILTVKGG TGAIVEYHGP GVDSISCTGM ATICNMGAEI GATTSVFPYN
301 HRMKKYLSKT GRADIANLAE EFKDHLVPDP GCQYDQVIEI NLNELKPHIN GPFTPDLAHP
361 VADVGTVAEK EGWPLDIRVG LIGSCTNSSY EDMGRSAAVA KQALAHGLKC KSQFTITPGS
421 EQIRATIERD GYAQILRDVG GIVLANACGP CIGQWDRKDI KKGEKNTIVT SYNRNFTGRN
481 DANPETHAFV TSPEIVTALA IAGTLKFNPE TDFLTGKDGK KFKLEAPDAD ELPRSDFDPG
541 QDTYQHPPKD SSGQRVDVSP TSQRLQLLEP FDKWDGKDLE DLQILIKVKG KCTTDHISAA
601 GPWLKFRGHL DNISNNLLIG AINIENGKAN SVRNAVTQEF GPVPDTARYY KKHGIRWVVI
661 GDENYGEGSS REHAALEPRH LGGRAIITKS FARIHETNLK KQGLLPLTFA DPSDYNKIHP
721 VDKLTIQGLK DFAPGKPLNC IIKHPNGTQE TILLNHTFNE TQIEWFRAGS ALNRMKELQQ
```

# 71 ALB	NP_599153	serum albumin precursor [Rattus norvegicus]

```
  1 MKWVTFLLLL FISGSAFSRG VFRREAHKSE IAHRFKDLGE QHFKGLVLIA FSQYLQKCPY
 61 EEHIKLVQEV TDFAKTCVAD ENAENCDKSI HTLFGDKLCA IPKLRDNYGE LADCCAKQEP
121 ERNECFLQHK DDNPNLPPFQ RPEAEAMCTS FQENPTSFLG HYLHEVARRH PYFYAPELLY
181 YAEKYNEVLT QCCTESDKAA CLTPKLDAVK EKALVAAVRQ RMKCSSMQRF GERAFKAWAV
241 ARMSQRFPNA EFAEITKLAT DLTKINKECC HGDLLECADD RAELAKYMCE NQATISSKLQ
301 ACCDKPVLQK SQCLAEIEHD NIPADLPSIA ADFVEDKEVC KNYAEAKDVF LGTFLYEYSR
361 RHPDYSVSLL LRLAKKYEAT LEKCCAEGDP PACYGTVLAE FQPLVEEPKN LVKTNCELYE
421 KLGEYGFQNA ILVRYTQKAP QVSTPTLVEA ARNLGRVGTK CCTLPEAQRL PCVEDYLSAI
481 LNRLCVLHEK TPVSEKVTKC CSGSLVERRP CFSALTVDET YVPKEFKAET FTFHSDICTL
541 PDKEKQIKKQ TALAELVKHK PKATEDQLKT VMGDFAQFVD KCCKAADKDN CFATEGPNLV
601 ARSKEALA
```

# 94 MMSDH	NP_112319	methylmalonate-semialdehyde dehydrogenase, mitochondrial precursor [Rattus norvegicus]

```
  1 MAAAVAAAAA VRSRILQVSS KVNSTWCPAS SFSSSSVPTV KLFIDGKFVE SKSDKWIDIH
 61 NPATNEVVGR VPQSTKAEME AAVAACKRAF PAWADTSILS RQQVLLRYQQ LIKENLKEIA
121 RLITLEQGKT LADAEGDVFR GLQVVEHACS VTSLMLGETM PSITKDMDLY SYRLPLGVCA
181 GIAPFNFPAM IPLWMFPMAM VCGNTFLMKP SERVPGATML LAKLLQDSGA PDGTLNIIHG
241 QHEAVNFICD HPDIKAISFV GSNQAGEYIF ERGSRNGKRV QANMGAKNHG VVMPDANKEN
301 TLNQLVGAAF GAAGQRCMAL STAVLVGEAK KWLPELVERA KNLRVNAGDQ PGADLGPLIT
361 PQAKERVCNL IDSGAKEGAS ILLDGRKIKV KGYENGNFVG PTIISNVKPS MTCYKEEIFG
421 PVLVVLETET LDEAIKIVND NPYGNGTAIF TTNGAIARKY AHMVDVGQVG VNVPIPVPLP
481 MFSFTGSRSS FRGDTNFYGK QGIQFYTQLK TITSQWKEED ATLSSPAVVM PTMGR
```

# 105 NDUFV1	NP_001006973	NADH dehydrogenase [ubiquinone] flavoprotein 1, mitochondrial precursor [Rattus norvegicus]

```
  1 MLAARHFLGG SVPVRVSVRL SSGTTAPKKT SFGSLKDEDR IFTNLYGRHD WRLKGAQRRG
 61 DWYKTKEILL KGPDWILGEM KTSGLRGRGG AGFPTGLKWS FMNKPSDGRP KYLVVNADEG
121 EPGTCKDREI MRHDPHKLVE GCLVGGRAMG ARAAYIYIRG EFYNEASNLQ VAIREAYEAG
181 LIGKNACDSD YDFDVFVVRG AGAYICGEET ALIESIEGKQ GKPRLKPPFP ADVGVFGCPT
241 TVANVETVAV SPTICRRGGT WFAGFGRERN SGTKLFNISG HVNHPCTVEE EMSVPLKELI
301 EKHAGGVLGG WDNLLAVIPG GSSTPLIPKS VCETVLMDFD ALVQAQTGLG TAAVIVMNSS
361 TDIVKAIARL IEFYKHESCG QCTPCREGVD WMNKVMARFV KGDARPAEID SLWEISKQIE
421 GHTICALGDG AAWPVQGLIR HFRPELEDRM QRFAQQHQAR QAAS
```

Table A.2continued: Amino acid sequences of differentially expressed proteins during DES-PC.

#129/130 CAII	NP_062164	carbonic anhydrase 2 [Rattus norvegicus]

```
  1 MSHHWGYSKS NGPENWHKEF PIANGDRQSP VDIDTGTAQH DPSLQPLLIC YDKVASKSIV
 61 NNGHSFNVEF DDSQDFAVLK EGPLSGSYRL IQFHFHWGSS DGQGSEHTVN KKKYAAELHL
121 VHWNTKYGDF GKAVQHPDGL AVLGIFLKIG PASQGLQKIT EALHSIKTKG KRAAFANFDP
181 CSLLPGNLDY WTYPGSLTTP PLLECVTWIV LKEPITVSSE QMSHFRKLNF NSEGEAEELM
241 VDNWRPAQPL KNRKIKASFK
```

# 131 CAI	NP_001101130	carbonic anhydrase 1 [Rattus norvegicus]

```
  1 MASADWGYDS KNGPDQWSKL YPIANGNNQS PIDIKTSEAK HDSSLKPVSV SYNPATAKEI
 61 VNVGHSFHVV FDDSSNQSVL KGGPLADSYR LTQFHFHWGN SNDHGSEHTV DGAKYSGELH
121 LVHWNSAKYS SAAEAISKAD GLAIIGVLMK VGPANPNLQK VLDALSSVKT KGKRAPFTNF
181 DPSSLLPSSL DYWTYFGSLT HPPLHESVTW VICKESISLS PEQLAQLRGL LSSAEGEPAV
241 PVLSNHRPPQ PLKGRTVRAS F
```

# 160 AST-1	NP_036703	aspartate aminotransferase, cytoplasmic [Rattus norvegicus]

```
  1 MAPPSFFAQV PQAPPVLVFK LIADFRDDPD PRKVNLGVGA YRTDDSQPWV LPVVRKVEQK
 61 IANDHSLNHE YLPILGLAEF RSCASQLVLG DNSPALRENG VGGVQSLGAT GALRIGADFL
121 ARWYNGTDNK NTPVYVSSPT WENHNGVFSA AGFKDIRSYR YWDAEKRGLD LQGFLNDLEN
181 APEFSIFVLH ACAHNPTGTD PTEEEWKQIA AVMKRRFLFP FFDSAYQGFA SGDLEKDAWA
241 IRYFVSEGFE LFCPQSFSKN FGLYNERVGN LTVVGKEHDS VLRVLSQMEK IVRITWSNPP
301 AQGARIVATT LSNPELFKEW KGNVKTMADR ILTMRSELRA RLEALKTPGT WSHITEQIGM
361 FSFTGLNPKQ VEYLVNEKHI YLMPSGRINM CGLTTKNLDY VATSINEAVT KFQ
```

# 201 LDH-B	NP_036727	L-lactate dehydrogenase B chain [Rattus norvegicus]

```
  1 MATLKEKLIA PVADDETAVP NNKITVVGVG QVGMACAISI LGKSLADELA LVDVLEDKLK
 61 GEMMDLQHGS LFLQTPKIVA DKDYSVTANS KIVVVTAGVR QQEGESRLNL VQRNVNVFKF
121 IIPQIVKYSP DCTIIVVSNP VDILTYVTWK LSGLPKHRVI GSGCNLDSAR FRYLMAEKLG
181 IHPSSCHGWI LGEHGDSSVA VWSGVNVAGV SLQELNPEMG TDNDSENWKE VHKMVVDSAY
241 EVIKLKGYTN WAIGLSVADL IESMLKNLSR IHPVSTMVKG MYGIENEVFL SLPCILNARG
301 LTSVINQKLK DDEVAQLRKS ADTLWDIQKD LKDL
```

# 501 UQCRC1	NP_001004250	ubiquinol-cytochrome c reductase core protein 1 [Rattus norvegicus]

```
  1 MAASAVCRAA CSGTQALLRT CRSPALLRLP ALRGTATFVQ ALQSVPETQV SVLDNGLRVA
 61 SEQSSHPTCT VGVWIDVGSR YETEKNNGAG YFLEHLAFKG TKNRPGNALE KEVESIGAHL
121 NAYSTREHTA YLIKALSKDL PKVVELLADI VQNISLEDSQ IEKERDVILR EMQENDASMQ
181 NVVFDYLHAT AFQGTPLAQA VEGPSENVRR LSRTDLTDYL SRHYKAPRMV LAAAGGVKHQ
241 QLLDLAQDHF SSVSQVYEED AVPSITPCRF TGSEIRHRDD ALPLAHVAIA VEGPGWANPD
301 NVALQVANAI IGHYDCTYGG GVHLSSPLAS VAVANKLCQS FQTFNISYSE TGLLGAHFVC
361 DAMSIDDMIF FLQGQWMRLC TSATESEVTR GKNILRNALI SHLDGTTPVC EDIGRSLLTY
421 GRRIPLAEWE SRIEEVDAQM VREVCSKYFY DQCPAVAGYG PIEQLSDYNR IRSGMFWLRF
```

Table A.3: Amino acid sequence of succinyl CoA ligase.

pI 9,9	M_r 37.6	NP_446204	Succinyl CoA ligase [GDP-forming] subunit alpha, mitochondrial precursor [Rattus norvegicus]

```
  1 MTAAVVAAAA TATMVSGSSG LAAARLLSRT FLLQQNGIRH GSYTASRKNI YIDKNTKVIC
 61 QGFTGKQGTF HSQQALEYGT KLVGGTTPGK GGKKHLGLPV FNTVKEAKEK TGATASVIYV
121 PPPFAAAAIN EAIDAEIPLV VCITEGIPQQ DMVRVKHKLT RQGKTRLIGP NCPGIINPGE
181 CKIGIMPGHI HKKGRIGIVS RSGTLTYEAV HQTTQVGLGQ SLCIGIGGDP FNGTNFIDCL
241 DVFLKDPATE GIVLIGEIGG HAEENAAEFL KEHNSGPKAK PVVSFIAGIT APPGRRMGHA
301 GAIIAGGKGG AKEKISALQS AGVIVSMSPA QLGTCMYKEF EKRKML
```

Table A.4: Theoretical MS/MS fragmentation of doubly oxidized peptides of Aco-2.

LTGTLSGW$_{2(ox)}$TSPK (aa 234-245)						
Unmodified peptide				**di-oxidized peptide**		
1247,663 Da $[M+H]^{1+}$				1279,663 Da $[M+H]^{1+}$		
b-ions	**residue**	**y-ions**		**b-ions**	**residue**	**y-ions**
114,092	1 L 12			114,092	1 L 12	
215,140	2 T 11	1134,580		215,140	2 T 11	1166,580
272,161	3 G 10	1033,532		272,161	3 G 10	1065,532
373,209	4 T 9	976,510		373,209	4 T 9	1008,510
486,293	5 L 8	875,463		486,293	5 L 8	907,463
573,325	6 S 7	762,379		573,325	6 S 7	794,379
630,346	7 G 6	675,347		630,346	7 G 6	707,347
816,426	8 W 5	618,325		848,426	8 fW 5	650,325
917,473	9 T 4	432,246		949,473	9 T 4	432,246
1004,505	10 S 3	331,198		1036,505	10 S 3	331,198
1101,558	11 P 2	244,166		1133,558	11 P 2	244,166
	12 K 1	147,113			12 K 1	147,113

EGW$_{2(ox)}$PLDIR (aa 371-378)						
Unmodified peptide				**di-oxidized peptide**		
985,54 Da $[M+H]^{1+}$				1017,60 Da $[M+H]^{1+}$		
b-ions	**residue**	**y-ions**		**b-ions**	**residue**	**y-ions**
130,050	1 E 8			130,050	1 E 8	
187,072	2 G 7	856,468		187,072	2 G 7	888,151
373,151	3 W 6	799,447		405,151	3 fW 6	831,151
470,204	4 P 5	613,367		502,204	4 P 5	613,367
583,288	5 L 4	516,315		615,288	5 L 4	516,315
698,315	6 D 3	403,231		730,315	6 D 3	403,231
811,399	7 I 2	288,204		843,399	7 I 2	288,204
	8 R 1	175,120			8 R 1	175,120

$_{2(ox)}$**WVVIGDENYGESSR** (aa 657-671)						
Unmodified peptide				**di-oxidized peptide**		
1667,80 Da $[M+H]^{1+}$				1699,80 Da $[M+H]^{1+}$		
b-ions	**residue**	**y-ions**		**b-ions**	**residue**	**y-ions**
187,087	1 W 15			219,087	1 W 15	
286,156	2 V 14	1481,687		318,156	2 V 14	1481,687
385,224	3 V 13	1382,619		417,224	3 V 13	1382,619
498,308	4 I 12	1283,550		530,308	4 I 12	1283,550
555,329	5 G 11	1170,466		587,329	5 G 11	1170,466
670,356	6 D 10	1113,445		702,356	6 D 10	1113,445
799,399	7 E 9	998,418		831,399	7 E 9	998,418
913,442	8 N 8	869,375		945,442	8 N 8	869,375
1076,505	9 Y 7	755,332		1108,505	9 Y 7	755,332
1133,527	10 G 6	592,269		1165,527	10 G 6	592,269
1262,569	11 E 5	535,248		1294,569	11 E 5	535,248
1319,591	12 G 4	406,205		1351,591	12 G 4	406,205
1406,623	13 S 3	349,184		1438,623	13 S 3	349,184
1493,655	14 S 2	262,152		1525,655	14 S 2	262,152
	15 R 1	175,120			15 R 1	175,120

EGW$_{2(ox)}$PLDIR (aa 371-378)

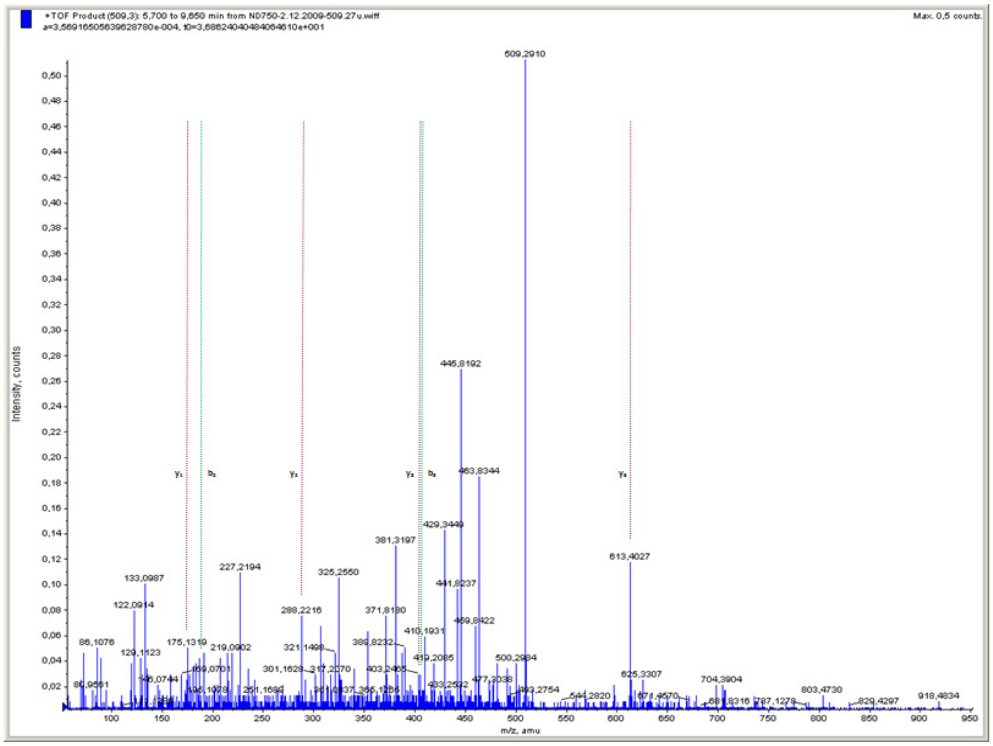

$_{2(ox)}$WVVIGDENYGESSR (aa 657-671)

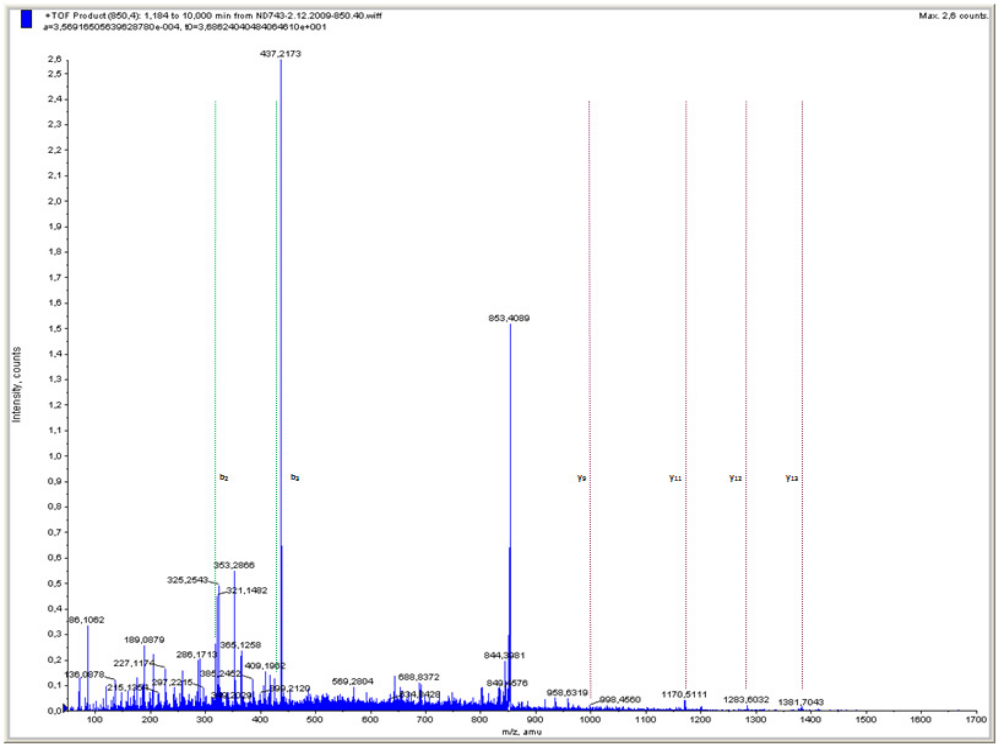

Figure A.2: MS/MS spectra of the doubly oxidized peptides of Aco-2. The respective b- and y-ions are indicated for unequivocal identification of the modified tryptophan.

B. Publications

Journal articles:

- **Dyballa N.** and Metzger S. (2009). Fast and sensitive colloidal coomassie G-250 staining for proteins in polyacrylamide gels. *J Vis Exp*. 2009 Aug **3**; (30). Doi 10.3791/1431
- **Dyballa N.** (2008). Sensitive Coomassie-Färbung. *Laborjournal*, Service-Magazin für Medizin und Biowissenschaften, Heft **4**/2008

Book chapter:

- **Dyballa N.** and Metzger S. Coomassie staining in quantitative proteomics. Contribution to *Methods in Molecular Biology*, Vol.xxx: *Quantitative Methods in Proteomics*, Humana Press (in preparation).

Abstracts:

- **Dyballa N.**, Schuh C., Vogt H., Metzger S., and Weber N. (2009). Cardiac proteome alterations during the time course of desflurane preconditioning in vivo. *European Journal of Anaesthesiology*, Vol. **26**, Suppl. 45
- **Dyballa N.**, Schuh C., Vogt H., Schlack W., Weber N.C., and Metzger S. (2008). Proteomic analysis of cardiac targets involved in anesthetic-induced preconditioning. *Wiley's GoProteomics*, HUPO Abstracts 2008, POS-WED-113
- **Dyballa N.**, Metzger S., Toma O., Schlack W., and Hauck-Weber N.C. (2007). An improved proteomics-based approach for the analysis of modifications in the cardioprotection by pharmacological preconditioning. *Naunyn-Schmiedeberg's Archives of Pharmacology*, Vol. **375**, Suppl. 1
- **Dyballa N.**, Weber N.C., Metzger S., Toma O., and Schlack W. (2006). Proteomic analysis of pharmacologically preconditioned rat myocardium by two-dimensional gel electrophoresis. *Naunyn-Schmiedeberg's Archives of Pharmacology*, Vol. *372*, Suppl. 1